EXPERIMENTAL STUDY ON POLYMER CEMENT MORTAR (PCM) WITH SILICA FUME TO ENHANCE CONCRETE-PCM INTERFACE BOND

シリカフュームを混入したポリマーセメントモルタル(PCM)によるコンクリート-PCM 界面接着性状改善効果に関する実験的研究

A dissertation submitted to the Division of Engineering and Policy for Sustainable Environment, Graduate School of Engineering, Hokkaido University in partial fulfillment of the requirements for the Degree of Doctor of Philosophy in Engineering

by
MAHMUDUL HASAN MIZAN

Examination Committee
Associate Professor Koji Matsumoto
Professor Takafumi Sugiyama
Professor Ryoma Kitagaki

Division of Engineering and Policy for Sustainable Environment
Graduate School of Engineering
Hokkaido University
Sapporo, Japan

September 2022

EXPERIMENTAL STUDY ON POLYMER CEMENT MORTAR (PCM) WITH SILICA FUME TO ENHANCE CONCRETE-PCM INTERFACE BOND

シリカフュームを混入したポリマーセメントモルタル(PCM)による コンクリートーPCM界面接着性状改善効果に関する実験的研究

Division of Engineering and Policy for Sustainable Environment
Graduate School of Engineering
Hokkaido University
Sapporo, Japan

September 2022

ABSTRACT

In twentieth century, strengthening of reinforced concrete (RC) structures is one of the fast-growing, challenging but crucial questions, thus it becomes a significant central issue all over the world to be solved for the practical application. The polymer cement mortar (PCM) overlay method is known as one of viable, economical, environment friendly and promising solution for strengthening the deteriorated concrete structures due to its superior properties in terms of mechanical strength, durability, and good adhesive strength with concrete than ordinary mortar. In this method, the substrate concrete-PCM bond is considered a threshold and the occurrence of premature debonding at the concrete-PCM interface prevents the strengthened structures from achieving full serviceability and designed load-carrying capacity. The exposure of composite specimens/structures to severe environmental conditions caused further degradation of the interface leading to significant reduction of intended service life of repaired structures. Therefore, it becomes a very urgent subjects to find out an efficient method to improve the concrete-PCM interfacial bond and simultaneously ensure the highest level of safety operation. With such aim, this study focused on how this interface can be strengthened more effectively to prevent brittle fractures. Number of experimentation at microscopic, material and member level were conducted considering the impact of different influencing factors to simulate the actual bonding situation in real retrofitting fields and investigated the effectiveness of adding silica fume to PCM, in order to achieve the great potential in practical design implications.

The research comprises of lot of experimental investigations of PCM-concrete bond properties with and without silica fume subjected to static loading. Experiments were conducted under tensile and shear stress condition along with the microstructure analysis using microscopic test to precisely understand the influence of silica fume in forming the chemical connection at the concrete-PCM interface. Performance evaluation of silica fume inclusion were also conducted considering experimental parameters, such as interface roughness, compressive strength of substrate concrete or moistness of the interface to clarify the effects of the considered parameters on the bonding mechanism. The issue of bonding durability of the concrete-PCM interface with the inclusion of silica fume under exposure to severe environmental condition were also evaluated. Meanwhile, PCM overlay strengthened beams with and without silica fume cementitious mortar having different cross-section area of the strengthening bar were tested under monotonic flexure loading. The major achievements through this research are summarized as follows:

The effectiveness of modified silica PCM as a repair material in forming a chemical connection at interface were evaluated qualitatively based on loading test (tensile and shear stress condition) using smooth and rough concrete surface roughness, and quantitatively based on microstructure analysis using scanning electron microscopy (SEM), energy-dispersive X-ray spectroscopy (EDS), X-ray diffraction (XRD) and thermogravimeter-differential thermal analysis (TG-DTA). As a repair layer mortar, PCM modified with silica fume caused an improvement in the interfacial strength, even with smooth concrete substrate surface where mechanical bonding had less influence. The inclusion of silica fume increases the splitting tensile strength by approximately 16% and 22%, and interfacial shear strength by approximately 114% and 30% compared to the normal PCM for smooth and rough concrete surfaces, respectively. This fact indicates a higher possibility of the formation of chemical connection at the concrete-PCM interface by transformation of harmful $Ca(OH)_2$ into more C-S-H. Furthermore, lower Ca/Si ratio was observed through microscopic SEM-EDS test and a decrease in the $Ca(OH)_2$ content was observed qualitatively through XRD analysis and quantitatively through TG-DTA at the modified silica PCM-concrete interface compared to normal PCM-concrete interface. This suggests an increase in the extend of bond formation between silica compound and free $Ca(OH)_2$ (modified silica PCM cases) compared to the bond formation in normal PCM cases, thus the inclusion of silica fume contributing to the improvement of the interfacial performance in former cases.

Because of the absence of information about the bonding performance of PCM modified by 5% silica fume as an overlay mortar under various influencing factors, more detailed experiments were designed to explore its effect on the interfacial bond performance. New research work was designed to study the effectiveness of modified 5% silica PCM as a repair material based on a bi-surface shear test using three level of surface roughness (high, medium and low), concrete compressive strengths (two types), moistness of the interface (wet, dry and saturated surface dry condition) and early age

behaviour (curing time) as an experimental parameter. It was observed that the inclusion of silica fume in the PCM significantly improves the interfacial bonding strength compared to normal PCM in each condition of surface roughness level and substrate concrete compressive strength. The moistness of the substrate concrete surface predominantly influenced the interfacial strength. The saturated surface dry interface state of substrate concrete facilitate bond strength development, especially in modified 5% silica PCM cases. Significant improvement of the bond strength with the inclusion of silica fume were observed from the very first day of pouring of overlay mortar due the predominant reaction of silica compound with $Ca(OH)_2$ during the early hydration stage.

From the perspective of practical application of modified PCM overlaying method, long-term performance of the interface (durability) under the harsh environmental exposure were investigated, considering an individual action of freezing and thawing cycle (FTC), elevated temperature (constant and cyclic), and moisture content (continuous immersion, and wetting/drying (W/D) cycle) in the laboratory which resembles with the real environmental conditions. It was observed that the interfacial strength of normal PCM specimen under FTC decreased more quickly than that of modified 5% silica PCM specimens. Mixing silica fume with PCM significantly increase interfacial bonding strength, provides better adhesion with substrate concrete, and improves the durability of the interfacial performance of concrete-PCM interface under harsh freeze-thaw environments. Normal PCM specimens resulted more decrease of interface strength than that of modified PCM specimens compared to their corresponding reference specimens under both constant and cyclic temperature exposure. Earlier occurrence of interface fracture and a greater number of pure interface fracture mode in normal PCM specimens compared to modified 5% PCM specimens indicates higher adhesion of modified PCM overlay with substrate concrete with better durability. The interfacial strength of normal PCM specimens significantly reduced under both W/D condition and continuous immersion compared to the reference specimens, whereas it reduced insignificantly under continuous immersion exposure and moderately under W/D cycle compared to reference specimens in case of modified 5% silica PCM specimens. The inclusion of silica fume significantly improves the interfacial bonding strength compared to without silica fume cases under the influence of moisture by wetting/drying and continuous immersion. The use of silica fume achieves adequate bond strength with concrete substrate, improves adhesion and durability under harsh environmental conditions.

For real application of the current work, performance of interface was also investigated at member level by conducting loading test of RC beams strengthened by both normal PCM and modified 5% silica PCM overlaying with different types (steel rebar, CFRP grid and CFRP strand sheet) and amounts of reinforcement. Failure load of all strengthened beams were observed more than the unstrengthened beams. The occurrence of debonding failure delayed with the incorporation of silica fume compared to normal PCM strengthened beam or failure mode shifted to classical failure. In all cases, the crack numbers in strengthened beam with modified PCM were more than those observed in strengthened beam with normal PCM. Significant increase of ductility, peak load, debonding load were observed in modified PCM strengthened beam compared to normal PCM strengthened beam. The strain distribution of the strengthening bar in normal PCM specimens were unstable (many sudden jumps/variations with the load increase) compared to the modified PCM specimens, confirming uniform shear stress transfer at the interface between the strengthening layer and the substrate RC beam.

Conclusively, considering easy applicability of silica fume with PCM in practical application, environmentally friendly nature, and ability to achieve adequate bond strength with concretes substrate, this study can provide an indication to practitioner for engineering application of silica fume in polymer cement-based repair materials.

Keywords: Polymer cement mortar, overlaying method, premature debonding failure, interfacial strength, silica fume.

ACKNOWLEDGEMENT

Firstly, the author expresses his praises to almighty ALLAH, who gave him ability to complete the project in due time.

This research work has been completed successfully under the kind supervision of Dr. Koji Matsumoto, from the Laboratory of Engineering for Maintenance System, Hokkaido University, Japan. I would like to express my special appreciation and thanks to my supervisor for his inclusive guidance, invaluable suggestions, dearly encouragement and constructive criticisms during the whole period of my graduate study at Hokkaido University. He not only provides me knowledge about the subject for my thesis, the knowledge, the wisdom, the guidance, and the patience throughout the course of my research but also supported me about many daily life's problems. That helps a foreign student like me to concentrated completely on the research. Without his time, patient advice and constant encouragement, this dissertation would not have been accomplished. It has been a great learning experience to carry out this research under his supervision.

Besides, I would like to express my sincere gratitude to my examination committee members, Professor Takafumi Sugiyama and Professor Ryoma Kitagaki for their instruction and advice. Their insightful comments, encouragements, and also the hard questions would make me widen my research from various perspectives. Furthermore, I am also obliged to my former supervisor, Professor Tamon UEDA, for his continuous guidance, valuable suggestion, encouragement, and invaluable input to carry out research in this topics.

I am also grateful to the Denka Co., Ltd. for providing polymer cement mortar and silica fume for this research. Besides, I am thankful to the Nippon Steel and Sumikin Materials Co. Ltd for their support by providing material in this research and their guidance in application. I am also thankful to Mr. Makoto Okubo of Maeda Kosen Co. Ltd for his discussion and information regarding practical implication of the PCM overlaying method.

Sincere thanks to Tatsuya Fukuda for his endless support during experimentation. I would like to extend my heartiest gratitude to the present and past members of our lab, especially Masamitsu Takase, Takuya Soma, Yuzuna Washio, Chinatsu Ryogoku, Ryosuke Nagai and Daichi Fujiwara for providing good cooperation and assistance during my experimental works over the years. Your helps and supports are really appreciated and will never be forgotten. Special thanks to Naoko Masaki (Secretary) for the continuous support and taking care of the financial issues for this research work as well as many of my personal issue. Your support contributes in many ways for the completion of this study. I am also thankful to technical staff Tatsuya Okuma, Kohei Tokuda, Takuya Sugimoto and Yoshiki Honda for their eager helpful nature that helped me in conducting my experiments smoothly. It would have been truly impossible to carry out such an extensive experimental work without our lab technicians. Thank you for your kind help and working together during specimen preparation and testing.

Of course, no acknowledgments would be complete without giving thanks to my family members; they prepared the best foundation for me and always encourage me to continue higher study, especially in abroad. I am too proud of them and love them very much. Later, I am very much indebted to my wife, Nasiba Afrin, she supported me in every possible way to see the completion of this work.

Finally, yet importantly, I would like to express my thanks to Japan Society for the promotion of Science (JSPS) for the financial support through my tenure, that make my dream come true and my future will become brighter. Besides, I am also thankful to English Engineering Education (e3) program staffs for their kind cooperation throughout this period.

CONTENTS

LIST OF TABLES

LIST OF FIGURES

Chapter 1

INTRODUCTION

1.1 Background

The twentieth century saw a dramatic increase in large construction projects made from reinforced concrete (RC) around the globe. Modern RC infrastructures such as buildings, bridges, power plants, roadways, dams etc. play a major role in Country's GDP growth. During the period of high economic growth after World War II in Japan, numerous large construction projects evolved, and structures were constructed with concrete. Over the time, these RC structures are getting old and have sustained severe damages. Due to the longer durability of RC structures, it had been considered as "maintenance-free" materials for many decades. Over the last few decades, this commonly holds view has changed significantly and large number of RC structures deteriorated before the end of intended service life due to different reasons viz. change in their use, overloading, inadequacy of design detailing and poor construction, new design standards, suffering from many adverse conditions such as severe environmental conditions, unseen mechanical loadings, natural disasters, etc. In a study [1], it was found that the deterioration of RC floor slab of a bridge caused by overloading is proportional to a vehicle's weight to the power of 12 i.e the impact of a truck with a 20 tons of axle load on a road bridge is equivalent to 4000 trucks with 10 tons of axle load. Several accidents have happened in the past where concrete structures didn't perform as per its expectation and caused lots of damages not only monetary but also livelihood, sometimes even cost humans lives. The Genoa Bridge collapse in Italy on August 14th, 2018, is a recent example, which caused 43 deaths.

To avoid such circumstances and restore the durability of concrete structures, it is a global issue to pay attention towards maintenance strategies such as repairing and strengthening of deteriorated structures. Instead of replacing these deteriorating structures, repairing, and strengthening them is a better solution from both economic and environmental viewpoints. To achieve the full serviceability of the deteriorated structures, several strengthening techniques based on practical experience and scientific research have been proposed over recent decades, such as continuous fibre sheet bonding, steel plate bonding, and fiber-reinforced polymer (FRP) jacketing [2-4]. Some unavoidable drawbacks due to the use of epoxy resin, such as low permeability, poor fire resistance, difficulties in applying on humid surfaces, susceptibility to UV radiation, and chemical damage hinder the worldwide application of these strengthening techniques. To overcome some of these obstacles, more innovative strengthening systems based on the cement matrix, such as textile-reinforced concrete [5], mineral-based composites [6], fibre reinforced cementitious mortar [7] and polymer cement mortar (PCM) [8-9] have been found in the technical literature.

Recently, the PCM overlay method has been widely used around the globe for the repair/retrofitting of deteriorated RC structures in which PCM is overlaid on pre-existing concrete by troweling or spraying as presented in Figure 1.1. PCM became the dominant material in the construction industry in 1980s, and it is currently used as a popular repairing material as PCM possesses very compatible properties with concrete in comparison to other repairing materials [10]. Besides, PCM is also advantageous over ordinary cement mortar because of its superior properties as it possesses better workability, higher compressive and adhesion strength [11], higher frost resistance [12], long-lasting durability [13], lower permeability [14], and a lower rate of shrinkage [15]. This strengthening method is also advantageous, as overlaying to the slab bottom surface enables the construction without any interruption in traffic and any weather conditions. This technique relies on the micro-filler and anchoring characteristics of PCM. The polymers in PCM are smaller than cement particles, and they fill the pores and voids on concrete surfaces due to the micro-filler effect. Additionally, polymers generate polymer films around aggregates and cement hydration forming an interpenetrating network structure with the cement hydration product, referred to as the anchoring effect of PCM. The coalescence of polymer particles in PCM reduces the porosity by filling all the pores and providing better adhesion and durability with concrete than ordinary mortar [16-17].

Previous experimental studies [8, 18-20] showed that the PCM overlay method often upgrades the flexural capacity and stiffness of strengthened RC structures. However, premature debonding,

which occurs before the yielding of rebar or upper concrete crushing hinders the worldwide application of this strengthening technique. Although PCM offers good adhesive properties as a repair material, in many studies [10, 19-22], the interface between the existing concrete substrate and new PCM overlay material has been reported as the weakest link. It is vital to avoid the delamination of the new overlay to reduce chloride intrusion or other physical-chemical degradation mechanisms affecting durability and serviceability requirements [23]. In PCM applications, an appropriate bond between two materials, concrete and PCM, that have undergone different aging processes is a key factor to ensure load transfer for restoring the monolithic character of the structure. In light of the weak bond at the concrete-PCM interface, it is now an issue gaining considerable attention to look for the measures to improve the interface more effectively to prevent the brittle debonding failure. Concerning the abovementioned issue, this research mainly highlights the improvement of the processes and procedures used in the PCM overlaying method (particularly, bond behavior at the concrete-PCM interface and enhancement of the interfacial bonding strength), in order to achieve the great potential in practical design implications.

(a) Spraying [Nara Construction Co., Ltd.] (b) Troweling [Maeda Kosen Co., Ltd.]

Figure 1-1 Application of PCM to the concrete bottom slab

1.2 Bonding mechanism of strengthening interface

The mechanisms of the bond strength at the interface between the new overlay layer and old substrate concrete are described under 'bond-adhesive' and 'bond-cohesive' mechanisms. The 'adhesive' mechanism is related to the embedding action between the reactive matrix materials of the new material and the old substrate concrete, and the 'cohesive' mechanism is linked to the 'overlay transition zone' of the new material. These two mechanisms are closely associated, and if the bond-adhesive strength is not developed, the interface cohesive mechanism will not be effective. Thus, good adhesion at the interface is required for a successful repair. In general, concrete and PCM are connected at the interface by micro filler and the anchoring effect of the PCM. The PCM overlaying interface is mainly bonded by mechanical bonding, as shown in Figure 1.2 (without chemical bonding), despite concrete and PCM parts relying on chemical bonding.

In the repair system, the composite specimens are considered a combination of three zones/layers: the PCM cohesion layer, concrete cohesion layer, and interface between the concrete and PCM termed the adhesion layer. Furthermore, the three layers of the interface have been proposed including penetration (first) layer, strongly affected (second) layer, and weakly affected (third) layer [24-25] as shown in Figure 1.2. The penetration layer is formed in the cavities and pores of the substrate concrete which contains mainly C-S-H and a little ettringite or calcium hydrate, thus this layer has no harmful influence on the strength of the interface. The strongly affected layer is formed adjacent to the physical boundary between substrate concrete and repairing material which contains mainly $Ca(OH)_2$ and needle-shaped AFt crystal. This layer has a significant influence on the interfacial performance and is regarded as the porous and weakest layer in the interfacial zone. The third layer has a similar microstructure of penetration layer in the repairing material; thus, it has no harmful influence on the strength of the interface.

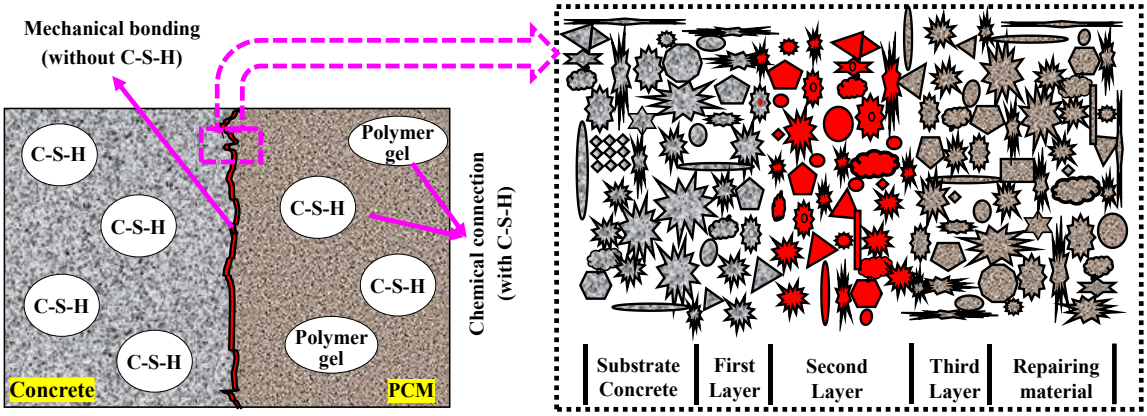

Figure 1-2 Phases of PCM strengthening techniques and three layers of the interface [25].

1.3 Aims and significance of this study

In PCM overlaying method, the bond behavior at the PCM-concrete interface that presents a weak link in the repaired structure, particularly influences the structural behavior. The occurrence of debonding failure from any discontinuity (boundary, joints or crack cutting the overlay) depicts that the retrofit structure fails at lower load than the designated load carrying capacity and cannot achieve full serviceability. In light of the debonding issue and weak bond between concrete and PCM, this study focused on the processes and procedures to increase interface bonding strength between existing concrete and PCM with a provision to prevent the brittle debonding failure to regards PCM overlay flexural strengthening as the main application background. It is common knowledge that the existence of C-S-H affects the bonding strength, but PCM overlaying interface is mainly bonded by mechanical bonding (without chemical connection). Therefore, if C-S-H could also be made at the interface between concrete and PCM by chemical reaction, it is expected that the interfacial bond strength will increase to prevent debonding failure. Thus, this study aims to increase the interface bonding strength more effectively by generating interface chemical bonding by using silica fume. The past research revealed that the silica fume in concrete provides greater cohesiveness, less segregation, reduced bleeding in concrete, and greatly improve the compressive strength and bond strength of paste-aggregate interface due to higher pozzolanic activity [27-28]. Silica fume also promote chemical reaction with free alkali after the hydration of cement to produce more C-S-H. It is expected that silica fume can strengthen the interface by the micro filler effect due to its extreme fineness. In addition, it is also expected that the high silica content in silica fume can generate more C-S-H by combining with calcium hydroxide (produced after hydration of cement) in the water supplied condition, which can enhance the interface bonding strength. Consequently, the purpose of silica fume is to cause more C-S-H at interface to increase strength and durability.

1.4 Objectives of the Study

The purpose of this study is to evaluate the effectiveness of using silica fume with PCM to improve the concrete-PCM interfacial bond to prevent the premature debonding. Detailed objectives of this study are listed as follows:

- To understand the fundamental stress-transferring mechanisms of the PCM-concrete interface and enhancement of the interfacial strength more effectively from the perspective of chemical reactions. Experimentation is conducted under tensile and shear stress condition along with the microstructure analysis using microscopic test to precisely understand the chemical bonding of the interface
- Performance evaluation of the bond between substrate concrete and PCM overlay with/without silica fume considering experimental parameters, such as interface roughness, compressive strength of substrate concrete, moistness of the interface, curing time to clarify the effects of the considered parameters on the bonding mechanism.
- To understand the bonding durability of the concrete-PCM interface with the inclusion of silica fume under environmental conditions (freeze-thaw cycle, hygrothermal condition),

which can be used in designing of structures strengthened by PCM overlay in given climatic condition.

- ❑ To explore the behavior of modified PCM strengthened RC beams in terms of ductility, failure load, failure mode, load deflection relationships, debonding strength to understand the influence of silica fume, which can be applied to the design of structures strengthened by PCM overlay.

1.5 Outline of the Dissertation

The present studies aim at a better understanding of the effectiveness of adding 5% silica fume with PCM from the perspective of microscopic, material, and structural point of view. The summary of the various types of tests along with specimen size and time interval of testing after PCM overlay is presented in Figure 1.3.

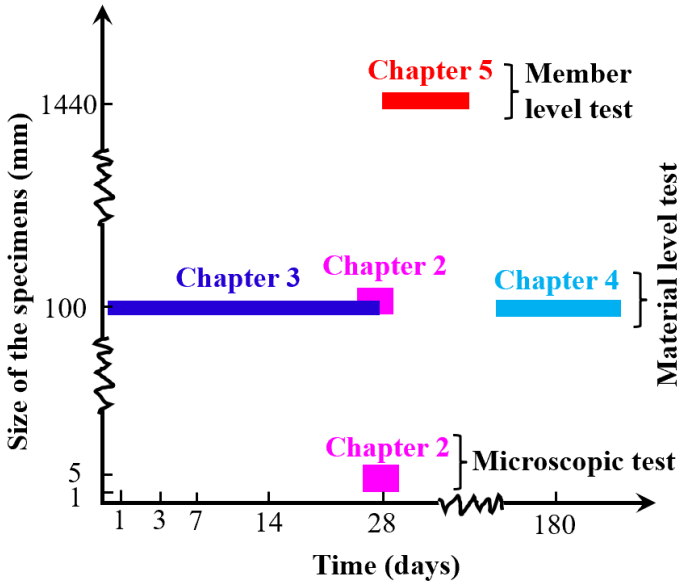

Figure 1-3 Illustration of the types of test performed in this study

This dissertation is divided into six main chapters. The basic contents of each chapter and research flow are illustrated in Figure 1.4 and listed as follows.

Chapter 1 describes the background, problem statement, objective, and significance of the present research. Chapter 2 to chapter 4 provides a description of the experimentation used in this study at material level test to increase the interfacial bonding strength using silica fume and crucial discussion of the obtained results.

Chapter 2 examines the influence of silica fume as a possible means to enhance the concrete-PCM interfacial bond. For the purpose of precise understanding of the influence of silica fume to enhance the interfacial bonding of the composite specimens, smooth roughness level of substrate concrete is considered where mechanical bonding has less influence. Several tests are conducted by incorporating primer at interface to understand the effectiveness of using silica fume with PCM as a repair mortar. In chapter 3, microstructural analysis are also discussed using different microscopic tests to quantify the transformation of harmful $Ca(OH)_2$ of the interface into more C-S-H and to precisely understand the chemical bonding of the interface with the inclusion of silica fume.

Chapter 3 describes the detailed experimentation of concrete-PCM interface of the composite specimens with/without silica fume. Several tests are conducted under shear stress condition and concrete substrate with different roughness level, different compressive strength of concrete, different moistness state of the substrate concrete interface, and curing time are considered to simulate the actual bonding situation in real retrofitting fields and concluded the significant effect of silica fume on the interface of the composite specimen.

Chapter 4 provides a description of the experimentation used in this study at material level test in tension and shear to investigate the bonding durability of the concrete-PCM interface under Freeze-

thaw cycle, elevated temperature, and moisture. The main efforts are put to evaluate the long-term performance of concrete-PCM composites under environmental conditions to simulate the actual bonding situation from the perspective of practical application of PCM overlaying method.

Chapter 5 discussed the experimental study of the PCM overlay strengthened RC beams to understand the behavior of interface at member level. The experimental failure mode, failure load and load deflection relationships of the strengthened RC beam with/without silica fume are discussed in detail in Chapter 5.

Chapter 6 presents the conclusion of the results obtained from Chapter 2 to Chapter 5, which clarify the objectives and significance of this study and includes very useful information for the practitioner. Some recommendations for the future study is included in this chapter as well.

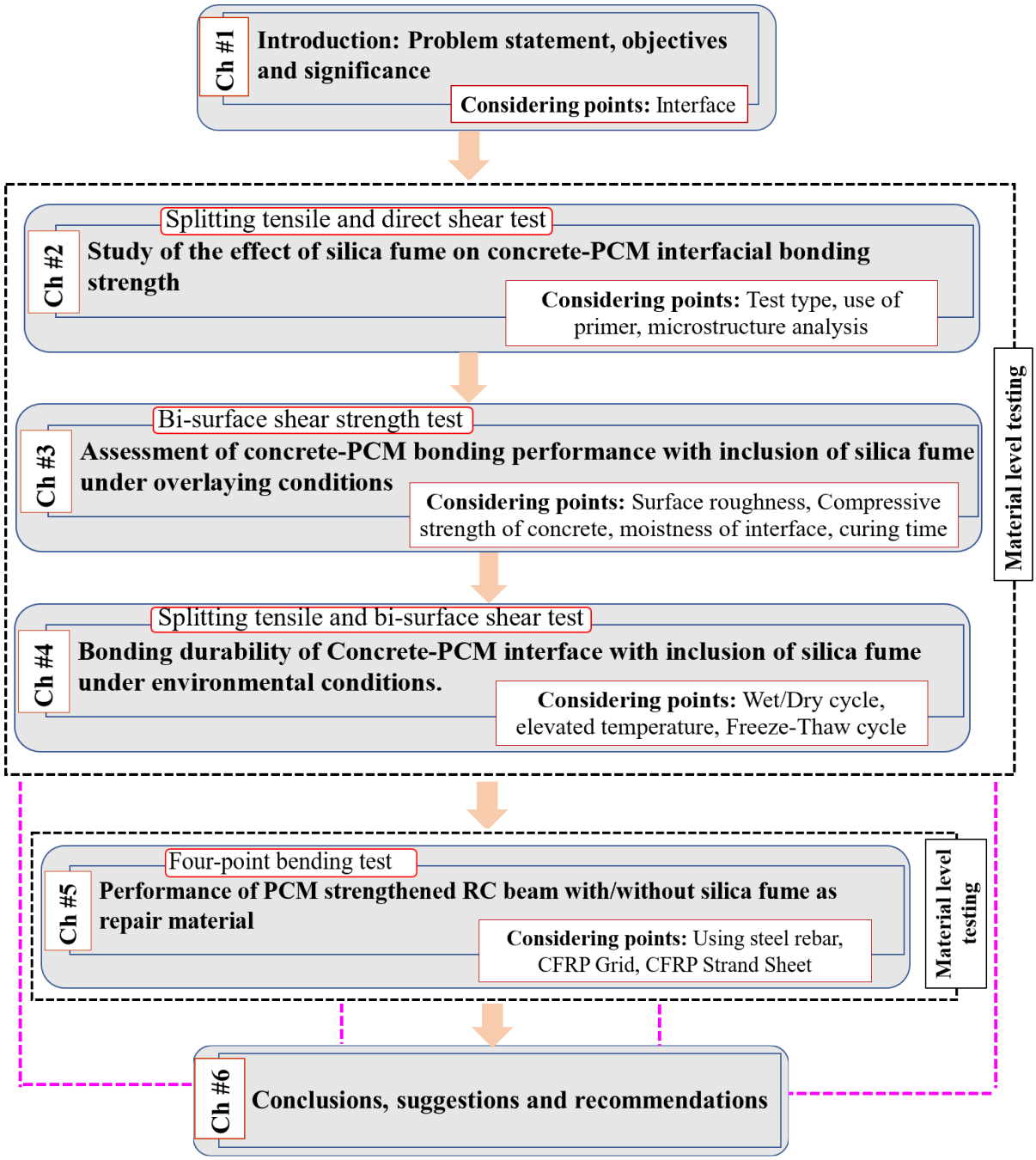

Figure 1-4 Research flow and organization of dissertation

References

[1] MLIT report. (2014). “Towards maintenance, management, and renewal of futures social infrastructures-social infrastructures that are passed on from aged to age.” Section 1, Chapter 1.

[2] Alam, M. S., Kanakubo, T. and Yasojima, A. (2012). “Shear-Peeling Bond Strength between Continuous Fibre Sheet and Concrete." ACI Structural Journal, 75-82.

[3] Alam, M. A., Ali, S. J., Zamin, M. J. and Kamal, N. M. (2014). “Effective method of repairing RC beam using externally bonded steel plate." Applied Mechanics and Materials, 567: 399-404.

[4] Tidarut, J., Zhang D. and Ueda, T. (2013). “Prediction of the post-peak behavior of reinforced concrete columns with and without FRP-jacketing.” Engineering Structures (Elsevier), 56:1511-1526.

[5] Bruckner, A., Ortlepp, R. and Curbach, M. (2005). "Textile Reinforced Concrete for Strengthening in Bending and Shear." Materials and Structures, 38, 741-748.

[6] Taljsten, B. and Blanksvard, T. (2007). "Mineral based bonding of CFRP to strengthen concrete structures." Journal of Composites for Constructions, 11(2): 120-128.

[7] D’Ambrisi, A., Feo, L. and Focacci, F. (2013). "Experimental and analytical investigation on bond between Carbon-FRCM materials and masonry." Composites Part B: Engineering, 46: 15-20.

[8] Satoh, K. and Kodama, K., (2005). “Central peeling failure behavior of polymer cement mortar retrofitting of reinforced concrete beam.” *Journal of Materials in Civil Engineering*, 17(2), 126-136.

[9] Zhang, D. W., Ueda. T. and Furuuchi, H., (2013). “Fracture mechanisms of polymer cement mortar: Concrete interfaces.” *Journal of Engineering Mechanics*, 139(2), 167-176.

[10] Hassan, K. E., Brooks, J. J. and Al-Alawi, L., (2001). “Compatibility of repair mortars with concrete in a hot-dry environment.” *Cement and Concrete Composites*, 23(1), 93-101.

[11] Chung, D. D. L., (2004). “Use of polymers for cement-based structural materials.” *Journal of Materials Science*, 39(9), 973-2978.

[12] Mirza, J., Mirza, M. S. and Lapointe, R., (2002). “Laboratory and field performance of polymer-modified cement-based repair mortars in cold climates.” *Construction and Building Materials*, 16(6), 365-374.

[13] Al-Zahrani, M. M., Maslehuddin, M., Al-Dulaijan, S. U. and Ibrahim, M., (2003). “Mechanical properties and durability characteristics of polymer and cement-based repair materials.” *Cement and Concrete Composites*, 25(4-5), 527-537.

[14] Yang, Z. X., Shi, X. M., Creighton, A. T. and Peterson, M. M., (2009). “Effect of styrene-butadiene rubber latex on the chloride permeability and microstructure of Portland cement mortar.” *Construction and Building Materials*, 23(6), 2283-2290.

[15] Wang, R. and Wang, P. M., (2010). “Function of styrene-acrylic ester copolymer latex in cement mortar.” *Materials and Structures*, 43(4), 443-451.

[16] Sakai, E. and Sugita, J. (1995). “Composite Mechanism of Polymer Modified Cement.” Cement and Concrete Research, 25(1):127–135.

[17] Brien, J. V. and Mahboub, K. C. (2013). “Influence of polymer type on adhesion performance of blended cement mortar.” International Journal of Adhesion and Adhesives, 43: 7–13.

[18] Mahmudul, H. M., Ueda, T. and Jun, T. (2019). “Finite element analysis of RC beam strengthened with PCM”, Proceedings of Japan Concrete Institute, Vol. 41, Japan.

[19] Zhang, D., Ueda, T. and Furruchi, H. (2012). "Concrete cover separation failure of overlay strengthened reinforced concrete beams." Construction and Building Materials, 26: 735-745.

[20] Zhang, D., Ueda, T. and Furuuchi, H. (2011). "Intermediate Crack Debonding of Polymer Cement Mortar Overlay-Strengthened RC Beam." Journal of materials in civil engineering, 23(6): 857-865.

[21] Khuram, R., Zhang, D., Ueda, T. and Weiliang, J. (2016). “Investigation on concrete-PCM interface under elevated temperature: At material level and member level.” Construction and Building Materials, 125: 465–478.

[22] Rashid, K., Ueda, T. and Zhang, D. (2016). “Study on Shear Behavior of Concrete-polymer Cement Mortar at Elevated Temperature.” Civil Engineering Dimension, vol. 18: 93–102.

[23] Zanotti, C., Talukdar, S. and Banthia, N. (2014). "A state-of-the-art on concrete repairs and some thoughts on ways to achieve durability in repairs." Infrastructure Corrosion and Durability-a Sustainability Study.
[24] Emmons, P. H. and Vaysburd, A. M. (1996). "System concept in design and construction of durable concrete repairs." *Construction and Building Materials*, **10**(1): 69-75.
[25] Xie, H., Li, G. and Xiong, G. (2002). "Microstructure model of the interfacial zone between fresh and old concrete." *Journal of Wuhan University of Technology-Mater. Sci. Ed.*, **17**(4), 64-68.
[26] Das, K. (2012). "The effect of Silica Fume on the Properties of Concrete as Defined in Concrete Society Report 74, Cementitious Materials." 37th Conference on Our World in Concrete and Structures, Singapore.
[27] Gao, J. M., Qian, C. X., Wang, B. and Morino, K., (2002). "Experimental study on properties of polymer-modified cement mortars with silica fume." *Cement and Concrete Research*, 32(1), 41-45.
[28] Jiang, C. H., Zhou, X. B., Huang, S. S. and Chen, D., (2017). "Influence of polyacrylic ester and silica fume on the mechanical properties of mortar for repair application." *Advances in Mechanical Engineering*, 9(1), 1-10.
[29] Sugawara S., Koizumi T., Harada S. and Okazawa K. (2007). "Effect of reaction ratio of silica fume on strength development of 150N/mm2 class concrete." Concrete Research Technology, 18(95).
[30] Kurdowski, W. and Nocun-wczelik, W. (1983). "The tricalcium silicate hydration in the presence of active silica." Cement and Concrete Research, 13(3), 341–348.

Chapter 2
STUDY OF THE EFFECT OF SILICA FUME ON CONCRETE-PCM INTERFACIAL BONDING STRENGTH

2.1 Introduction

Recently, the PCM overlay method has gained popularity worldwide as a strengthening material for concrete structures and pavements due to its superior properties (relatively high compressive strength, high adhesion strength, and low permeability) compared with normal mortars. The concrete-PCM interface is the most critical component of PCM strengthening method to be considered in practical applications as the interface is weak attributed by the mismatch of the material properties between concrete and PCM. The lower modulus of PCM compared to its concrete counterpart results more deformation under load and causes the accumulation of stresses over the interface zone. The debonding failure happened when the accumulated stress exceeds the bond strength. As far as the author's reviewed literatures are concerned, premature debonding failure was observed in numerous studies as a major failure modes in repaired or strengthened structure such as FRP strengthening, steel plate strengthening, etc., which led the strengthened structure to not fully utilization of its capacity. From the past experimental study [1-4], it can be said that the PCM overlaying method is also prone to debonding unlike other strengthening methods. For example, the interface of substrate concrete of existing slabs and new PCM layer is subjected to self-equilibrated state of tension combined with shear [4-5]. In bridge retrofitting, interface zone between new and old material are subjected to shear stress due to application of load. In columns strengthened with PCM jackets, longitudinal forces are transferred through interface shear stresses from old cross-section to new cross-section [5-6]. Premature debonding failure results undesirable deficiency of the bond and ineffectiveness of the whole composite structures. Considering this premature debonding failure issue, it is important to understand how the interface between concrete and PCM can be improved more effectively to prevent this premature debonding failure of the PCM strengthened RC structures. With an aim to increase the interfacial bonding strength between the concrete and the PCM, this present study utilizes silica fume as a possible means to improve the interface properties to prevent premature debonding failure.

Silica fume is commonly known as micro silica, which is an ultrafine powder collected as a byproduct of silicon and ferrosilicon alloy production. Silica fume is expected to strengthen the interface by micro filler effect because of the extreme fineness (mean dia. of about 0.15 microns i.e., approximately 100 times smaller than the average size of cement particle). Extremely fine particle size, high surface area, and a high percentage of SiO_2 (approximately 85%) of silica fume make the repair material highly reactive [7]. Additionally, Kurdowski and Nocun-wczelik [8] stated that the silica fume accelerates the hydration of the main constituents of cement, i.e., A-lite (C_3S), B-lite (C_2S), and ferrite (C_4AF). After the hydration of cement, the free alkali, in the form of calcium hydroxide [$Ca(OH)_2$], reacts with the silica compound of silica fume under the water supply condition to form an additional binder called calcium silicate hydrate (C-S-H) [9], which strongly affects the bonding strength. The past research revealed that the silica fume in concrete provides greater cohesiveness, less segregation, reduced bleeding in concrete, and greatly improve the compressive strength and bond strength of paste-aggregate interface due to higher pozzolanic activity [10-11]. Despite the positive influence of silica fume in polymer concrete, few studies [12] have investigated the basic utilization of silica fume to enhance interfacial performance but almost no studies have been done to evaluate quantitatively the influence of silica fume in forming chemical connection to enhance interfacial performance, although it is common knowledge that the silica compound of silica fume reacts with free alkali to produce more C-S-H. In the past, Xie [13] proposed a microstructure model of the interfacial zone between substrate concrete and repair material in which they stated that the physical boundary of substrate concrete-repair material is characterized by high porosity and highly oriented crystal constituents: mainly $Ca(OH)_2$ and ettringite. In the presence of water, this $Ca(OH)_2$ reacts with the silica compound of silica fume to form more C-S-H, thus reduces the orientation and percentage of $Ca(OH)_2$ gathered at the interface and increases the interfacial performance. Consequently, the purpose of using silica fume is to cause more C-H-S at the interface to increase the interfacial strength and durability.

In previous study [12], an improvement in the interfacial shear strength were observed with the PCM modified with 5% silica fume compared to the normal PCM. The chemical bonding at the concrete-PCM interface with the inclusion of silica fume was difficult to understand due to the use of higher roughness levels of the concrete substrate, where mechanical bonding plays a dominant role. To understand it more precisely, in this study, concrete substrate with a smooth surface is used where mechanical bonding had less influence. Primers are also utilized to understand the effectiveness of silica fume with PCM as a repair mortar. It is thought that the use of primer can acts as a protective layer of the substrate concrete to resists penetration of moisture from the repair layer to the concrete substrate. Thus, silica fume in the repair layer cannot perform its function in expected way to improve interfacial performance (chemical reaction with free alkali in substrate concrete and silica compound in repair layer under water supplied condition and micro-filler effect). Conclusively, this research work is designed to study the effectiveness of modified 5% silica PCM as a repair material in forming a chemical connection at the interface based on direct single-surface shear test and splitting tensile strength test using smooth and rough concrete surface roughness, along with microstructure analysis using scanning electron microscopy (SEM), energy-dispersive X-ray spectroscopy (EDS), X-ray diffraction (XRD) and thermogravimeter-differential thermal analysis (TG-DTA) to quantitatively understand the formation of chemical connection at the interface.

2.2 Outline of the test

2.2.1 Materials and mix proportion of substrate concrete

Substrate concrete was fabricated by mixing a commercially manufactured high early strength cement having specific surface area of 4550 cm^2/g and density of 3.14 g/cm^3, crushed stone with a maximum size of 19 mm and true density of 2750 kg/cm^3, sand with 2.68 fineness modulus and true density of 2680 kg/cm^3, and water. A liquid of poly carboxylic acid with a density of 1.05 g/cm^3 was used as a water reducer. The proportion of concrete used in this study is shown in Table 2.1

Table 2-1 Mix proportion of substrate concrete

W/C (%)	Amount (kg/m^3)					Compressive strength (MPa)
	Water	Cement	Sand	Stone	Water reducer	
40	164	411	844	1045	8	37.84

2.2.2 Polymer cement mortar (PCM)

Polymers have been used in a wide range of applications in the construction industry to prepare cementitious and non-cementitious repair materials. Polymers, in the form of polymer concrete, polymer-modified concrete, or polymer impregnated concrete, are used in the repair of structures because of its superior properties to those of ordinary Portland cement [14]. PCM is prepared by mixing either polymers or monomers in a dispersed form with cement. In this study, polyacrylic acid ester (PAE) powder polymer mixed type commercially available PCM supplied by the company was used. The manufacturer mixed all the ingredient in specific ratio to fabricate PCM in such a way that, at the time of application, only the predetermined water amount is required to be added (water/PCM ratio of 15% used in this study as suggested by supplier) and the mixture becomes ready to be used. The polymers in PCM act as a micro-filler, resulting in lower permeability, which makes it possible to use thinner layers in construction and obtain better resistance to penetration of chloride ions and other environmental factors. Many types of polymers or monomers, such as redispersed polymer latex powder, water-soluble polymers, liquid resins, etc. have been used in the past to prepare PCM [15]. In this study, a commercially available polyacrylic ester (PAE) polymer was used.

2.2.3 Silica fume

In the last four decades, many studies have been conducted on the applications of silica fume in concrete as a partial replacement for cement. As supplementary material, silica fume is largely used to increase strength and ductility. In this study, commercially available silica fume with technical characteristic as presented in Table 2.2 is utilized as a modifier with PCM to increase the interfacial strength between the concrete and PCM. Silica fume has a micro-filler effect and fills the gaps between the cement particles because of its extreme fineness. It is also expected that the use of silica

fume will cause more chemical bonds in the interface. The use of silica fume in PCM causes a need for more water, as the high surface area and small particle size of silica fume demand more water. A small amount of silica fume results in less C-S-H at the interface, which does not satisfy the interface requirement, whereas material stagnation is caused by using a large amount of silica fume [16]. Based on the findings of previous studies [12], 5% silica fume of PCM mass with a water/binder ratio of 15% was used in this study. Following the outcome of trial flow test by the author and previous group research in our team [9], a superplasticizer (1% by mass of PCM) was used during the preparation of modified 5% silica PCM to prevent the formation of silica lumps, whereas superplasticizer was not used to prepare PCM without silica fume.

Table 2-2 Technical characteristics of silica fume

Appearance	Specific surface area (m^2/g)	Relative density (kg/m^3)	Specific gravity	Average particle size (μm)	pH
Grey ultrafine	15-30	150-700	2.2-2.3	0.15	7-8

2.2.4 Primer

Primers have been widely used as adhesives to increase the bonding performance of interfaces in repair systems. In this study, commercially available primer with technical characteristics as shown in Table 2.3 were utilized to understand the effectiveness of using silica fume with PCM as a repair mortar. The primer was brushed over the concrete surface by mixing with water in a 2:1 ratio before three hours of the casting of PCM, as suggested by the manufacturer. The application of primer over the concrete surface is shown in Figure 2.1(a).

Table 2-3 Technical characteristics of primer

Appearance	Main component	Solid content (%)	Density (g/cm^3)	Stickiness (mPa · s)	pH
Milky white liquid	Modified Vinyl Acetate-Ethylene Copolymer Emulsion	45-48	1.06	800-1200	4.5-6.5

2.2.5 Substrate concrete surface preparation

Considering ease and suitability, two roughness levels of concrete substrate (smooth and rough) were used in this study as shown in Figure 2.1(b). A retarder was sprayed over the concrete surface after casting the concrete to delay the hardening of concrete and to prepare the rough surface. The soft concrete surface was then sprayed with a strong jet of water until coarse aggregates were exposed to make the surface rough for better bonding. The smooth surface of substrate concrete was prepared by cutting cured concrete using a diamond saw. In general, the interface strength is affected by the mechanical interlock induced by a rough surface, whereas the smooth surface induced less mechanical interlocking. Thus, our initial thought to form more C-S-H at the interface by using silica fume in PCM can be evaluated by comparing the outcome of the composite specimens with rough and smooth surfaces, as mechanical bonding has less influence on smooth surfaces. The considered roughness level as shown in Figure 2.1(b) can be easily identified with visual inspection with minimal scattered roughness value. Thus, qualitative assessment based on the visual inspection was used to define the roughness level in this study rather than quantitative analysis that widely used by many researchers.

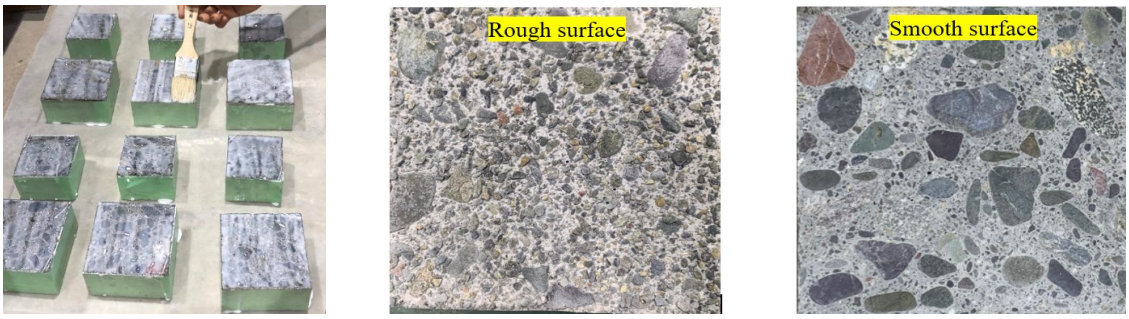

(a) Application of primer (b) Concrete substrate roughness level used in this research work

Figure 2-1 Treated surface of substrate concrete interface

2.2.6 Preparation of the composite specimens

The composite specimens were prepared by casting concrete and PCM on different dates having 14 days interval between pouring two materials. The time difference was chosen to allow prepared concrete using high early strength cement to attain its strength before repairing, to resemble existing concrete of the real infrastructure. The procedure of preparing the composite specimen for the splitting tensile test, as an example, is shown in Figure 2.2. After sufficient curing of half of the concrete specimens, the treated surfaces were kept facing up in the mould for the PCM application. The treated surfaces were cleaned with high-pressure air to remove dust before casting the PCM. After that, the concrete surfaces were wetted for 24 hours. At the time of casting, the free water from the top of the concrete surface was wiped with a towel to provide a saturated concrete substrate with a dry surface for adequate bonding. In past research [4-5, 17], it has been reported that prewetting results in better bonding. Therefore, attention was given to the wetness of the treated concrete surfaces before PCM application.

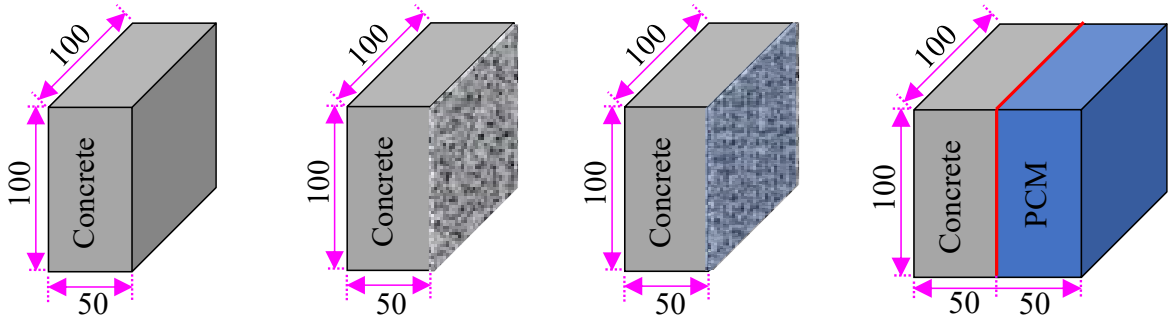

Figure 2-2 Composite specimen preparation procedure with primer for splitting tensile test (unit: mm)

PCM was cast over the treated concrete surfaces by trowelling to prepare composite specimens of sizes 100 cubic mm and 100x75x75 mm for splitting tensile and direct single-surface shear tests, respectively. After casting, specimens were covered with plastic sheets and wet cloths to maintain the moisture content. All the formworks were demoulded after 24 hours of casting and cured in water for 7 days to help the hydration process following by dry curing for 21 days. Curing under dry conditions benefits the formation of polymer films that can fill the voids and strengthen the PCM [17]. The total number of composite specimens cast for this research work is shown in Table 2.4.

Table 2-4 Numbers of specimens and types of tests performed

Repair material of composite specimen	Use of primer at the interface	Test type and roughness level of substrate concrete			
		Splitting tensile		Direct single-surface shear	
		Smooth (S)	Rough (R)	Smooth (S)	Rough (R)
NPCM	No	3	3	3	3
SPCM	No	3	3	3	3
NPCM with primer	Yes	3	3	3	3
SPCM with primer	Yes	3	3	3	3

Note: "NPCM" denotes normal PCM and "SPCM" denote PCM modified with 5% silica.

2.2.7 Testing procedure

The splitting tensile prism test was conducted in this study to determine splitting tensile strength which is widely used due to its ease of sample preparation, low variation in test results, and simple loading method. In general, the splitting tensile strength was measured by split tensile test on cylindrical specimens following ASTM C496 and using Equation 2.1. In this study, it was measured using cubical specimens according to the process described by Li [18], as shown in Figure 2.3(a). For even load distribution, steel strips of size 200x12x6 mm were used between loading plates and the corrected splitting tensile strength was calculated by incorporating the influence of the strip using Equation 2.2 [19]. To evaluate interfacial shear strength, many test methods have been proposed in

the past, as summarized by Santos [20]. The slant shear test has been adopted by some international codes [21], but there is no general agreement among researchers regarding the appropriateness of this test for non-resinous materials such as PCM [22]. The discussions of many in-house testing methods had been found, but these were not widely accepted due to their complex test setups. Single surface shear tests which were used in this study, have been widely used and developed to evaluate the interfacial shear strength due to their simple loading method. The scheme of the direct single-surface shear test is shown in Figure 2.3(b) and the strength was evaluated using Equation 2.3. Both tests were done with displacement control at a rate of 0.1 mm/min until the specimen failed using UTM.

$$f_{st} = \frac{2P_u}{\pi A} \tag{2.1}$$

$$f_{st}(\beta) = \frac{2P_u}{\pi A}\left[(1-\beta^2)^{\frac{5}{3}} - 0.0115\right] \tag{2.2}$$

$$\tau_{max} = \frac{P_u}{A} \tag{2.3}$$

where f_{st} is the split tensile strength (MPa); $f_{st}(\beta)$ is the corrected split tensile strength considering the effect of the strip (MPa), τ_{max} = maximum shear strength (MPa), P_u is the ultimate load (kN), A is the area of the specimen interface (m^2), and β is the ratio of the width of the strip to the height of the specimen.

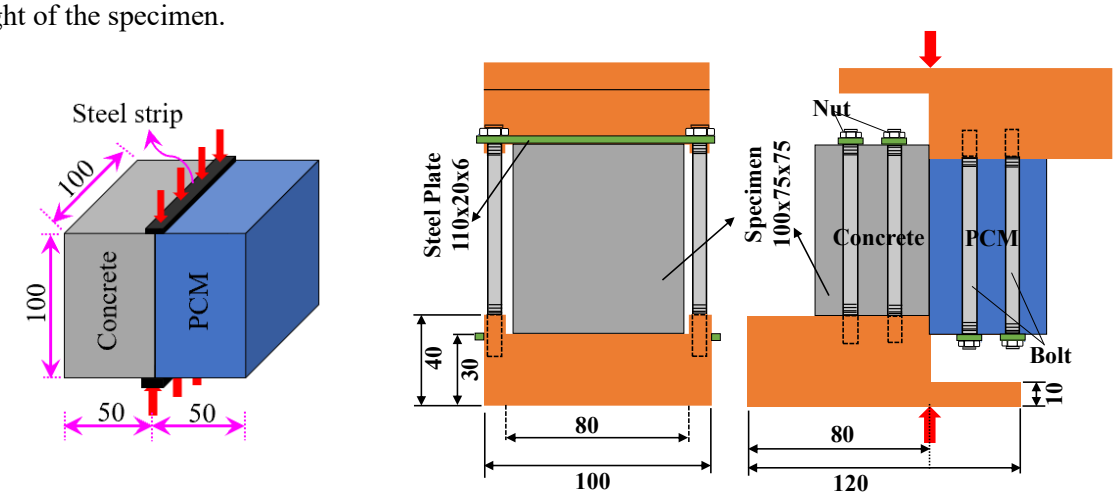

(a) Splitting tensile strength test (b) Direct single-surface shear test

Figure 2-3 Schematic diagram of the test performed with the loading condition (unit: mm)

2.2.8 Microstructure test

SEM-EDS was employed to identify the interfacial layer and to precisely understand the chemical bonding of the interface. A rectangular parallelepiped of size 15x15x5 mm including substrate concrete, PCM overlay, and substrate concrete-PCM interface was cut to fit the size into the SEM chamber as shown in Figure 2.4. The prepared samples were vacuumed for 7 days in a vacuum chamber to keep them dry. The specimen surface was coated with a platinum coating to enhance electrical conductivity and to get a high-quality interface image.

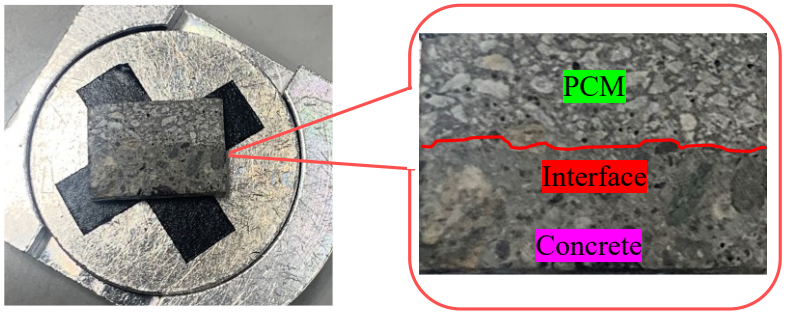

Figure 2-4 Composite specimen samples for SEM tests

XRD analysis of the samples (in the form of powder) collected from the interface after the loading tests were performed at 40kV and 40mA with a Cu-K alpha radiation source to identify the intensity of $Ca(OH)_2$ at the interface. In XRD analysis, a continuous 2θ scan mode from 10° to 75° was applied at a step size of 0.02 and scan speed of 1.5°/min. In addition, TG-DTA of the powdery samples collected from the interface were also performed up to 1000°C using platinum top-opened crucible with experimental conditions; N_2 gas dynamic atmosphere (60mL/min rate), heating rate (20°C/min) to quantitatively identify the amount of $Ca(OH)_2$ and $CaCO_3$ at the interface.

2.3 Test results and discussions

2.3.1 Maximum stress capacity

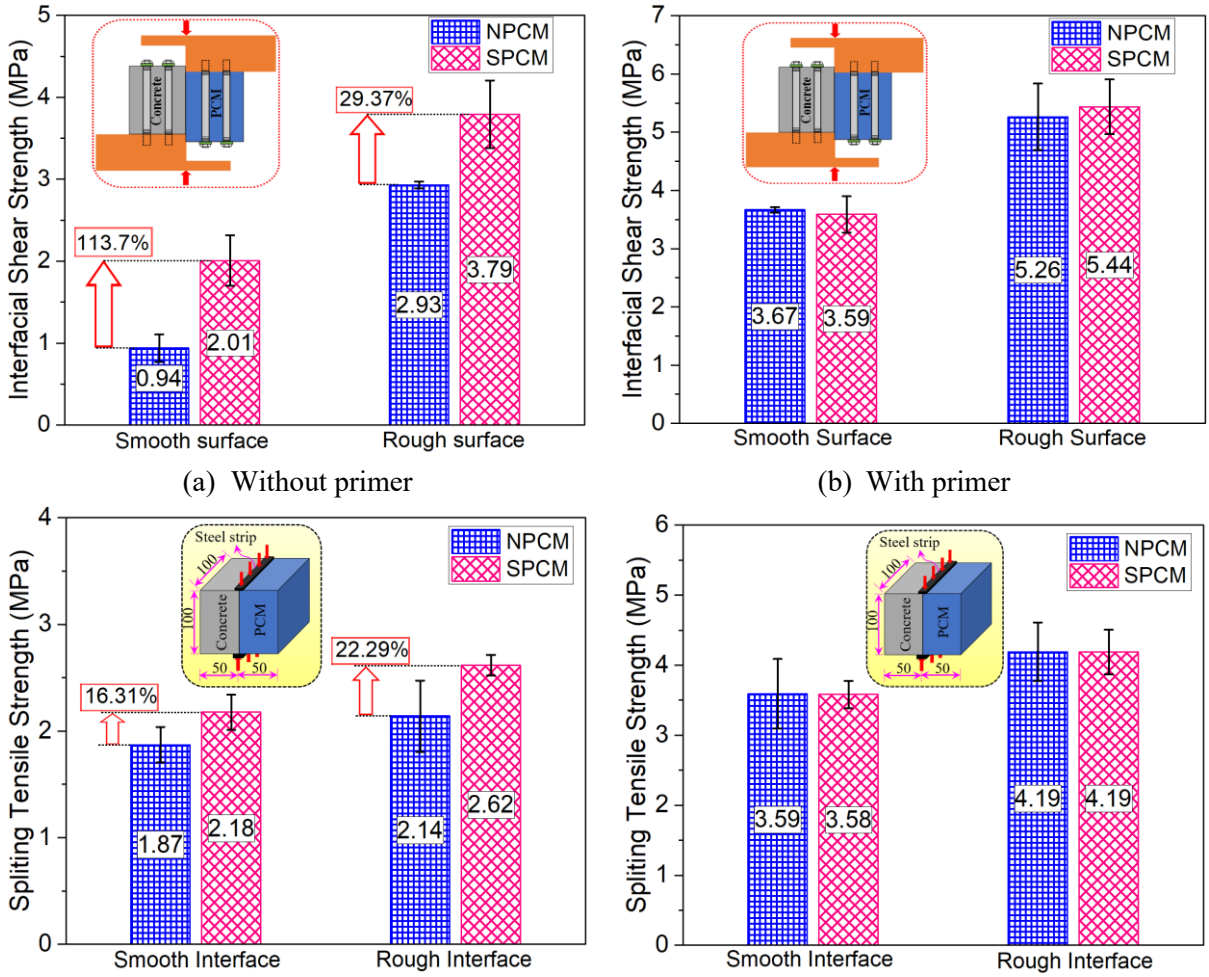

Figure 2-5 Influence of the addition of 5% silica fume to PCM on the interfacial bonding strength

The average strength of the three specimens was recorded as the interfacial shear strength under specific conditions and presented in Fig 2.5(a-b) with the standard deviation (SD). The average interfacial strength was calculated after excluding the data when the difference between any measured value and the mean value exceeded 20% of the mean value. The median value of the three specimens in each group is taken as the mean value. Large variations in SD and COV (1.24% and 17.87%) was observed in this study due to variability of cementitious composites, which was also observed in previous study [23-24]. The silica fume inclusion greatly increased the interfacial strength compared to the normal PCM (without primer cases), as shown in Figure 2.5(a). An increase of interfacial strength with the smooth surface where mechanical bonding had less influence indicates a higher possibility of causing a chemical reaction at the concrete-PCM interface with silica fume addition. In the case of the primer used at the interface, only a slight variation in the interfacial strength for the NPCM and SPCM cases was observed, as shown in Figure 2.5(b), which can be considered as

experimental scatter. The use of primer at the interface results in a protective layer that prevents the small silica fume particles from filling the gaps among the cement particles of the substrate and hinders the flow of the water required for hydration to the cured concrete, thus, silica fume cannot perform in the expected way to strengthen the interface by the micro-filling effect or by chemical connection. Considering the negative impact of primer on the environment and the positive influence of silica fume (no primer cases) for enhancing concrete-PCM interface bonding, the inclusion of silica fume with overlay material is suggested in practical application.

The average interfacial tensile strength of the three specimens, after excluding data when the difference between any measured value and the mean value exceeded 20% of the mean value, is shown in Figure 2.5(c-d). The measured coefficient of variance ranged between 3.711% and 13.82%, which is within the considerable range for cementitious composites. The constituent of the overlay material attached to the concrete substrate has an insignificant influence on the interfacial performance in the case of primer used at the interface, whereas it has a significant influence in the case of no primer at the interface. The improvement of the bond strength occurs because of chemical reactions of $Ca(OH)_2$ with pozzolans. Additionally, silica fume particles can fit between cement particles and inside pores on the surface of the concrete, resulting in a denser microstructure with higher intermolecular forces and mechanical interlocking. Consequently, the bond strength increases significantly with the inclusion of silica fume.

2.3.2 Effect of surface roughness level

Many available reports [25-27] have discussed and concluded that the surface roughness treatment is significantly enhanced interface bonding between the concrete and overlay materials. The positive influence of the surface roughness level on the interfacial bonding performance is also confirmed in this study. The percentage increase of the interfacial shear strength and splitting tensile strength in both normal PCM and modified 5% silica CPM cases with different surface roughness levels is shown in Figure 2.6(a) and Figure 2.6(b), respectively. The interfacial strength is very sensitive to the variation in the surface roughness of the concrete substrate. This is likely because the area of contact between the substrate and overlay material primarily affects the bond failure mechanism, and an increase in the contact surface area increases the interfacial performance. The surface contact area is larger on a rough surface, which results in greater bonding strength than on a smooth surface. Consequently, the surface roughness level greatly influences the interfacial bonding performance in both the normal PCM and PCM modified with 5% silica cases.

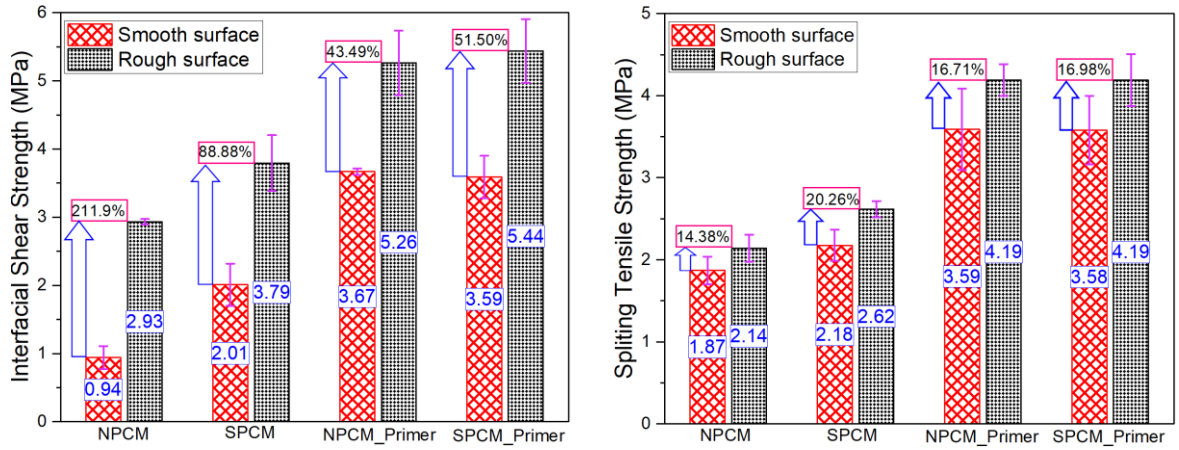

(a) Direct single surface shear test (b) Splitting tensile test

Figure 2-6 Interfacial strength with different surface roughness levels

2.3.3 Fracture modes of the composite specimens

2.3.3.1 Definition of the fracture mode

The fracture modes are named by identifying the fracture location on the surface of the composite specimens. A fracture mode was named concrete cohesion (C) or PCM cohesion (P) when a fracture occurred either in the concrete substrate or in the PCM part, while an interface fracture

mode (I) was named when a fracture occurred purely through the interface, with or without tiny cracks in the concrete or PCM. Composite fracture modes include partial concrete partial adhesive (I-C) fracture modes, in which some amount of concrete substrate or coarse aggregate attached on the PCM side; partial PCM partial adhesive (I-P) fracture modes, when some PCM is attached to the concrete substrate; and mixed concrete and PCM (C-P) fracture modes, where the fracture occurs in both the concrete and the PCM layer. The possible fracture modes of the composite specimens are shown in Figure 2.7.

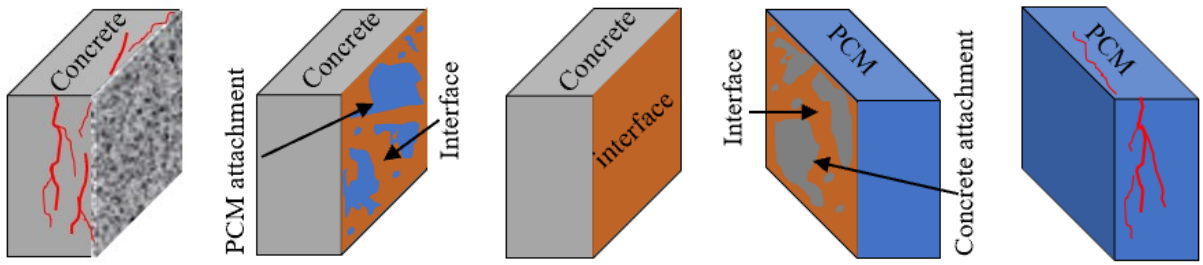

Figure 2-7 Classification of the fracture surface of the composite specimens

2.3.3.2 Observed fracture modes in the composite specimens

Visual observations were made carefully during and after the tests of the composite specimens to determine whether the specimens failed along with the shear plane (interface) or the fracture was due to significant cracking in the overlay or concrete substrate. Examples of adhesive and composite fracture modes of the composite specimens observed in this study are shown in Figure 2.8(a-d).

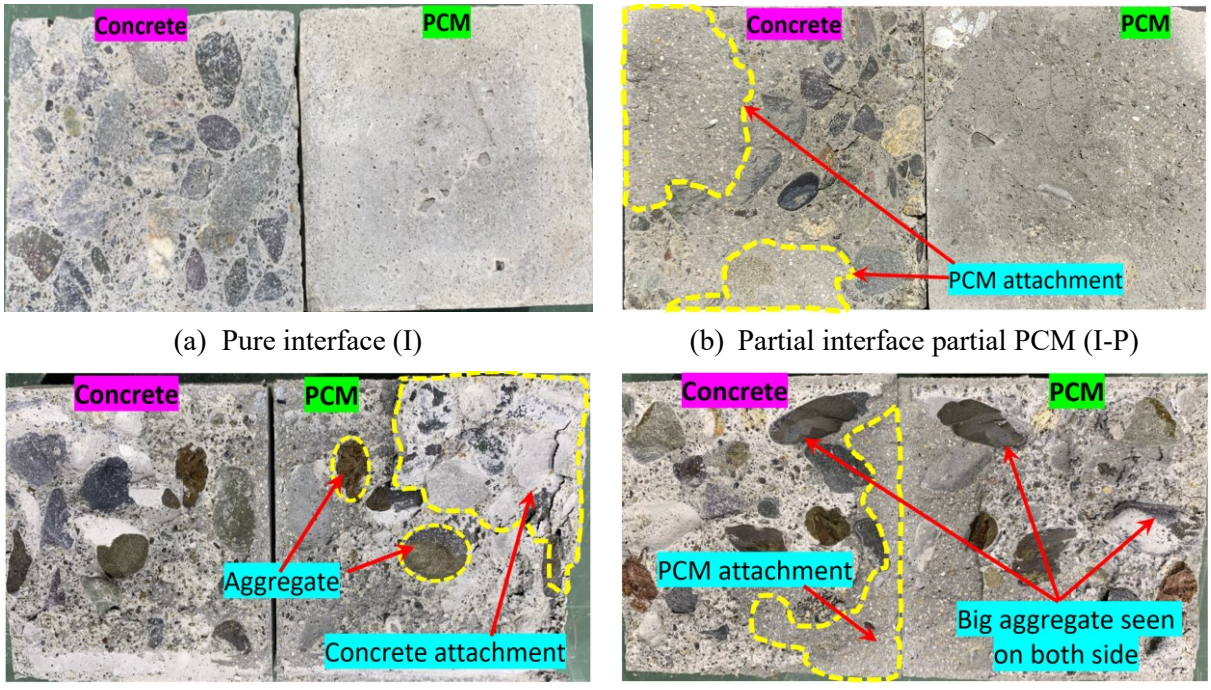

Figure 2-8 Sample fracture surfaces of the composite specimens

The direct single-surface shear test results indicate that the fracture modes of the composite specimens with normal PCM included pure interface fractures (I) irrespective of the surface roughness level, as shown in Figure 2.9(a). The specimen with 5% silica PCM exhibited two cases of composite or mixed fracture mode, such as (I-P) or (C-P), and only one pure interface fracture (I). This result indicated that the inclusion of silica fume enhanced the interfacial performance and shifted the pure interface fracture mode to a composite or mixed fracture mode. The splitting tensile test results for the

composite specimens with normal PCM also exhibited pure interface fracture (I) irrespective of the surface roughness level, while the specimens with 5% silica PCM did not include any pure interface fractures (I), as shown in Figure 2.9(b). All the 5% silica PCM specimens showed composite or mixed fracture modes, such as (I-C), (I-P), or (C-P). The fracture modes differed among the three specimens with the same conditions due to the composite nature of the concrete and PCM. The positive influence of the inclusion of 5% silica fume in the PCM can be attributed to the chemical reactions between the active SiO_2 in the PCM and $Ca(OH)_2$ in the substrate concrete to form secondary C-S-H. Because of the secondary chemical reactions of $Ca(OH)_2$ and pozzolans, the microstructure of the interface can improve with time, leading to the creation of a denser interfacial zone with better durability. Consequently, mixing silica fume with PCM enhances the interfacial performance and shifts the fracture mode from pure interfacial to composite or mixed-mode fracture in both splitting tensile and direct shear tests.

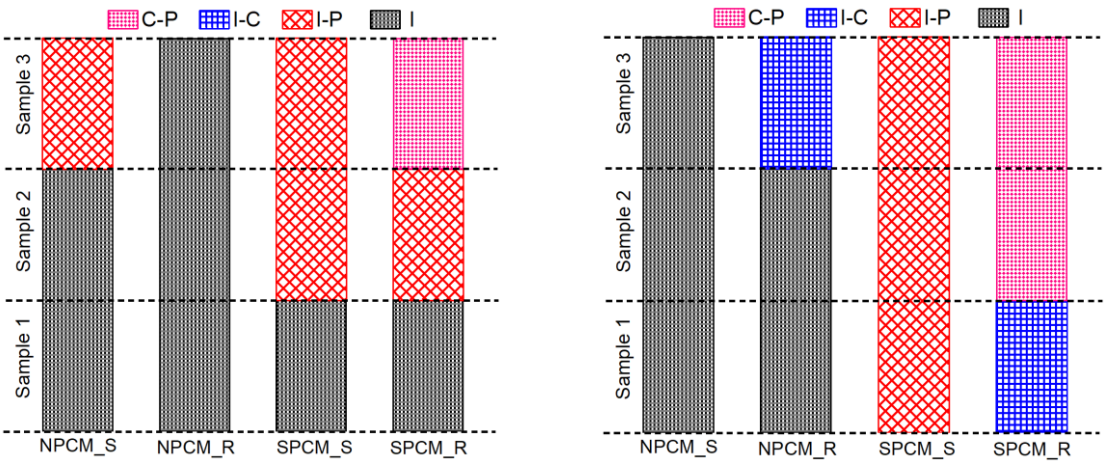

(a) Direct single-surface shear test (b) Splitting tensile test

Figure 2-9 Influence of silica fume on fracture modes of composite specimens (without primer)

2.3.4 Fracture energy

The fracture energy was obtained from the area under the load-displacement curve. As an example, the load-displacement relationship of the specimens tested under shear and tensile stress condition with smooth and rough surface, respectively are shown in Figure 2.10(a-b). For the other conditions, the corresponding load-displacement relationships were also similar; thus, these are omitted here.

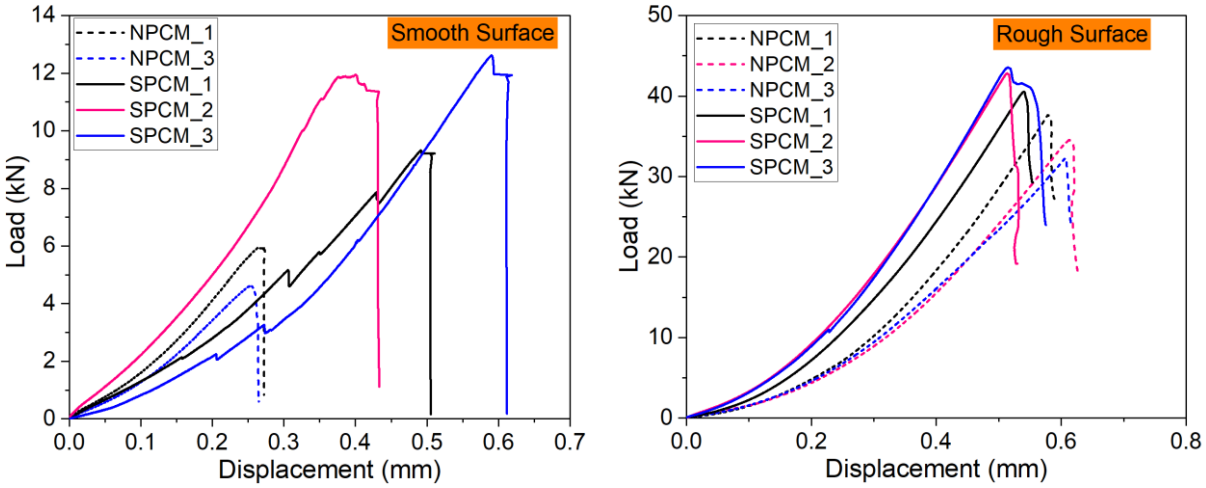

(a) Single-surface shear test (without primer) (b) Splitting Tensile test (without primer)

Figure 2-10 Load-displacement relationship of the normal and modified 5% silica PCM specimens

The fracture energy was calculated considering the ascending and descending branches of the load-displacement diagram, in cases there is sudden drop of load value after peak load. When there is gradually decreasing tendency after the peak, it was calculated considering the ascending branch up to the peak stress level. In such cases, stress shifts from the interface to the concrete or PCM part and continues loading even though the interface has a crack, causing an impure fracture. The calculated shear and tensile fracture energies of all the composite specimens along with the corresponding fracture mode are shown in Figure 2.11(a-d). The pure interface (I) fracture corresponds to lower fracture energy, whereas the concrete (C) or PCM (P) cohesive or concrete-PCM (C-P) mixed fracture mode corresponds to higher fracture energy.

The constituent of the overlay material attached to the concrete substrate influenced the calculated shear and tensile fracture energy in no primer cases, as shown in Figure 2.11(a) and Figure 2.11(c), respectively. The composite specimen with PCM modified with 5% silica fume has a shear fracture energy that is approximately 5 times and 2.5 times greater compared to the normal PCM for smooth and rough interfacial surfaces, respectively. The tensile fracture energy also increased by a factor of approximately 2 times in the PCM modified with 5% silica fume compared to the normal PCM. On the other hand, in the case of primers used at the interface, the shear and tensile fracture energies seem almost similar under particular conditions, indicating that the constituent of the overlay material attached to the concrete substrate does not influence the fracture energy consumption, as shown in Figure 2.11(b) and Figure 2.11(d), respectively. Consequently, it can be said that the fracture energy increases with the inclusion of silica fume, which also affects the fracture mode of the composite specimens.

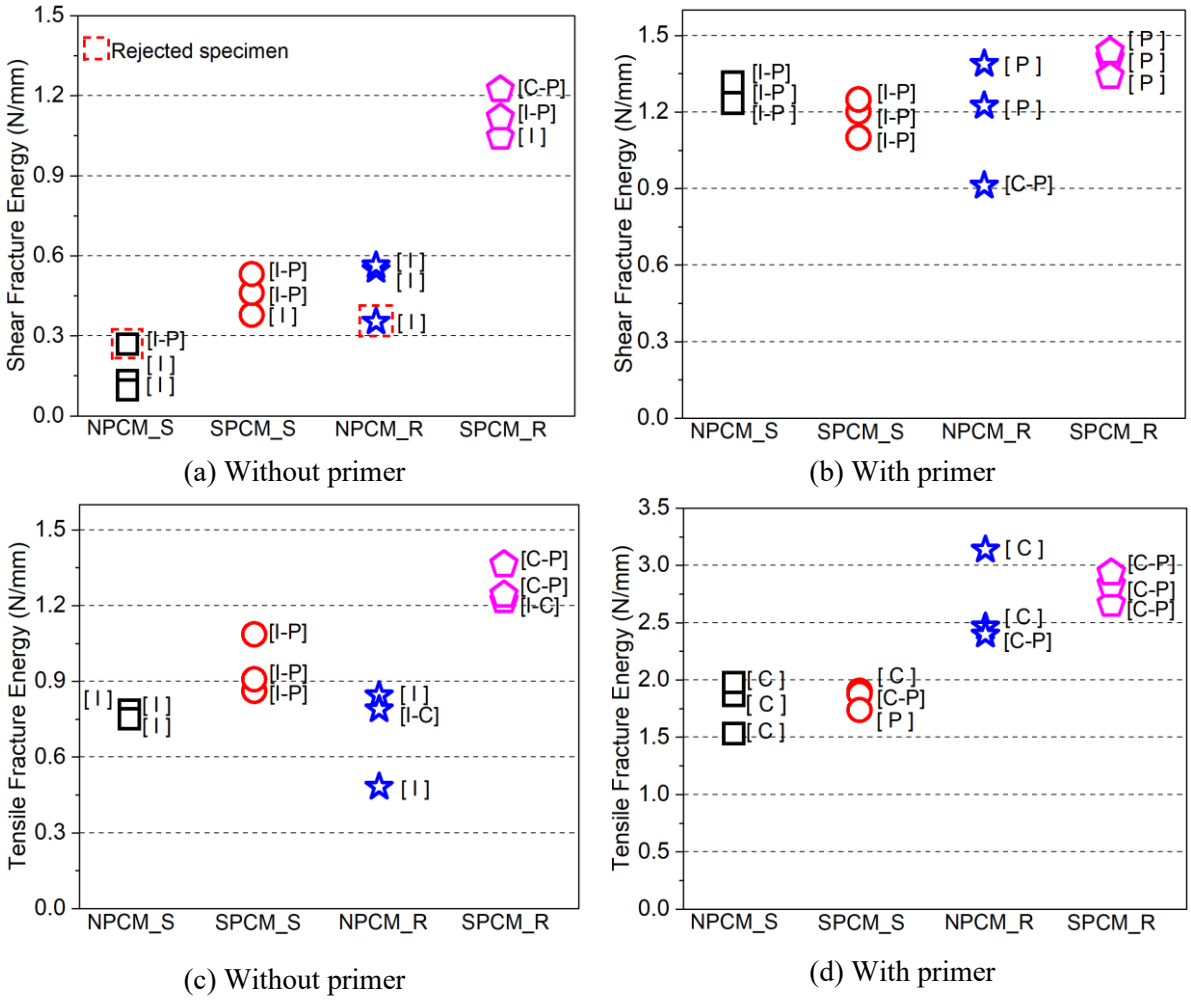

Figure 2-11 Fracture energy of all the composite specimens with fracture modes

2.3.5 Microstructural analysis

SEM-EDS (JSM-6510LA) was employed to explore the microstructure of the interfacial layer of the composite specimens. The SEM images was further analyzed using EDS attached in the SEM to precisely identify the interface and for quantitative elemental analysis. The EDS uses an X-ray source for the identification and quantification of the element present at detectable concentrations. The prepared sample for this microstructure analysis contains both concrete and PCM parts with different elemental compositions. Therefore, EDS results of particular element distribution over a selected area help to identify the interface precisely as the EDS technique is capable of producing relative elemental distribution maps using different color index as presented in Figure 2.12(a-b).

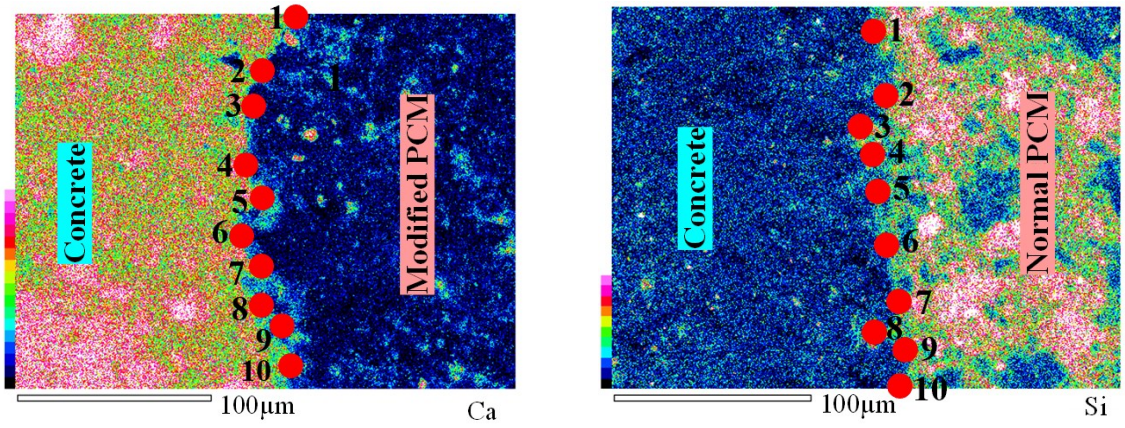

(a) Modified 5% silica PCM (b) Normal PCM

Figure 2-12 Element distribution using EDS over a selected area at 500 magnification level (X500)

The mapping of elemental distribution of all the element mentioned in Table 2.5 were observed over a selected area using EDS technique. The specific area was selected assuming it contains all the three phases of the composite specimens: concrete substrate, repair material, and the interface between them. The three phases of the composite specimen were easily identifiable by looking at the mapping of the elemental distribution of all the element. As an example, the relative distribution of "Ca" for modified 5% silica PCM specimen and "Si" for normal PCM specimen is presented in Figure 2.12(a-b). The blue color reflects lower concentration of specific element i.e presence of Ca in repair part [Figure 2.12(a)] and Si in concrete part [Figure 2.12(b)], whereas reddish color indicates higher concentration i. e presence of Ca in concrete part [Figure 2.12(a)] and Si in repair part [Figure 2.12(b)]. As PCM and Concrete part has different elemental composition, it was clearly identifiable the interface seeing the elemental distribution map.

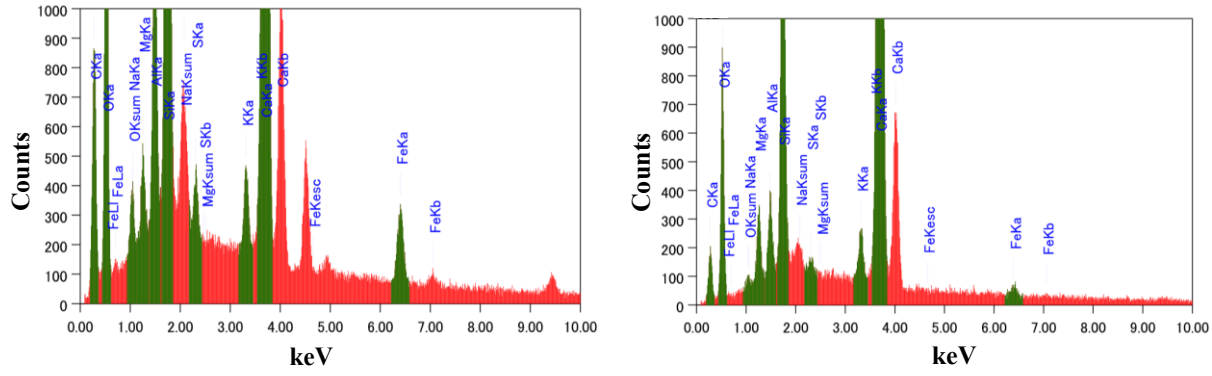

(a) Normal PCM (b) Modified 5% silica PCM

Figure 2-13 EDS elemental spectrum at a specific point along the interface of composite specimen

Once the three phases of the composite specimen were confirmed, the interface was further analyzed to record the elemental information using EDS that can detect the element with a concentration up to 0.1 wt%. In this study, the EDS was performed to know the elemental information of the interface layer by selecting points along the bond line (interface layer). Ten different points

were selected along the interface for the elemental analysis as presented in Figure 2.12(a-b) and the average value of ten EDS measurements was recorded as the concentration of the particular element at the interface. Typical examples of EDS elemental spectrum at a specific point along the interface of normal PCM specimen and modified 5% silica PCM specimen, are shown in Figure 2.13(a-b) respectively and the average quantification results of ten EDS spectrum are tabulated in Table 2.5.

Table 2-5 EDS elemental quantification results

Element	Normal PCM		Modified 5% silica PCM	
	Weight%	Atomic%	Weight%	Atomic%
O	44.38	59.86	43.55	53.67
Fe	0.82	0.32	2.36	0.83
Mg	1.46	1.30	0.66	0.54
Al	1.17	0.94	2.20	1.61
Si	7.20	5.53	9.57	6.72
K	0.74	0.41	0.55	0.28
Ca	37.53	20.21	23.95	11.78
C	6.10	10.96	13.89	22.81

The Ca to Si (C/S) ratio is an indirect measure of C-S-H and calcium hydroxide (CH). A high C/S ratio implies that it has high CH and low C-S-H, and vice versa [28]. It is common knowledge that the interface with high C-S-H results in high strength. The C/S value at the interface is calculated from the EDS elemental quantification result shown in Table 2.5, which is 5.21 at the interface of normal PCM specimen and 2.5 at the interface of modified 5% silica PCM specimen. As a trial basis, the elemental distribution in inside of PCM (both normal and modified 5% silica PCM) were performed and it was found that C/S ratio in the inside of PCM (both normal and modified 5% silica PCM) was lower than that of at the interface in corresponding cases. The results of C/S value at the interface reflects that there is a high possibility of formation of more C-S-H at the interface with silica fume inclusion with PCM.

The observed XRD pattern were analyzed with standard compiled Profex software (v-4.2.3) to identify $Ca(OH)_2$ phase. The XRD results of modified 5% silica PCM and normal PCM specimen is presented in Figure 2.14 which indicates some qualitative differences in the hydration rate due to the incorporation of silica fume in the repair material. For the comparison between two samples, the peak intensity in the region of $2\theta = 18°$ has been considered as a measurement of the intensity of $Ca(OH)_2$ [29-30]. Lower peak intensity for $Ca(OH)_2$ was found in modified 5% silica specimen compared to normal PCM specimen (Figure 2.14). Conclusively, the inclusion of silica fume caused a decrease of $Ca(OH)_2$ content at the interface, thus, contributing to the improvement of the interfacial performance.

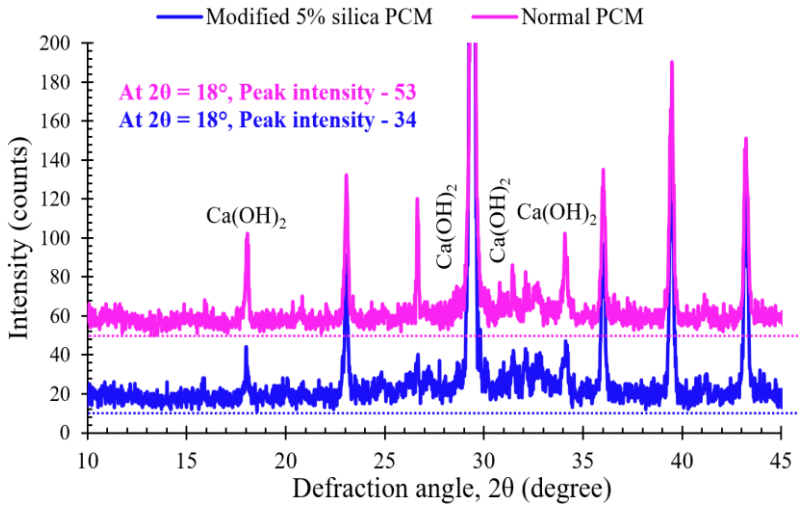

Figure 2-14 XRD pattern of powdery sample collected from the interface of the composite specimen

Figure 2.15 showed the TG-DTA curve of the powdery samples collected from the interface of modified 5% silica PCM and normal PCM specimen. TG-DTA curves show the typical reactions occurring in the cement mortars when subjected to a progressive temperature increase from room temperature to 1000 °C. The mass loss % of the samples, including the control during TG analysis occurred in three main steps: dehydration of water molecules in hydrates such as C–S–H and ettringite (first step), dihydroxylation of calcium hydroxide (second step) and decarbonation of $CaCO_3$ and escape of CO_2 from the cement matrix (third step) [31-35]. The mass loss % in TG at different steps was calculated following corresponding DTA peak and presented in Figure 2.15.

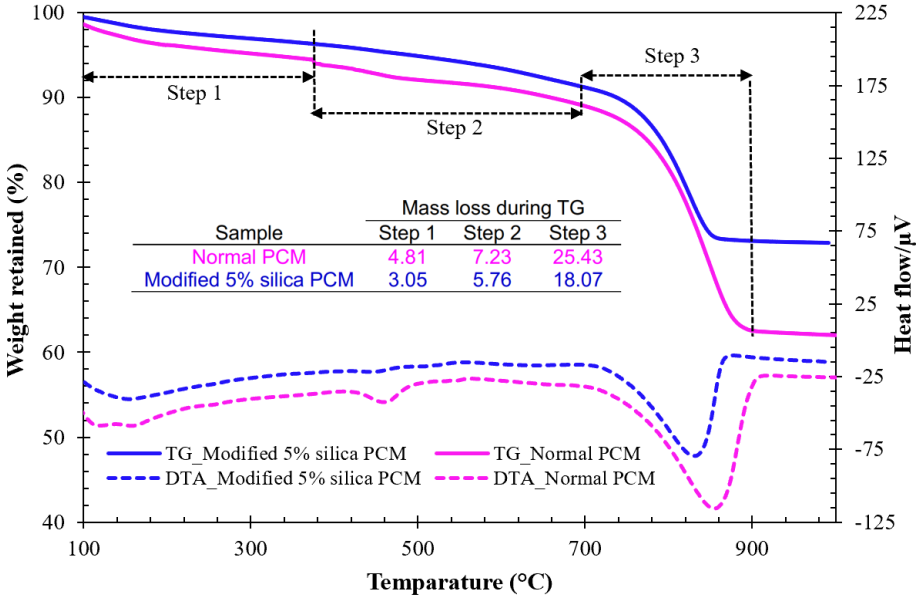

Figure 2-15 TG-DTA curve of the sample collected from the interface of composite specimen

As mentioned in the literature [10], the mass % of $Ca(OH)_2$ and $CaCO_3$ in the samples were calculated by multiplying molar mass ratios of $Ca(OH)_2/H_2O$ and $CaCO_3/CO_2$ with the corresponding mass loss obtained in the second and third steps of TG curves (Figure 2.15) and presented in Table 2.6. The amount of both free $Ca(OH)_2$ and $CaCO_3$ was found higher in the normal PCM cases compared to modified 5% silica PCM cases. This finding indicates an increase in the extend of bond formation between silica compound and free $Ca(OH)_2$ (modified 5% silica PCM cases) compared to the bond formation in without silica fume (normal PCM) cases.

Table 2-6 Mass % of $Ca(OH)_2$ and $CaCO_3$ at the interface of normal and modified 5% silica PCM

Sample	Second Step of TG Mass % of $Ca(OH)_2$	Third step of TG Mass % of $CaCO_3$	Total mass % of $Ca(OH)_2$ and $CaCO_3$
Modified 5% silica PCM	23.68	41.07	64.75
Normal PCM	29.73	57.80	87.53

2.4 Conclusions

The following conclusions can be drawn from this experimental investigation:

- In the absence of primer at the substrate concrete interface: (i) The effect of the constituents of the overlay material attached to the concrete substrate on the bond strength is significant. The modified 5% silica PCM specimen showed stronger bonding strength than the normal PCM specimens. The inclusion of silica fume significantly increases the interfacial shear and tensile strength for both smooth and rough concrete surfaces; (ii) Surface preparation (texture) significantly affects bond strength. The interfacial shear strength and splitting tensile strength increase with increasing surface roughness for both the normal PCM and PCM modified with 5% silica cases; (iii) The mixing of silica fume in the PCM shifts the interfacial fracture (I) with lower fracture energy to a composite fracture mode (I-P) or (I-C) or mixed (C-P) fracture mode with higher fracture energy.

- With primed substrate concrete surface, the interfacial bond performance does not depend on the inclusion of silica fume with PCM as primer act as a protective layer and hinders the functionality of silica fume.
- Lower C/S ratio observed through microscopic SEM-EDS test at the modified 5% silica PCM-concrete interface implies high C-S-H contents that results in high strength. This is mainly due to the transformation of harmful $Ca(OH)_2$ into a large amount of C-S-H, which indicates the possibility of formation of chemical connection at the modified 5% silica PCM-concrete interface.
- A decrease in the $Ca(OH)_2$ content observed qualitatively through XRD analysis and quantitatively through TG-DTA at the modified 5% silica PCM-concrete interface compared to normal PCM-concrete interface. This suggests an increase in the extend of bond formation between silica compound and free $Ca(OH)_2$ (modified 5% silica PCM cases) compared to the bond formation in without silica fume (normal PCM) cases, thus, contributing to the improvement of the interfacial performance in former cases.

In conclusion, the use of silica fume can achieve adequate bond strength with concrete substrate and there is a higher possibility of chemical reaction at the concrete-PCM interface with silica fume addition that can enhance the chemical bonding between the concrete substrate and overlay material. Considering easy applicability of silica fume with PCM in practical application, environmentally friendly nature and ability to achieve adequate bond strength with concretes substrate, this study can provide an indication for engineering application of silica fume in polymer cement-based repair materials.

References

[1] Rashid, K., Ueda, T. and Zhang, D., (2016). "Study on Shear Behavior of Concrete-polymer Cement Mortar at Elevated Temperature." Civil Engineering dimensions, 18(2), 93-102.

[2] Rifadli, B., Shinichi, F., Kohei, Y. and Atsuya, K., (2015). "Flexural strengthening effect of CFRP strand sheet and PCM on RC beams." Proceedings of Japan Concrete Institute, 37(2), Japan.

[3] Satoh, K. and Kodama, K., (2005). "Central peeling failure behavior of polymer cement mortar retrofitting of reinforced concrete beams." *Journal of Materials in Civil Engineering*, 17(2), 126-136.

[4] Zhang, D. (2009). "Research on PCM-Concrete Interface and PCM-Strengthened RC Beam." Doctoral Thesis, Hokkaido University, Japan.

[5] Rashid, K. (2016). "Behaviour of Interface between concrete-PCM at elevated temperature at material and member level", Doctoral Thesis, Hokkaido University, Japan.

[6] Espeche, A. D. and Leon, J. (2011). "Estimation of Bond Strength Envelopes for Old to New Concrete Interfaces based on a Cylinder Splitting Test." Construction and Building Materials, 25(3): 1222-35.

[7] Das, K. (2012). "The effect of Silica Fume on the Properties of Concrete as Defined in Concrete Society Report 74, Cementitious Materials." 37th Conference on Our World in Concrete and Structures, Singapore.

[8] Kurdowski, W. and Nocun-wczelik, W. (1983). "The tricalcium silicate hydration in the presence of active silica." Cement and Concrete Research, 13(3), 341–348.

[9] Sugawara S., Koizumi T., Harada S. and Okazawa K. (2007). "Effect of reaction ratio of silica fume on strength development of 150N/mm^2 class concrete." Concrete Research Technology, 18(95).

[10] Gao, J. M., Qian, C. X., Wang, B. and Morino, K., (2002). "Experimental study on properties of polymer-modified cement mortars with silica fume." *Cement and Concrete Research*, 32(1), 41-45.

[11] Jiang, C. H., Zhou, X. B., Huang, S. S. and Chen, D., (2017). "Influence of polyacrylic ester and silica fume on the mechanical properties of mortar for repair application." *Advances in Mechanical Engineering*, 9(1), 1-10.

[12] Hayato, S., Mahmudul, H. M., Ueda, T., Katsuichi, M. and Jun, T. (2019). "A study on the effect of silica fume and surface penetrant on bonding strength for overlaying." Journal of Asian Concrete Federation, 5(1):1-14.[31].

[13] Xie, H., Li, G. and Xiong, G. (2002). "Microstructure model of the interfacial zone between fresh and old concrete." Journal of Wuhan University of Technology (Material Science Edition), 17(4), 64-68.

[14] Fowler, D. W. (1992). "Polymers in Concrete: A Vision for the 21st Century." Cement and Concrete Composites, 21(5-6):449-52.

[15] Brien, J. V. and Mahboub, K. C. (2013). "Influence of polymer type on adhesion performance of blended cement mortar." International Journal of Adhesion and Adhesives, 43: 7–13.

[16] Kanezuka, T., Ito, M., and Katori, K. (2005). "Fresh state, strength, and structure system by changing the ratio of mixing silica fume." An investigation by SOC Group.

[17] Ohama Y. (1995). "Handbook of polymer-modified concrete and mortars-properties and process technology." New Jersy: Noyes Publications.

[18] Li, G., Xie, H., and Xiong, G. (2001). "Transition zone studies of new-to-old concrete with different binders." Cement and Concrete Composites, vol. 23: 381–387.

[19] Rocco, C., Guinea, G.V., Planas, J., and Elices, M. (1999). "Size effect and boundary conditions in the Brazilian test: experimental verification." Materials and Structures, 32(3): 210–7.

[20] Santos, P. M. D. and Julio, E. N. B. S., (2011). "Factors affecting bond between new and old concrete." ACI Materials Journal, 108(4), 449-456.

[21] Saldanha, R., Julio, E., Dias-da-Costa, D. and Santos, P., (2013). "A modified slant shear test designed to enforce adhesive failure." *Construction and Building Materials*, 41, 673-680.

[22] Li, S., Geissert, D.G., Li, S.E., Frantz, G.C. and Stephens, E.J. (1997). "Durability and bond of high-performance concrete and repaired Portland cement concrete." Joint Highway Research Advisory Council, Project JHR 97- 257, University of Connecticut.

[23] Shuling, G., Xiaochong Z., Jinli, Q., Yadong, G. and Guanhua, H. (2019). "Study on the bonding properties of Engineered Cementitious Composites (ECC) and existing concrete exposed to high temperature." Construction and Building Materials, 196: 330–344.
[24] Alireza, V., Azadeh, J. J., Islam M. M. and Atorod A. (2020). "Experimental evaluation of concrete-to-UHPC bond strength with correlation to surface roughness for repair application." Construction and Building Materials, 238: 1–11.
[25] Sahmaran, M., Yücel, H. E. and Yildirim, G. (2013). "Investigation of the bond between the concrete substrate and ECC overlays." Journal of Materials in Civil Engineering, 26 (1): 167–174.
[26] Yu, J. T., Xu, W. L. and Zhang, Y. M. (2015). "Experiment study on fracture property of ECC-concrete interface." Journal of Building Materials and Structures, 18(6): 958–963.
[27] Wang, B., Xu, S. and Liu, F. (2016). "Evaluation of tensile bonding strength between UHTCC repair materials and concrete substrate." Construction and Building Materials, 112:595-606.
[28] Zhifu, W. (2011). "Interfacial shear bond strength between old and new concrete." Master Thesis, Louisiana State University, Louisiana.
[29] Afridi, M., Ohama, Y., Iqbal, M.Z. and Demura, K. (1989). "Behavior of $Ca(OH)_2$ in polymer-modifed mortars" *The International Journal of Cement Composites and Lightweight Concrete*; 11(4):235-244.
[30] *Alessandra, E. F. A. and Eduvaldo, P. S.* (2006). "Thermogravimetric Analyses and Mineralogical Study of Polymer Modified Mortar with Silica Fume." Materials Research, Vol. 9, No. 3, 321-326.
[31] Senff, L., João, A.L., Victor, M.F., Dachamir, H. and Wellington, L.R. (2009). "Effect of nano-silica on rheology and fresh properties of cement pastes and mortars" *Construction and Building Materials*; 23(7):2487-2491.
[32] Ashraf, M., Naeem, K. A., Ali, Q., Mirza, J., Goyal, A. and Anwar, A.M. (2009). "Physico-chemical, morphological and thermal analysis for the combined pozzolanic activities of minerals additives." *Construction and Building Materials*, 23, 2207-2213.
[33] Wongkeo, W. and Chaipanich, A. (2010). "Compressive strength, microstructure and thermal analysis of autoclaved and air cured structural lightweight concrete made with coal bottom ash and silica fume*." Materials Science and Engineering*. 527, 3676-3684.
[34] Aly, M., Hashmi, M.S.J., Olabi, A.G., Messeiry, M., Abadir, E.F. and Hussain, A.I. (2012). "Effect of colloidal nano-silica on the mechanical and physical behavior of waste-glass cement mortar*." Materials Design*, 33, 127-135
[35] Hasan, B. and Nihal, S. (2014). "Comparative Study of the Characteristics of Nano Silica, Silica Fume and Fly Ash–Incorporated Cement Mortars", *Materials Research*; 17(3): 570-582

Chapter 3
ASSESMENT OF CONCRETE-PCM BONDING PERFORMNACE WITH INCLUSION OF SILICA FUME UNDER OVERLAYING CONDITIONS

3.1 Introduction

It was concluded from previous chapter that the use of silica fume with PCM as a repair material can achieve adequate bond strength with concrete substrate and there is a higher possibility of chemical bonding between the concrete substrate and overlay material with silica fume addition to enhance interfacial performance. Although modified PCM with silica fume addition as repair material has been found to possess good mechanical and chemical properties, there is absence of information of the influence of various factors on the concrete-PCM interface. As reported in the technical literature [1], the bonding between substrate concrete and repair material is highly influenced by various factors such as surface roughness preparation techniques, temperature, moisture contents, strength and stiffness of substrate concrete and overlay material, etc. Therefore, with present data and scope, it is hard to confirm the applicability of this overlaying method using silica fume with PCM as a repair material in practical strengthening cases. For practitioners better understanding and with an aim to achieve the great potential in practical design implications of the PCM overlay strengthening method, new work was designed and presented in the following sections exploring the effect of various factors on the concrete-PCM interfacial bond performance.

A lot of experimental study have been found in the technical literature [2-5] that emphasized on the importance of substrate concrete surface preparation and the effect of roughness for the good bonding of repairing material to the substrate concrete. The roughness level of substrate concrete highly influences the interfacial strengths as because the higher roughness level produce a larger surface area than the lower roughness level for the PCM attachment. Water jetting and sand-blasting techniques are considered to be the most suitable techniques for roughening the substrate concrete [6-7] to produce good bond as these methods generates less micro-cracks in substrate layer, whereas grinding [8] and the needle-gun [9] method of surface preparation result into lower bond strength. In the experimental study by Miura [10], it was found that the interfacial shear strength increased with the increase of surface roughness (from grinding to high sand blasting techniques). The moistness state of substrate concrete interface [11-13] and compressive strength of substrate concrete [14-16] is also regarded as one of the important factors in achieving bond between two layers. It was reported in a study [17] that too much dry surface of substrate concrete absorb water from the newly overlaid material, while excessive moisture in substrate concrete clog the pores and prevent absorption, resulting into weaker bond strength. Thus, many researchers suggested to consider the saturated surface dry condition in order to attain good bonding strength. Zhang [18] investigated the effect of the difference between the compressive strengths of PCM and substrate concrete, it was found that the interface bond strength decreases with increase in the difference of the compressive strength for a given kind of PCM. In case of compatible strength between concrete and PCM, fracture in the PCM side or interfacial fracture are most likely to occur. Hence, the substrate concrete surface should be roughened enough to ensure the aggregate interlock phenomenon to act.

For the successful strengthening technique, it is also important to withstand the induced stress by the continuous traffic movement during/after the construction work from the early stages as the PCM overlaying method enables its construct without preventing traffic. As far as the author's reviewed literatures are concerned, not many study have been found evaluating the performance of the interface from the early stages of overlay material application. In general, silica fume is expected to perform better in long run. Therefore, it is essential to evaluate the performances of silica fume to enhance the interfacial strength at early stages.

Although different factors have an impact on the concrete-PCM interfacial bond, the influence of some of these factors on concrete-PCM interface were considered as an experimental parameter as a priority basis. Series-I of this research work was designed to study the effectiveness of modified 5% silica PCM as a repair material based on bi-surface shear test using three levels of surface roughness (high, medium and low) and two different concrete compressive strengths (low strength type (LS) with 16.73 MPa and normal strength type (NS) with 29.59 MPa). In series-II and Series-III, the

performance evaluation of the bonding strength under shear stress conditions based on bi-surface shear test using rough concrete surface were explored with/without silica fume with three different states of moisture at the interface and at early ages, respectively.

3.2 Experimental outline

3.2.1 Materials and mix proportion of substrate concrete

Two kinds of concrete with mix ratio as shown in the Table 3.1 were cast in the laboratory to facilitate Serie-I experiment. Concrete with higher water to cement ratio was termed as low strength "LS" concrete and with lower water to cement ratio was referred as normal strength "NS" concrete. Concrete were cast with commercially manufactured ordinary portland cement (OPC) in case of "LS" type of concrete and with high early strength cement in case of "NS" type of concrete. Similar properties of coarse aggregate and fine aggregate mentioned in Chapter 2 (Section 2.2.1) was used to prepare concrete. Water was sprinkled 24 hours before on the coarse and fine aggregates to make them saturated. Tap water was used and all the mixes were prepared at room temperature using mixing machine. To prepare composite specimen for Series-II and Series-III experiment, same concrete as mentioned in Chapter 2 (Section 2.2.1) was used.

Table 3-1 Mix proportion of concrete

Type of Concrete	W/C (%)	Water (L)	Amount(kg/m^3)		
			Cement	Sand	Aggregate
LS	60.0	160	267	817	1067
NS	40.0	160	400	788	1128

3.2.2 Materials of repairing

As an overlay repairing material, PCM and silica fume having similar properties as reported in detail in Chapter 2 (Section 2.2.2 and 2.2.3, respectively) were used. As a second improving material of the interfacial bonding strength between concrete and PCM, a reactive type of surface penetrant (SP) supplied by the Fuji Chemical Co., Ltd. was used in Series-I experiment. It was intending to use to re-react cured concrete (as the cured substrate concrete cannot easily undergo chemical reactions) to cause cured concrete hydration. It was thought that the hydration of both cured concrete and PCM simultaneously helps to form a chemical bonding between these two materials. The main component of the surface penetrates was "sodium silicate". Surface penetrant was applied to the concrete surface 8 hours before the application of PCM following the outcome of the previous study [19]. Pipette was used for the uniform application of surface penetrant over the entire concrete surface as shown in Figure 3.1. It was applied in two times with time interval of 60 minutes and the amount was maintained 0.15 l/m^2 for each of the 1st and 2nd application. When it was applied to the roughed concrete surface, the surface was wettened according to guideline on design and application methods of silicate-based surface penetrants used for concrete structures [20]. Though the moisture content of the substrate concrete was not measure, but a good attention was paid to the wet condition of the surface of concrete before application of surface penetrant. Water was sprayed on the roughed substrate concrete surface and surface penetrant was applied after water stagnation had disappeared. In cases, if some portion of surface penetrant remained over the concrete surface, it was wiped before the application of PCM layer.

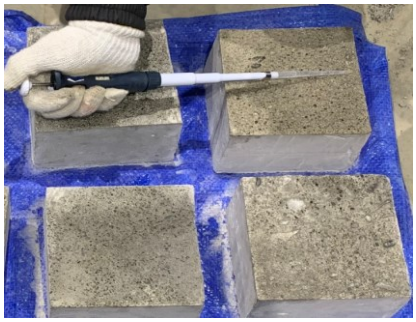

Figure 3-1 Application of the surface penetrant over the concrete surface

3.2.3 Specimen preparation

The surface roughness of concrete substrate is considered as a key factor in the performance of bonding between substrate concrete and new overlay layer. For the preparation of composite specimens of Series-I experiment, one surface was roughened by steel wire brushing (WB) or sandblasting (SB) for better interlocking of the overlay layer to the substrate layer, as these methods generate fewer micro-cracks in the substrate layer [6]. Two types of roughness levels were prepared by the WB technique and categorized as low (L) and high (H). Eight hours after the concrete was cast, steel wire brushing was performed in the laboratory by the author. The types of cement used in the specimen preparation results in the difference in the surface roughness level. The use of high early strength cement resulted in a lower roughness level with no exposure of coarse aggregate, as shown in Figure 3.2(a), whereas the use of normal strength portland cement resulted in a higher roughness level with some exposed aggregates, as shown in Figure 3.2(b), thus named WB(L) and WB(H), respectively. Sandblasting was performed after 14 days of curing of the concrete, and roughness level is shown in Figure 3.2(c). To ease surface preparation and considering large number of specimen, a retarder was used to prepare substrate concrete roughness level for series-II and Series-III experimentation. In this method of surface preparation, retarder was sprayed over the concrete surface after casting the concrete to delay the hardening of concrete. The soft concrete surface was then washed spraying a strong jet of water until coarse aggregates were exposed as shown in Figure 3.2(d) to make the surface rough (R) for better bonding. Following the outcomes of the trial test (in WB cases) by the author and previous group research in our team [10, 19] (in SB cases), paying good attention, it is possible to get similar roughness level of the three specimens used in each group by visual inspection. Although many researchers quantitatively assess roughness, qualitative (visual inspection) was used, following the outcomes of the trial test and previous research by our team [10,19,21].

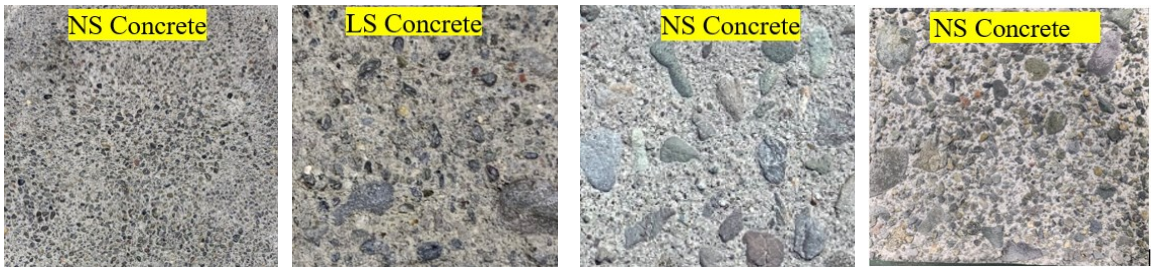

(a) WB(L) (b) WB(H) (c) Sandblasting (SB) (d) Using retarder (R)

Figure 3-2 Surface roughness used in this test

3.2.4 Preparation of composite specimen

The composite specimens were prepared by casting concrete of size 150 x 150 x 100 mm and 100 x 100 x 50 mm, followed by pouring PCM after 14 days to prepare composite specimens of sizes 150x150x150 mm for Series-I experiment and 100x100x75 mm for experiment of Series-II and Series-III. Considering a large number of composite specimens, different sizes of composite specimens were selected to reduce the material use of PCM. Concrete specimens were put into the moulds, and the roughened surface was kept facing up in the mould. Before casting the PCM, the top surface of the concrete specimens was cleaned with high air pressure to remove any dust as well as to create microporosity which helps in good adhesion. After that water was sprayed at the top concrete surface and free water on the rough surface was removed (if any) with a towel just before casting the PCM to provide a saturated concrete substrate with a dry surface for adequate bonding [22]. Once water stagnation had disappeared, PCM was trowelled over the treated surface of the concrete. The PCM was trowelled in two layers with a time interval of 180 minutes to prepare composite specimen of size 150x150x150 mm and 100x100x75 mm, respectively for different series experimentation.

To study the influence of moistness of the interface, the composite specimen of size 100 x 100 x 75 mm was fabricated with the moisture state of the interface as air dry (AD), saturated surface dry (SSD), and wet. The AD state was achieved by placing the specimen in a natural dry environment in the laboratory for one week before pouring a new mortar layer. The SSD condition was achieved by

immersing the specimens in water for 1 day, removing the samples from water, waited for about 2 hours, and wiping out the excess moisture (if any) at the surface with a towel before placing PCM. The wet state was made by putting the substrate concrete in water for 3 days, removing the specimen from the water immediately before casting PCM, and overlay mortar was placed without wiping surface water. The state of the moistness of the interface used is shown in Figure 3.3(a-c).

(a) AD (b) SSD (c) Wet

Figure 3-3 Moisture state of the interface used in this study

Table 3-2 Numbers of composite specimens for the interfacial shear test

Test type		Specimen level	Surface roughness preparation method	Moistness of the interface	Surface penetrant application	No. of specimen
Bi-surface shear (Specimen size - 150 mm)	Series-I	N_WB(L)_SSD_NS	Steel wire brushing	SSD	No	1 x 3
		M_WB(L)_SSD_NS	Steel wire brushing	SSD	No	1 x 3
		M_WB(L)_SSD_NS*	Steel wire brushing	SSD	Yes	1 x 3
		N_WB(H)_SSD_LS	Steel wire brushing	SSD	No	1 x 3
		M_WB(H)_SSD_LS	Steel wire brushing	SSD	No	1 x 3
		M_WB(H)_SSD_LS*	Steel wire brushing	SSD	Yes	1 x 3
		N_SB_SSD_NS	Sandblasting	SSD	No	1 x 3
		M_SB_SSD_NS	Sandblasting	SSD	No	1 x 3
		M_SB_SSD_NS*	Sandblasting	SSD	Yes	1 x 3
		N_SB_SSD_LS	Sandblasting	SSD	No	1 x 3
		M_SB_SSD_LS	Sandblasting	SSD	No	1 x 3
		M_SB_SSD_LS*	Sandblasting	SSD	Yes	1 x 3
Bi-surface shear (Specimen size - 100x100x100 mm)	Series-II	N_R_SSD_1	Using retarder	SSD	No	1 x 3
		M_R_SSD_1	Using retarder	SSD	No	1 x 3
		N_R_SSD_3	Using retarder	SSD	No	1 x 3
		M_R_SSD_3	Using retarder	SSD	No	1 x 3
		N_R_SSD_14	Using retarder	SSD	No	1 x 3
		M_R_SSD_14	Using retarder	SSD	No	1 x 3
		N_R_SSD_28	Using retarder	SSD	No	1 x 3
		M_R_SSD_28	Using retarder	SSD	No	1 x 3
	Series-III	N_R_AD_14	Using retarder	AD	No	1 x 3
		M_R_AD_14	Using retarder	AD	No	1 x 3
		N_R_AD_28	Using retarder	AD	No	1 x 3
		M_R_AD_28	Using retarder	AD	No	1 x 3
		N_R_Wet_14	Using retarder	Wet	No	1 x 3
		M_R_Wet_14	Using retarder	Wet	No	1 x 3
		N_R_Wet_28	Using retarder	Wet	No	1 x 3
		M_R_Wet_28	Using retarder	Wet	No	1 x 3

Note: * indicates the application of surface penetrant at the substrate concrete interface

Once the specimens were cast, the molds were wrapped with a polythene sheet to avoid the evaporation of moisture. Twenty-four hours after casting, all the formworks were demolded, and the specimens were cured in water following the procedure described in detail in Chapter 2 (Section 2.2.6). The total number of composite specimens cast is shown in Table 3.2. The acronym designation adopted for each group of the specimens are as follows: the first letter "N" or "M" refers to normal or modified 5% silica PCM followed by surface roughness level of the interface (WB(L), WB(H), SB or R), and moisture state of the interface (SSD, AD and wet) and substrate concrete compressive strength (LS or NS). For example, N_SB_SSD_LS refers to a composite specimen with normal PCM and low strength concrete which was bonded by roughness level prepared by sandblasting technique with moisture state of saturated surface dry condition of the interface. Moreover, N_SB_SSD_3 represented the composite specimens N_R_SSD which were tested three days after casting of the PCM layer.

3.2.5 Testing procedure

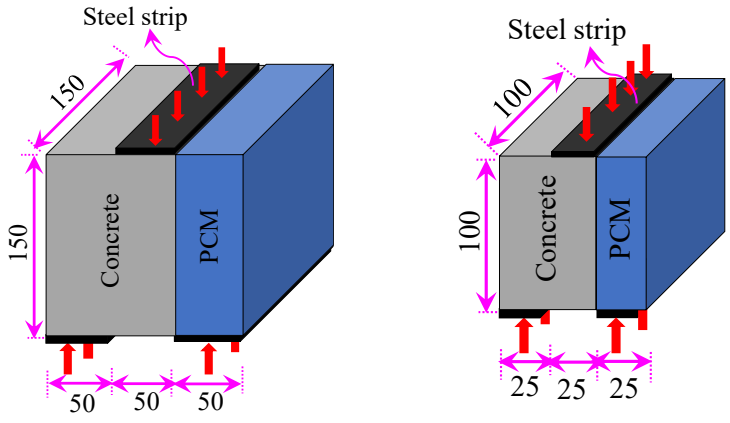

(a) (b)

Figure 3-4 Schematic of bi-Surface shear strength composite specimen; (a) for Series-I, (b) for Series-II and Series-II experiment (unit: mm)

The interfacial shear strength is one of the major interface properties that need to be carefully investigated. The measurement of the "pure" shear strength has always been a challenge for researchers, as it is a very difficult condition to achieve in reality. Many previous methods have been proposed to quantify the interfacial shear strength [23,24]. Single or double shear tests have been widely used and developed to evaluate the interface shear strength due to their simple loading method, but it has a disadvantage in the possibility to cause not adhesive failure but local compressive failure at the edge of loading plate or bending crack [25]. The slant shear test that evaluated under a combination of compression/tension and shear action at the interface has also been investigated by some researchers and has been developed as a design standard such as ASTM C 882 [26]. The presence of a compression force in the slant shear test leads to higher bonding strength than that in the pure shear stress condition due to the increase in friction. Meanwhile, the test method is greatly influenced by the difference between the stiffness of substrate concrete and repair material, the geometry of the test such as size and axis at the shear plane [24]. Some researchers have used their developed testing method for the pure interfacial shear strength measurement, but these methods were not widely accepted due to their complex test setups. Each of these tests has been reported to have some advantages and disadvantages compared with one another. Momayez et al. [23] proposed a new direct shear test named bi-surface shear strength test that does not require any special form and can be fabricated easily as well as gives less variation in the results. Thus, this method is widely used for the evaluation of the interfacial shear strength. Consequently, considering the fact of a large number of specimens and to ease the complexity in specimen preparation, the bi-surface shear test was adopted to measure interface shear strength using Eq. 3.1 in this study. The scheme of the test method used for the measurement of the interfacial shear strength is shown in Figure 3.4.

$$\tau_v = \frac{P_u}{2A} \tag{3.1}$$

where τ_v = the shear bond strength (MPa), P_u = the ultimate load (N) and A = the area of the connected interface (mm^2).

3.2.6 Statistical analysis

The laboratory test data of interfacial strength were further analyzed statistically using a one-way analysis of variance (ANOVA) to evaluate the influence of silica fume as a repair mortar and the impact of different influencing factors. The relevant calculation principles and significant criterial of one way ANOVA is shown in Table 3.3 and 3.4, respectively. The formulas for the calculation of parameters of the Table 3.3 is presented in literature [27]. The degree of influence of considered factor on the interfacial bond was designated by "a", "b", "c"," or "d" following the significant criteria as shown in Table 3.4.

Table 3-3 Analysis of One way ANOVA

Source of variation	Sum of squares deviation (SS)	Degree of freedom (DF)	Mean square deviations (MS)	F value
Between groups	S_A	r-1	$MS_A = S_A/(r-1)$	MS_A/MS_E
Within groups	S_E	n-r	$MS_E = S_E/(n-r)$	
Total variance	S_T	n-1		

Note: "r" represent levers number for each influencing factor; and "n" represent the total number of outcomes of different levers for each influencing factor

Table 3-4 Significant analyses based on one way ANOVA

Criteria	Result
If $F > F_{0.01}$ (r-1,n-r) or p-value < 1%	Highly significant effect (a)
If $F_{0.01}$ (r-1,n-r) > F > $F_{0.05}$ (r-1,n-r) or p-value; 1% ~ 5%	Significant effect (b)
If $F_{0.05}$ (r-1,n-r) > F> $F_{0.1}$(r-1,n-r) or p-value; 5% ~ 10%	Little effect (c)
If $F < F_{0.10}$ (r-1,n-r) or p-value > 10%	No or Very little effect (d)

3.3 Test results and discussions

3.3.1 Series-I (Interfacial shear strength of composite specimens)

The average interfacial shear strength along with the standard deviation of all the composite specimens are presented in Figure 3.5. The data of the specimens were excluded when the difference value between any measured value and the mean value calculated exceeds 20% of the mean value, the median value measured is taken as the mean value. The COV values ranged from 1.41% to 14.71% which are reasonable considering the variability of production of cementitious composites.

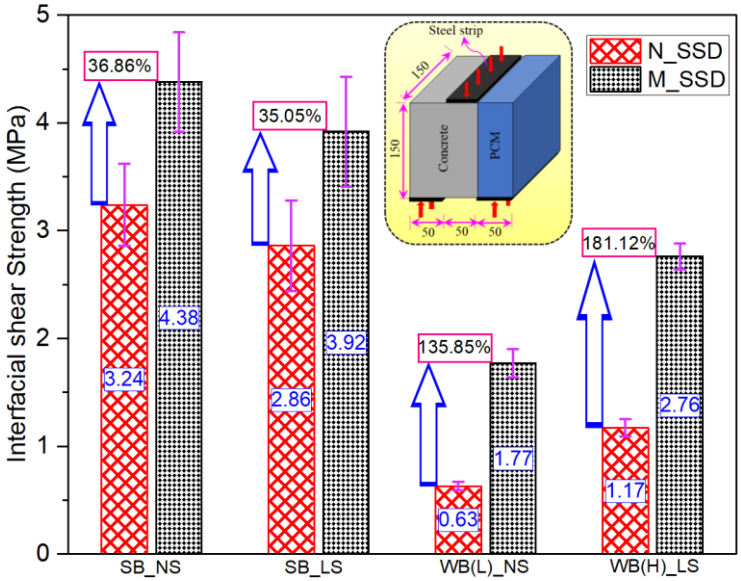

Figure 3-5 Increase in the interface shear strength by the inclusion of silica fume in PCM

The constituent of the overlay material attached to the substrate concrete influenced the interfacial bonding strength. The inclusion of 5% silica fume of the PCM mass in the overlay material greatly increased the interfacial strength in each substrate concrete compressive strength and surface roughness case. The percentage increases in the interfacial strength for the case of 5% silica PCM compared to the normal PCM cases are presented in Figure 3.5. The increasing percentage is very high for the steel wire brushing cases with both the medium and lowest surface roughness levels compared to the sandblasting case that has the highest surface roughness level. This fact indicates that silica fume inclusions can enhance the chemical bonding at the concrete-PCM interface. Therefore, in practical PCM strengthening applications, the inclusion of silica fume in the overlay material is highly suggested if the substrate concrete cannot meet the roughness requirements.

The composite specimens (modified 5% silica PCM with surface penetrant) show less interfacial shear strength compared to normal PCM composites irrespective of the types of concrete or surface roughness level as shown in Figure 3.6 which indicates that our initial thought on the possible enhancement of the bond strength by silicate-based surface penetrant was not correct.

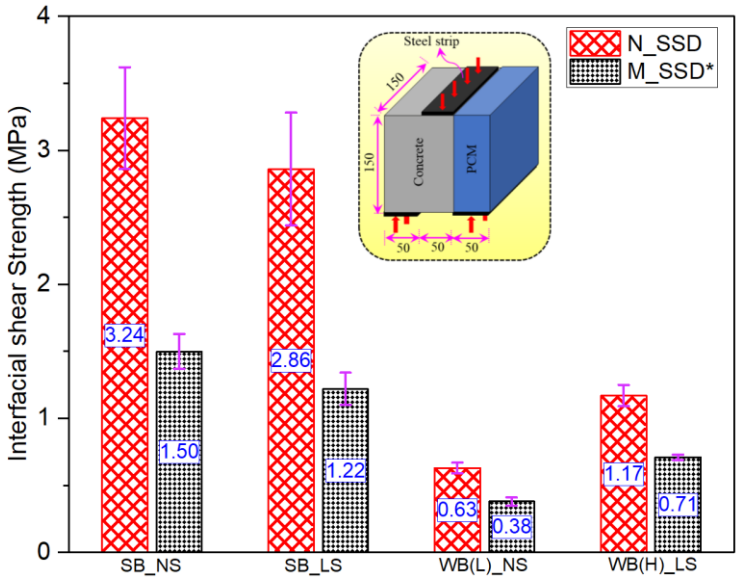

Figure 3-6 Decrease in the interface shear strength in modified %5 silica PCM with surface penetrant compared to normal PCM composite

One of the reasons for the reduction in the interfacial bonding strength is the presence of a white compound in both the concrete and PCM parts in the specimens with the surface penetrant, as shown in Figure 3.7(a). In a previous study [19], this white compound was also observed at the interface of the specimens with surface penetrant, and the presence of 44% $CaCO_3$ was found by X-ray diffraction analysis of the white compound, which was higher compared to that of the normal concrete cases (approximately 20%). This white compound cannot be seen in the normal PCM cases or the cases without the surface penetrant, as shown in Figure 3.7(b).

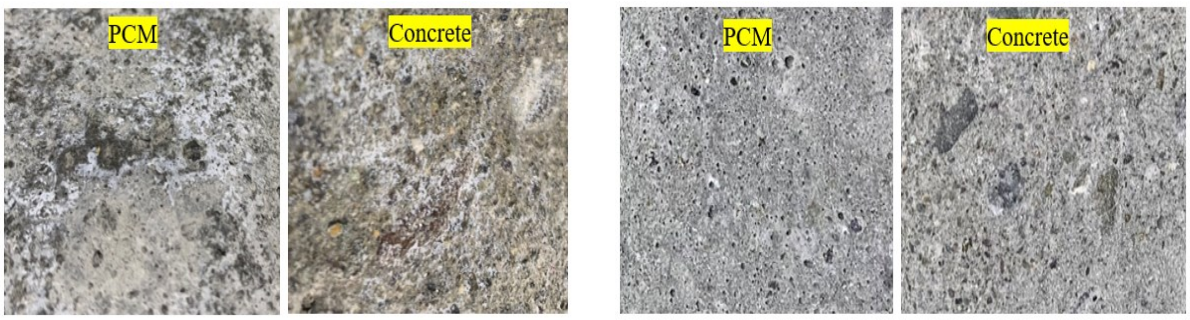

(a) With surface penetrant (b) Without surface penetrant

Figure 3-7 White compound in the interface

Another cause for the reduction in the interface shear strength is that the layer of the surface penetrant over the substrate concrete acts as a protective layer. In general, this material is used over the cured concrete surface as a surface modifier to protect the surface from abrasion, water penetration, etc. This protective layer hinders the flow of the water to the cured concrete, which is required for hydration and prevents the small silica fume and PCM particles from filling the gaps among the cement particles of the substrate, resulting in a weak bond between the substrate concrete and overlay layer. In the SP application, it is realized that it is very important to adjust the chemical reaction time of SP and PCM. The intensive chemical reaction time between concrete and SP which depends on the kinds of SP used has not been studied so well. Therefore, it is important to know the exact surface penetrant reaction time to realize effective interface bonding.

3.3.1.1 Effect of substrate concrete compressive strength

The results of interfacial bond strength of the composite specimens with different substrate concrete compressive strengths are compared in Figure 3.8(a) when the surface is roughened by sandblasting. An increase in the interfacial shear strength was found for "NS" concrete compared to that of "LS" concrete. Higher compressive strength of substrate concrete formed lower autogenous shrinkage of composite that results in higher bond strength [16]. The increase of compressive strength of substrate concrete also increases its elastic modulus. It reduced the difference of elastic modulus of composite specimens and increased the mechanical compatibility [15], subsequently increased interfacial strength. In addition, in the case of the low substrate concrete compressive strength cases, cracks occur in the concrete earlier and propagate towards the interface, causing failure of the specimens through the interface or with the concrete cohesion fracture mode, subsequently resulting in lower interfacial bonding strength. The increase in the interfacial bonding strength with the increases in the substrate concrete compressive strength was also observed when 5% silica PCM specimens were compared to the normal PCM specimens. The increase percentages were 36.84% for "LS" concrete and 35.05% for "NS" concrete. Figure 3.8(b) shows that the interfacial bonding strength decreases with increasing substrate concrete compressive strength. This is because the roughness level is high for the case of the specimens with a lower substrate concrete compressive strength. Conclusively, there is an optimum surface roughness level of the substrate concrete up to which the substrate concrete compressive strength is not effective on the interfacial bonding performance. After the optimum surface level, the interfacial strength increases with increasing substrate concrete compressive strength.

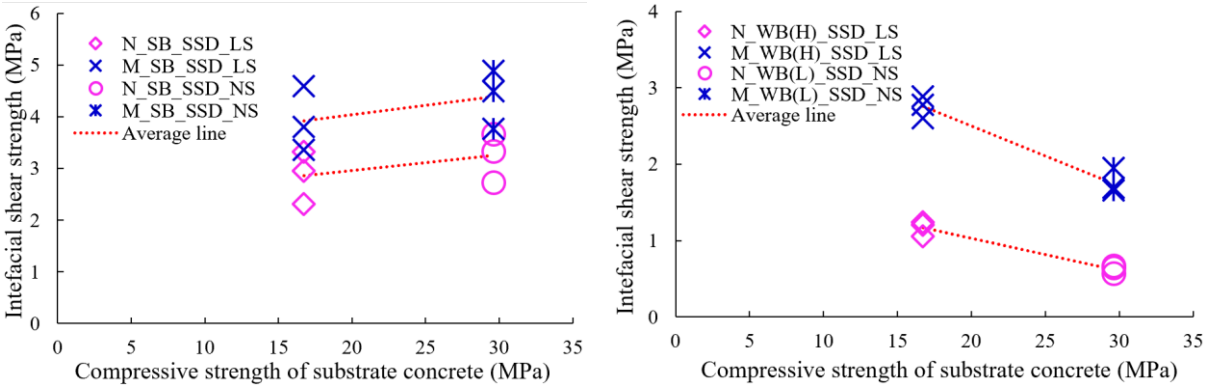

(a) Sandblasting (b) Steel wire brushing

Figure 3-8 Effect of the substrate concrete compressive strength on the interfacial bonding at different surface roughness levels.

3.3.1.2 Effect of surface roughness

The positive influence of surface roughness level of substrate concrete on the interfacial bonding performance between the concrete and PCM was found in this research work. Figure 3.9 showed that the surface roughness prepared by sandblasting, that has a higher surface roughness level, results in a higher interfacial shear strength than that of the steel wire brushing cases that have a lower surface roughness level for the case of both normal PCM and 5% silica PCM composite specimens. In the

case of the normal PCM composite specimens, sandblasted specimens with the highest level of roughness have higher interfacial strengths of approximately 5 times and 2.5 times compared to the specimens roughened by steel wire brushing (lowest and medium roughness level). Consequently, the surface roughness level greatly influences the interfacial bonding performance both in normal PCM and 5% silica PCM cases.

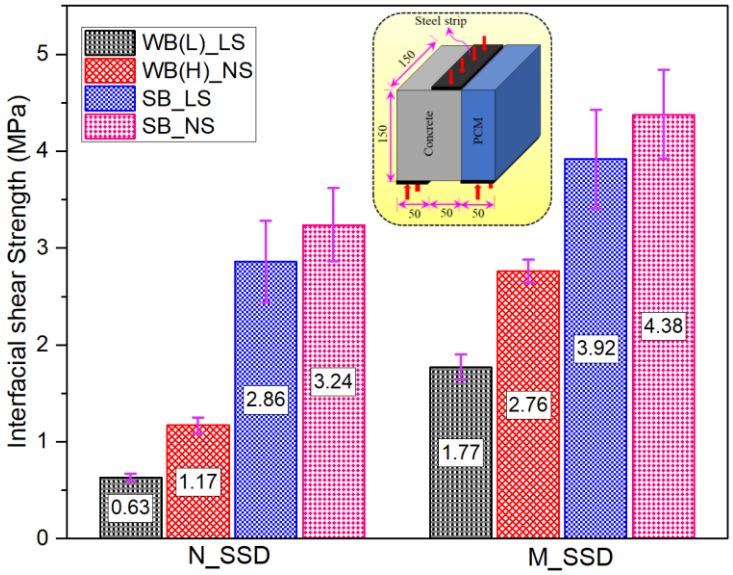

Figure 3-9 Variation in the interfacial strength with different surface roughness techniques

3.3.1.3 Fracture mode of the composite specimens

The fracture modes are named according to the location of the fracture on the surface of the specimens. During and after the loading tests of the composite specimens, visual observations were made carefully to determine the location of failure and named according to the definition of fracture mode mentioned in Chapter 2 (Section 2.3.3.1). Examples of four types of fracture modes of the composite specimens observed in this research work is shown in Figure 3.10(a-d).

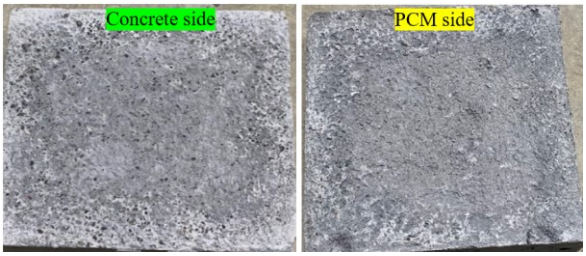

(a) Pure interface fracture (I)

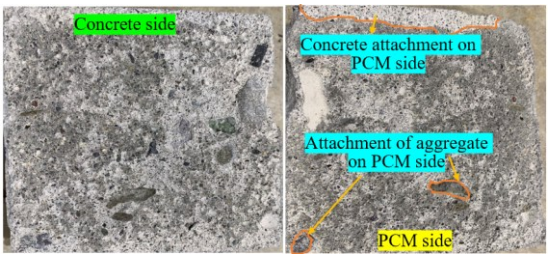

(b) Interface-concrete composite fracture (I-C)

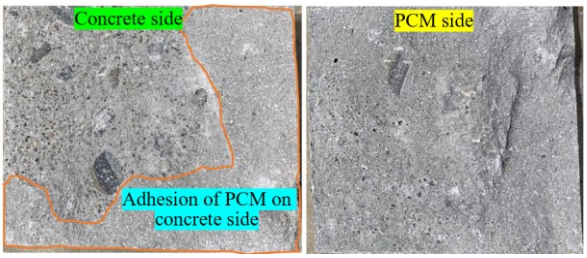

(c) Interface-PCM composite fracture (I-P)

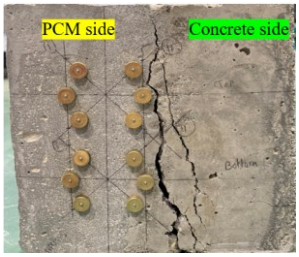

(d) Concrete cohesion fracture (C)

Figure 3-10 Sample fracture surface of the composite specimens in Series-I experiment

In this research work, all the composite specimens with surface penetrant showed pure interface (I) fracture. The fracture modes of the specimens other than the surface penetrant specimens are shown in Figure 3.11. The sandblasted specimens showed an increase in the number of specimens that failed at the mixed-mode or concrete cohesion mode in 5% silica PCM cases compared to normal

PCM cases. For example, one pure interface fracture mode (I) was observed in the case of specimen N_SB_SSD_LS, but no pure interface fracture mode (I) was observed in the case of specimen M_SB_SSD_LS; rather, the fracture mode shifted to one mixed-mode (I-C) and two concrete cohesion modes (C). It may be considered that concrete cohesion fracture occurred when the interface shear strength was higher than the concrete shear strength. However, for both the normal PCM and 5% silica PCM cases, all the specimens show pure interface fracture mode (I) when the surface is roughened by steel wire brushing (both high and low steel wire brushing cases). Consequently, it can be said that the increase in the surface roughness shifted the failure surface closer to the concrete cohesion (C) side for the case of the low substrate concrete compressive strength and to the mixed-mode (I-P) for the case of the high substrate concrete compressive strength.

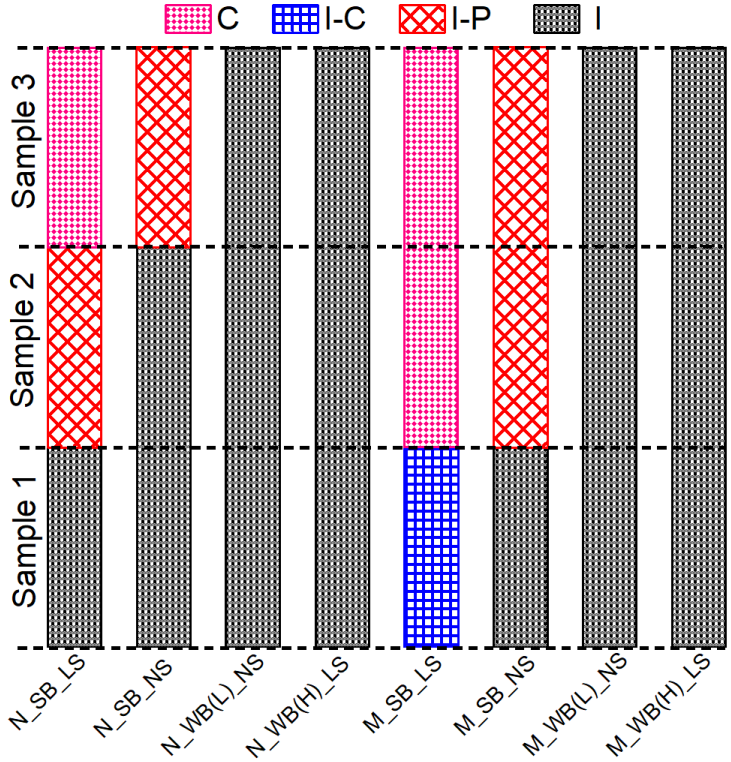

Figure 3-11 Fracture mode observed for the composite specimens in Series-I experiment

3.3.2 Series-II (Effect of moisture state of the interface)

Figure 3.12(a-b) showed three specimens' average values of all the composite specimen with different moisture state at the interface along with their standard derivation. The interfacial bonding strength was higher with the SSD condition of the substrate concrete interface compared to air-dry or wet conditions of substrate concrete interface. The wet condition of the interface results in the lowest interfacial strength in all cases. The dry substrate may accelerate water migration from repair mortar that leads to incomplete hydration near the interface and induces less bonding between substrate concrete and overlay mortar. Alternatively, the presence of excessive moisture at the interface (wet moisture state cases) may clog the pores of the substrate concrete and prevent absorption of new material which results in weaker bond strength. The bond strength in the SSD state of normal PCM is 24% and 4% higher than that of wet state at 14 and 28 days, respectively. The outcome of statistical analysis (p-value of 0.204 and 0.669, and degree of influence "d"), as presented in Figure 3.12(a) confirmed that there is no or very little influence of the moistness of the interface on the bonding strength in normal PCM specimens. The same phenomenon was also observed in the previous study [10] in case of normal PCM over mortar. However, the percentage increase of bonding strength in the SSD state of modified 5% silica PCM compared to the wet state at 14 and 28 days is 40% and 55%, respectively. The outcome of the statical analysis (p-value of 0.013 and 0.042, and degree of influence "b"), as presented in Figure 3.12(b) suggests that there is a significant effect of the moistness of the interface on the bonding strength.

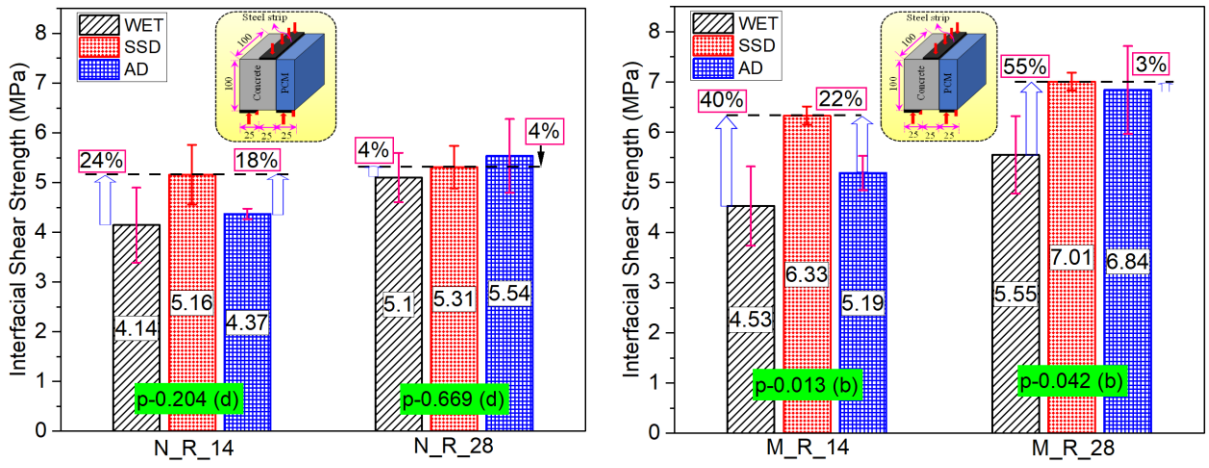

(a) Normal PCM (b) Modified 5% silica PCM

Figure 3-12 Influence of moistness states of interface on the interfacial bond strength

A typical example of calculation and analysis of the relativity of the impact factors of the bond interface between substrate concrete and overlay layer using one way ANOVA is presented in Table 3.5. As an example, the influence of the moistness of the interface on the bond interface strength of modified 5% silica PCM-concrete at 14 days was considered. The calculated *F*-value is compared with critical value (F_x) obtained using *F* distribution at 1% ($F_{0.01}$), 5% ($F_{0.05}$) and 10% ($F_{0.1}$) significant level to determine the level of significance of the concerned factor. Following the significant criteria as shown in Table 3.4 and comparing the calculated and critical values, it can conclude that the concerned factor (interface moisture state) has significant effect on the bonding strength. The statistical results of the all the composite specimen with different moisture states of the interface is presented in Figure 3.12 and Figure 3.13. Conclusively, the experimental and statistical test results imply that moisture condition of the interface in substrate concrete is very important to achieve good interfacial bonding strength, especially in using silica fume with overlay mortar.

Table3-5 A typical example of calculation and analysis of the relativity of the impact factors

Factor		Interfacial shear strength (MPa)			*SS*	*DF*	*MS*	*F* value		Level of Significance
Interface moisture state	AD	3.80	5.36	4.43	4.992	2	2.496		$F_{0.1} = 3.46$	
	SSD	6.13	6.38	6.48	1.532	6	0.255	9.777	$F_{0.05} = 5.14$	Significant effect (b)
	Wet	5.40	5.36	4.80	--	--	--		$F_{0.01} = 10.92$	

The influence of silica fume in the interfacial shear strength of the composite specimen under different moisture states of the substrate concrete interface is shown in Figure 3.13. In all states of moisture of the interface, the modified 5% silica PCM specimens showed higher interfacial bonding strength compared to normal PCM specimens. The SSD state results in the highest percentage increase of bonding strength, followed by AD and Wet state, respectively. The percentage increase of interfacial strength with the inclusion of silica fume with PCM as a repair material compared to without silica fume cases is also presented in Figure 3.13. With SSD state of the substrate concrete interface, it accelerates the hydration process and rate of chemical reaction of silica compound and $Ca(OH)_2$ to form secondary C-S-H that leads to acquiring good bond between substrate concrete and overlay mortar. The presence of a very small amount of water in the AD state helps in the formation of fewer C-H-S at the interface, which does not satisfy the interface strengthening requirement resulting in less bonding strength than SSD condition. The presence of a high amount of water at the wet state clogs the pores of the substrate concrete and prevents absorption of new material indicating that silica fume cannot perform in the expected way to strengthen the interface by the micro-filling effect or by chemical connection.

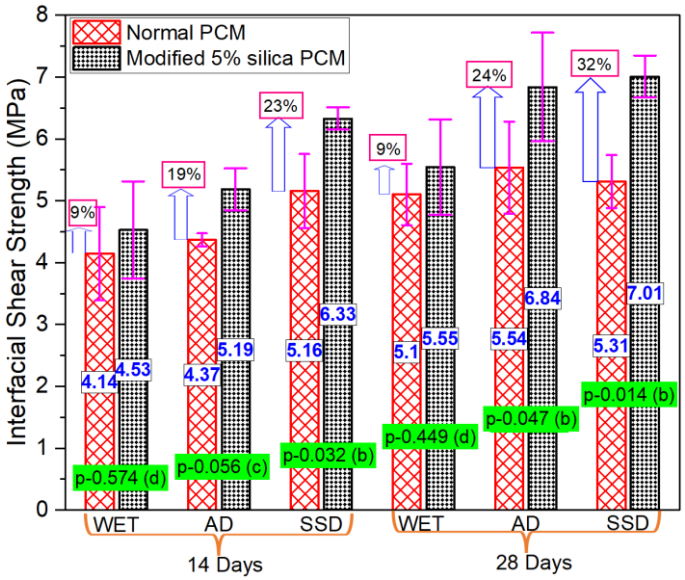

Figure 3-13 Influence of silica fume on bonding performance with different moisture conditions

The fracture mode of all the composite specimens tested at different moisture states of the interface is presented in Figure 3.14(a-b). The modified 5% silica PCM specimens with SSD state of the interface do not include any pure interface fractures (I) as presented in 3.14(b). This indicates higher adhesion of modified PCM overlay with substrate concrete with better durability. Consequently, the moisture condition at the interface of substrate concrete has a significant impact on the interfacial bonding performance, especially in using Silica fume, SSD condition is very important to achieve a good bond.

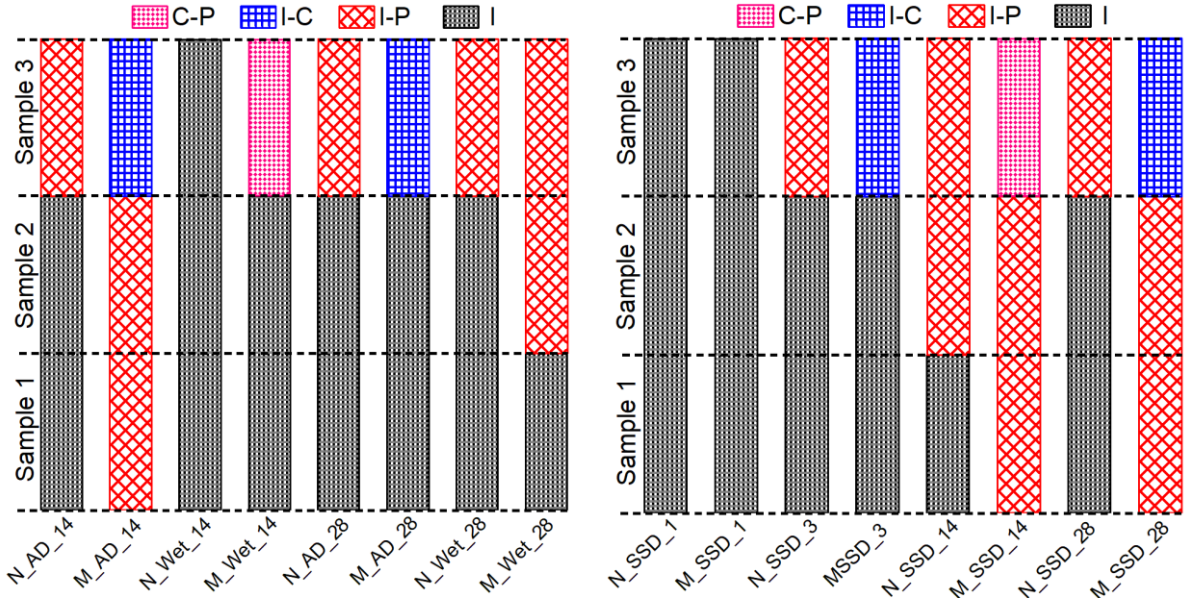

(a) Different moisture content at the interface (b) Specimens tested at early ages

Figure 3-14 Fracture mode of all the composite specimens of Series -II and Series-III

3.3.3 Series-III (Effect of silica fume at early ages)

3.3.3.1 Monolithic specimen

The compressive strengths of normal PCM and modified 5% silica PCM were evaluated using cylindrical specimens (50x100 mm) according to the standard test method ASTM C39 [28]. The influence of silica fume was checked by comparing the percentage increase of strength of the modified 5% silica PCM and normal PCM specimens, as shown in Figure 3.15.

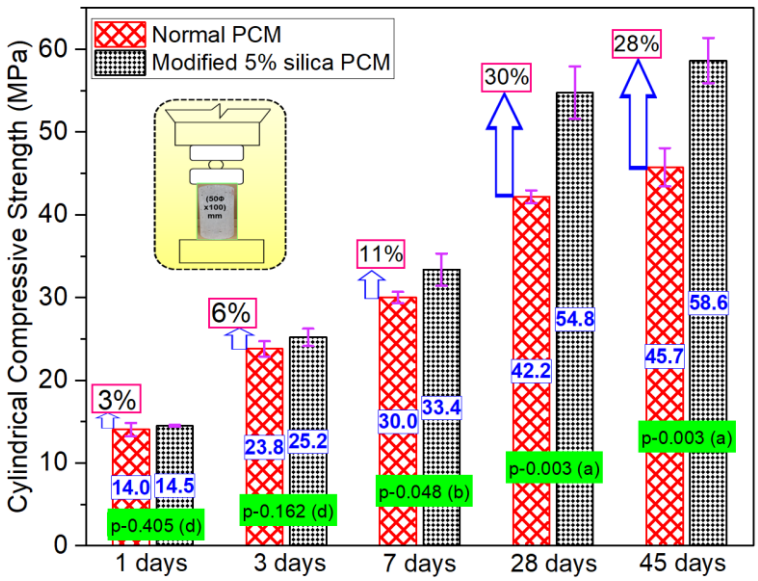

Figure 3-15 Influence of silica fume on monolithic specimens

The strength gain in the modified 5% silica PCM specimen was slightly higher which is considered insignificant up to 3 days of curing compared to normal PCM specimen. There is a possibility that due to presence of higher SiO_2 (about 29%, identified by XRF analysis) in PCM, silica compound can react with $Ca(OH)_2$ produced in the early-age hydration stage and increase its strength causing marginal strength difference between normal PCM and modified 5% silica PCM at initial stage. This gaining of strength become pronounced for modified 5% silica PCM specimen beyond seven days. A high amount of strength gain was achieved in between the ages of 7 days and 28 days of about 64% in modified PCM mortar whereas it is about 40% in the normal PCM overlay mortar. The result of the statistical analysis shows no significance in between the ages of 1 day and 3 days, which shifted to a significant and very significant level at the ages of 7 days and 28 days, respectively, presented with p-values and degree of influence in Figure 3.15. This finding is partially a result of pozzolanic reactions of the silica fume due to its large specific surface area. The self-cementitious activity of silica fume, the predominant reaction of silica compound with $Ca(OH)_2$ during the early hydration stage seems to contribute to the higher strength of modified 5% silica PCM mortar. In conclusion, the addition of 5% silica fume significantly increased the compressive strength of the monolithic specimens with time, though it has a marginal effect at early ages.

3.3.3.2 Composite specimen

The average interfacial shear strength of the three specimens, after excluding data when the difference between any measured value and the mean value exceeded 20% of the mean value, is shown in Figure 3.16. One-day curing specimens showed higher interfacial strength in modified 5% silica PCM specimen than in the normal PCM specimen. This indicates that the hydration of the silica PCM mixtures occurs at the relatively young ages of casting. The interfacial strength further increased with ages of curing in the modified 5% silica PCM compared to normal PCM. The bond strength of one-day curing specimens was roughly half the three days strength in both normal and modified PCM overlay mortar. In between age 14 days and 28 days, normal PCM specimens showed similar results, whereas the modified PCM specimens showed approximately 20% higher bond strength. The outcomes of statistical analysis showed a positive influence of silica fume on interface performances from the young ages of casting. The bonding improvement can be attributed to the chemical reactions of $Ca(OH)_2$ of substrate concrete and SiO_2 of silica PCM of the overlay mortar to form secondary C-S-H. Additionally, silica particles can fit between cement particles and inside pores on the surface of the concrete substrate, resulting in a denser microstructure with higher intermolecular forces and mechanical interlocking. Consequently, the bond strength increases significantly with the inclusion of silica fume from the very first day of pouring of overlay mortar. The addition of silica fume to PCM is strongly suggested for practical PCM strengthening applications to withstand the induced stress by the continuous traffic movement during/after the construction work from the early ages.

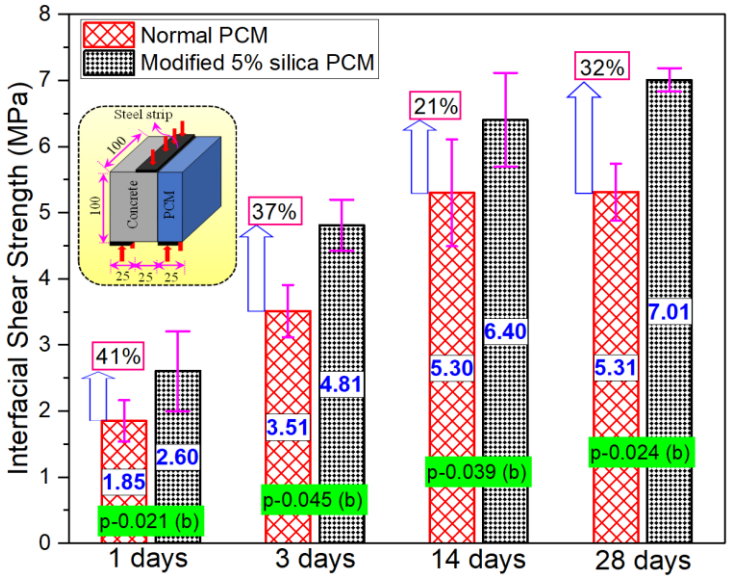

Figure 3-16 Interfacial strength of normal PCM and modified 5% silica PCM specimen at early ages

After the mechanical testing, visual observations were made to determine the failure mode of the composite specimens whether it failed due to a crack along the interface (shear plane) or failed due to significant cracking in the overlay material or substrate concrete. The failure mode was named comparing the classification of the fracture surface as discussed in Section 2.3.3.1. The fracture mode of all the specimens tested at early ages is shown in Figure 3.14(b), which shows a smaller number of pure interface fracture (I) in modified 5% silica PCM specimens compared to normal PCM specimens. Consequently, the adhesion of overlay mortar to substrate concrete increased with the inclusion of silica fume that kept the interface from failing.

3.4 Conclusions

The following conclusions can be made from this material level test:

- The interfacial shear strength increases with the increase in the surface roughness level for both the normal PCM and 5% silica PCM cases.
- The substrate concrete compressive strength is not effective in increasing the interfacial bonding strength up to a certain surface roughness level (optimum level) of the substrate concrete. If the roughness level exceeds that of the optimum level, the interfacial bonding strength increases with increasing substrate concrete compressive strength.
- The inclusion of silica fume in the PCM increases the interfacial bonding strength. Additionally, the incorporation of silica fume shifts the failure surface closer to the concrete cohesion (C) for the case of the low strength concrete and to the composite fracture mode (I-P) for the case of the high strength concrete if the surface roughness level is high. However, the surface roughness prepared by steel wire brushing having lower surface roughness level result in pure interfacial fracture mode (I) for both the normal PCM and 5% silica PCM cases.
- The fracture energy is affected by the fracture mode of the composite specimens, i.e., the interfacial fracture mode (I) results in smaller fracture energy, whereas the composite fracture (I-P) or (I-C) and concrete cohesion fracture mode (C) results in higher fracture energy.
- Applying the surface penetrant at the interface decreases the interfacial shear strength and results in the pure interfacial fracture mode (I), even if the surface roughness is high.
- The interfacial strength is predominantly influenced with the moistness of the substrate concrete surface, the saturated surface dry interface state of substrate concrete facilitate bond strength development. Interface moisture state exert a positive influence on the modified 5% silica PCM-concrete bonding performance, while it has no/insignificant impact on the normal PCM-concrete interface.
- There is a high possibility that the bond strength increases significantly with the inclusion of silica fume from the very first day of pouring of overlay mortar due the predominant reaction of silica compound with $Ca(OH)_2$ during the early hydration stage.

References

[1] Beushausen, H. (2010). "The influence of concrete substrate preparation on overlay bond strength." *Magazine of Concrete Research*, 62, 845-852.

[2] Sholar G.A., Page G.C., Musselman J.A., Upshaw P.B. and Moseley H.L. (2004) "Preliminary investigation of a test method to evaluate bond strength of bituminous tack coats." *Journal of the Association of Asphalt Paving Technologists*, 73:771-801.

[3] Eduardo, N.B.S.J., Fernando, A.B.B. and Vitor, D.S. (2004) "Concrete-to-concrete bond strength. Influence of the roughness of the substrate surface." Construction and Building Materials,18, 675–681.

[4] West R.C., Zhang J. and Moore J. (2005). "Evaluation of bond strength between pavement layers." *NCAT Report 05-08, National Center for Asphalt Technology*, Auburn University, Auburn, Alabama, USA.

[5] He, Y., Zhang, X., Hooton, R. D. and Zhang, X. W. (2017). "Effects of interface roughness and interface adhesion on new-to-old concrete bonding." *Construction and Building Materials*, 151, 582-590.

[6] Santos D. and Júlio S. (2013). "A state-of-the-art review on roughness quantification methods for concrete surfaces." *Construction and Building Materials,* 38: 912–923.

[7] Furuuchi H., Sakai R., and Ueda T. (2006). "Influence of maximum aggregate size and interface roughness for interface bonding strength of Polymer Cement Mortar." *Proceeding of Japan Concrete Institute*, vol. 28.

[8] Talbot C., Pigeon M., Beaupre D., and Morgarn D.R. (1994). "Influence of Surface Preparation on Long-term bonding of Shotcrete." ACI Materials Journal, 91(6):560-566.

[9] Abu-Tair A.I., Rigden S.R., and Burely E., (1996). "Testing the Bond between Repair Materials and Concrete Substrate." ACI Materials Journal, 553-558.

[10] Miura S. (2017). "A Study on Interface Shear Behavior of PCM-Strengthened Concrete under High Temperature." Master Thesis, Hokkaido University, Japan.

[11] Fu, X. and Chung, D.L. (1998). "Effects of Water-Cement Ratio, Curing Age, Silica Fume, Polymer Admixtures, Steel Surface Treatments, and Corrosion on Bond between Concrete and Steel Reinforcing Bars," ACI Materials Journal, 95(72), 725-734.

[12] Momayez, A., Ehsani, M. R., Ramezanianpour, A. A. and Rajaie, H., (2005). "Comparison of methods for evaluating bond strength between concrete substrate and repair materials." *Cement and Concrete Research*, 35(4), 748-757.

[13] Igor, D.L.V., Jose, M., Dale, P. B. and Benjamin, G. (2015). "Effect of the Interface Moisture Content on the Bond Performance between a Concrete Substrate and a Non-Shrink Cement-Based Grout." National Accelerated Bridge Construction Conference, USA.

[14] Zhang D., Furuuchi H., Hori A., Fujima S. and Ueda T. (2008). "Influence of Interface Roughness on PCM-Concrete Interfacial Fracture Parameters." Proceedings of 3rd ACF International Conference, HCM City, Vietnam, 15: 919-924.

[15] Hu, Y. Y., (2014). "*Compatibility of repair materials with the existing substrate in concrete structure repair*." Thesis (PhD). Hunan University, China.

[16] Diab, A. M., Elmoaty, A. M. A. E. and Eldin, M. R. T., (2017). "Slant shear bond strength between self-compacting concrete and old concrete." *Construction and Building Materials*, 130:73-82

[17] Austin S., Robins P. and Pan Y. (1995). "Tensile Bond Testing of Concrete Repairs." Materials and Structures, 28: 249-59.

[18] Zhang, D. (2009). "Research on PCM-Concrete Interface and PCM-Strengthened RC Beam." Doctoral Thesis, Hokkaido University, Japan.

[19] Hayato, S., Mahmudul, H. M., Tamon, U., Katsuichi, M. and Jun, T. (2019). "A study on the effect of silica fume and surface penetrant on bonding strength for overlaying." Journal of Asian Concrete Federation, 5(1):1-14.

[20] Fuji chemical Co. Ltd. (2009). "Guideline on the procedure of the application of silicate based surface penetrant over the concrete surface." Japan.

[21] Ueda, T., Rashid, K., Qian, Y., and Zhang, D. (2017). “Effects of Temperature and moisture on concrete-PCM interface performance.” Sustainable Civil Engineering Structures and Construction Materials, 171:71-79.
[22] Ohama, Y. (1995). “Handbook of polymer-modified concrete and mortars-properties and process technology.” New Jersy, Noyes Publications.
[23] Momayez, A., Ramezanianpour, A., Rajaie, H. and Ehsani, M.R. (2004). “Bi-Surface Shear Test for Evaluating Bond between Existing and New Concrete.” ACI Materials Journal, 99-106.
[24] Santos, P. M. D. and Júlio, E. B. S. (2010). “Assessment of the Shear Strength between Concrete Layers.” 8th fib International Ph.D. Symposium in Civil Engineering, Denmark, 1-6.
[25] Tanaka, H., Yoshitake, I., Yamaguchi, Y. and Hamada, S. (2003). “A study of prototype of simple loading device giving pure shear force” Proceedings of the Japan Concrete Institute, 25(2):1003-1008.
[26] Rui, S., Júlio, E. B. S., Daniel, D.C and Santos, P. M. D. (2012). “Modified Slant Shear Test to Enforce Adhesive Failure.” Structural Faults and Repair, Edinburgh, Scotland.
[27] Kan, L., Zhiqiang, W., Hongxia, Q., Chenggong, L. and Hakuzweyezu, T. (2021). “PCM-Concrete Interfacial Tensile Behavior Using Nano-SiO2 Based on Splitting-Tensile Test.” Journal of Advanced Concrete Technology, Vol. 19, 321-334.
[28] ASTM C39/C39M-05 (2013). “Standard Test Method for Compressive Strength of Cylindrical Concrete Specimens.” American Standard of Testing Materials.

Chapter 4

BONDING DURABILITY OF CONCRETE-PCM INTERFACE WITH INCLUSION OF SILICA FUME UNDER ENVIRONMENTAL CONDITIONS

4.1 Introduction

It was concluded form previous two chapters that the inclusion of silica fume with PCM as a repair material significantly improve the concrete-PCM interfacial bonding strength. In practice, the strengthened structures put into immediate service based on achieving adequate substrate concrete-repair materials bond strength in a short duration. However, in many cases, the short-term strength gain of the strengthened members does not ensure long-lasting and durable repairs as because the long-term properties of the substrate concrete and repair material can be significantly different from the properties measured at early ages. The strengthened members are frequently in harmful media and severe environment in service life stage causing early degradation and performance deterioration [1]. The emphasis in selecting suitable repair techniques of the deteriorated structures is placed on the bonding properties measured at early ages alone with not much consideration on the degradation properties during long term exposure though the environmental exposure (freeze-thaw cycle, elevated temperature) of strengthened members have significant response in its performance. Therefore, from the perspective of practical application of polymer cement mortar (PCM) overlaying method, long-term performance of strengthened members under severe environmental exposure should be achieved along with short-term bonding strength of newly overlaid PCM layer with substrate concrete.

In some country, the temperature can be seen below -20°C in winter, thereby inducing different degrees of freeze–thaw damages affecting the durability of the concrete structures. The positive and negative temperature alterations during freezing and thawing cycle (FTC) in service environments causes scaling and cracking in structures resulting significant influence on the mechanical performance and service life of the concrete structure [2-3]. Many researcher have investigated mechanical properties of concrete after freeze-thaw cycles [4-7] along with degradation prediction model under FTC for evaluating concrete degradation behaviour [8-10] and confirmed negative influence of FTC on the long-term performances of concrete structure. Not only the material itself is damaged by FTC, the adhesive interface, which is regarded as the weakest part of composite system, is also degraded under FTC [11-13]. In an experimental study by Qian [11], the interface and outer surface of PCM containing composite specimen were found subjected to damage under FTC though PCM itself possesses good freeze-thaw resistance over conventional mortar due to the reduction of porosity as a result of decreased water-cement ratio, low permeability, high percentage of polymer film and filling of pores by polymers. Since polymer film is an important mechanism to bond the components of PCM and increase the bonding strength, the weakening of polymer under water or freeze-thaw cycles would weaken the PCM or interface resulting flakes at interface and at outer PCM surface. Also, higher porosity at the interface due to wall effect increase water absorption which subsequently weaken the interface under FTC.

Temperature and moisture is also considered as one of the major factor affecting the durability of the concrete structures. Due to rapid industrialization, global warming and non-sustainable development, temperature in some regions exceeds 50℃ and may rise to 60℃ [14, 15], which may deteriorate concrete structure rapidly. In our real environment, concrete structures are also exposed to cyclic temperature instead of constant temperature. In such environmental conditions, mismatch properties between concrete and repair material may be dominant causing damage to the adhesive bonding between them. Therefore, both concrete and repair materials must be durable in severe environmental exposure. Many researchers have investigated the change in the microstructure of the concrete [16–18] and mechanical performance degradation of the concrete [19–21] after exposure to high temperatures. It was observed that the mechanical behavior of concrete degraded to different degrees after exposure to high temperatures. Repair materials like PCM is also sensitive to high temperature, Ries [22] noticed 91.6% reduction in flexural strength at 90 ℃. The degradation of the properties of concrete and repair materials directly influenced the interfacial bonding strength under severe environment condition as the interfacial strength is depends upon the intrinsic properties of the

constituent material [23]. In the past experimental study [24-26], reduction of interfacial shear strength of around 18% and 35% was reported for specimens exposed to 40°C and 60°C respectively compared to 20°C. Additional stress is generated at the interface when exposed to hot dry environment leading to failure of the interface at lower load [27]. Owing to high temperature and moisture absorption, volumetric change in two constituents' material also generates additional stress at the interface and creates a condition of generating cracks [28].

The inclusion of silica fume with PCM as a repair material is expected to perform better in long run under harsh environment as silica fume can cause chemical reaction to form more C-S-H with strong binding force. Due to extreme fineness of silica fume, it fills the void resulting lower porosity at the interface that can hold less moisture at the beginning. Thus, it may reduce the effect of volumetric change under severe environmental conditions. Although different individual and coupling environmental condition have an impact on the concrete-PCM interfacial bond, the influence of some of the individual environmental conditions on concrete-PCM interface were considered as an experimental parameter as a priority basis. Series-I of this research work was designed to study the effectiveness of modified 5% silica PCM as a repair material under FTC based on a splitting tensile strength test using rough concrete. In series-II and Series-III, the performance evaluation of the bonding strength under shear stress conditions based on bi-surface shear test using rough concrete surface were explored with/without silica fume with different temperature exposure and moisture condition, respectively.

4.2 Experimental outline

4.2.1 Materials

In this experimental work, three types of materials were used. First one was the substrate concrete which was fabricated by mixing commercially available high-early strength cement, coarse and fine aggregate, tap water, water reducer and air entraining agent having technical characteristics as mentioned in Chapter 2 (Section 2.2.1) and with mix ratio as shown in the Table 4.1. Second type of the material was the pre-mixed PCM containing poly acrylic ester (PAE) provided by company having same properties as reported in detail in Chapter 2 (Section 2.2.2). Third material was silica fume which was used with PCM as a repair material for proper adhesion between concrete and PCM. Since silica fume powder is not liquid and difficult to spread in an interface, it was used by mixing into PCM powder right before overlaying and hydrated together. Super plasticizer of 1.0% of the PCM mass were mixed in preparing modified 5% silica PCM repair material to prevent the formation of silica fume lumps. The mix proportion of repair material is shown in Table 4.2.

Table 4-1 Mix proportion of substrate concrete

W/C (%)	Amount (kg/m^3)					Air entraining agent (ml/ m^3)	Compressive strength (MPa)
	Water	Cement	Fine aggregate	Coarse aggregate	Water reducer		
40	160	500	818	1018	8	187.5	41.57

Table 4-2 Mix proportion of repair material

Overlay material	Water/PCM (%)	Silica fume (% of PCM mass)	Superplasticizer (% of PCM mass)
Normal PCM	15.0	0	0
Modified 5% silica PCM	15.0	5	1

4.2.2 Specimen preparation

Wooden molds were prepared for casting of concrete and PCM of following sizes; 100 cubic mm (as monolithic specimen), 100 x 100 x 50 mm (for interfacial splitting tensile and shear test) as shown in Figure 4.1(a). Thermocouple was placed at the middle of some molds to measure the inside temperature of the specimen under different environmental exposure. At the bottom of the molds, some amount of retarder were spread after mixing with water to prepare surface roughness level for composite specimen, except of cubic mold. Once the concrete were cast in all molds, it was compacted and covered with polythene sheet to avoid evaporation of moisture. Prior to demolding,

the bottom layer of the mold were removed first and concrete surface was exposed to environment after 24 of casting. Due to use of retarder, the exposed concrete surface was not fully hard. The soft concrete surface was then sprayed with a strong jet of water until coarse aggregates were exposed to resemble rough substrate concrete surface as shown in Figure 4.1(b). After 48 hours of casting, all molds were removed and concrete was cured in wet condition for more than 2 weeks followed by dry curing for about 3 months to resemble existing concrete of the real infrastructure. To prepare composite specimens, cured concrete specimens of size 100 x 100 x 50 were put into the mold of 100 cubic mm (for splitting tensile strength test) and 100 x 100 x 75 mm (for bi-surface shear strength test). The rough surface was kept upside in the mold. Before casting PCM, the rough concrete surface was cleaned with high air pressure to remove any dust followed by immersing the concrete specimens in water for 48 hours. Wet specimens were put in molds and free water on the rough surface was removed by towel just before casting of repair material to provide saturated concrete substrate with dry surface for adequate bonding. Though moisture content of the substrate concrete was not measured quantitively, good attention was paid to the wet condition of the surface of substrate concrete before casting PCM. Once water stagnation had disappeared, PCM was trowelled over the treated surface of the concrete in two layers with a time interval of 180 minutes to prepare 100 cubic mm (for splitting tensile strength test) and 100 x 100 x 75 mm (for bi-surface shear strength test). Methodology of specimen preparation at material level testing is explained in Figure 4.1(a-e). The specimens containing fresh PCM was cured in wet condition for about one week to facilitate the hydration to took place. After wet curing, it was placed in the basement of the laboratory in dry condition as polymer film formed during dry curing and filled the voids and makes PCM stronger [29].

(a) Wooden molds

(b) Rough concrete surface

(c) PCM mixing by hand mixer

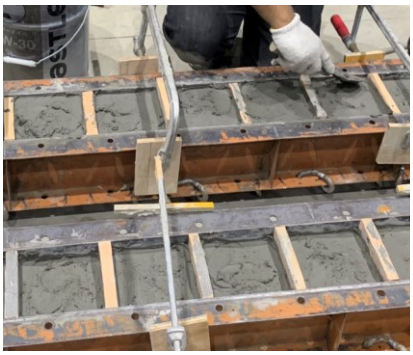

(d) Casting of PCM in two layers

(e) Covered to reduce evaporation

(e) Curing in wet condition

Figure 4-1 Preparation of composite specimens for material level testing

4.2.3 Exposure condition

All the composite specimens were exposed to different environmental conditions in the laboratory which resemble with the real environmental conditions. The specimens were divided into three series to study the influence of freezing and thawing, elevated temperature, and moisture content. Detail exposure condition of the composite specimens is described in the following section. The Summary of exposure conditions, test performed and number of specimens considered in this research work is shown in Table 4.3

4.2.3.1 Freeze-thaw cycle (FTC)

The most important durability problem of concrete structures under cold climate is freeze-thaw effect. Durability of the repair material and its adhesive bonding to substrate concrete may also be affected by negative and positive temperature fluctuations. To investigate this effects in details, concrete repaired with normal PCM and modified 5% silica PCM were exposed to different freeze-thaw cycle. Two types of experimental condition named “Type A” and “Type B” were considered. The composite specimen for “Type A" exposure condition was prepared by applying epoxy resin in all surface excect the top PCM surface as indicated in Figure 4.2(a) to resist water intake from all surface except the free surface to ressemble real situation. In “Type B” composite specimen, all the surface of the composite specimen were kept open so that water can intrude from all surface as shown in Figure 4.2(b). It was intended to kept all surface open to simulate the worse case of the structures with wide opening (cracks). In such cases, water can penetrate through that crack, subsequently damage the properties of the materials.

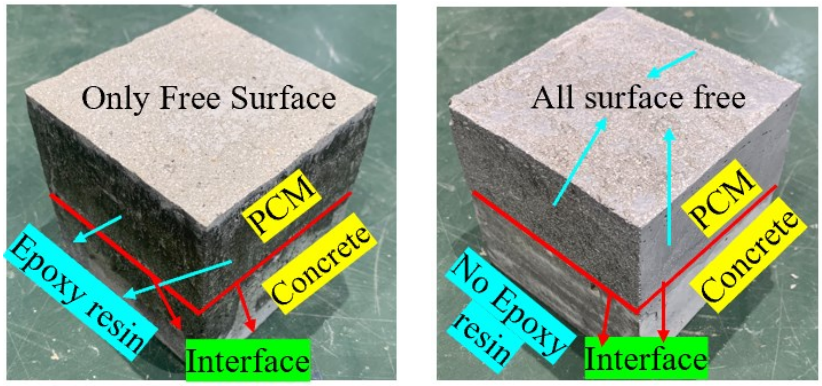

(a) Type A (b) Type B

Figure 4-2 Exposure condition of composite specimen used for FTC

The freeze-thaw test was performed in accordance with ASTM C-666A [30] in water with the length of each FTC ranging between +20°C and -20°C. The temperature was set to drop from 20°C to -20°C for 2 hours, keep at -20°C for 10 hours, rise from -20°C to +20°C for another 2 hours, and keep at +20°C for 10 hour. Prior to FTC test, the specimens was submerged in water for proper saturation inside the specimens. Then, the specimens was put inside self-designed mold as shown in Figure 4.3(a) filled with water such that the top surface of specimen is located around 5 mm below the level of water. The experimental setup of all the specimens in chamber is shown in Figure 4.3(b). The inside and outside temperature was measured with thermocouples which were attached inside of the specimen during casting. At the end of specific number of FTC, the specimens was taken out from FT chamber and the fundamental transverse frequency was recorder through ultrasonic pulse wave velocity method to evaluate relative dynamic elastic modulus (RDME). The RDME was measured using Eq. 4.1 to predict the damage progress of the specimens. The summary of exposure conditions and number of specimens considered in this series of research work is shown in Table 4.3

$$RDME = \left(\frac{F_n}{f_0}\right)^2 \quad (4.1)$$

Where F_n and F_0 is fundamental transverse frequency after n cycles and 0 cycle of freezing and thawing, respectively.

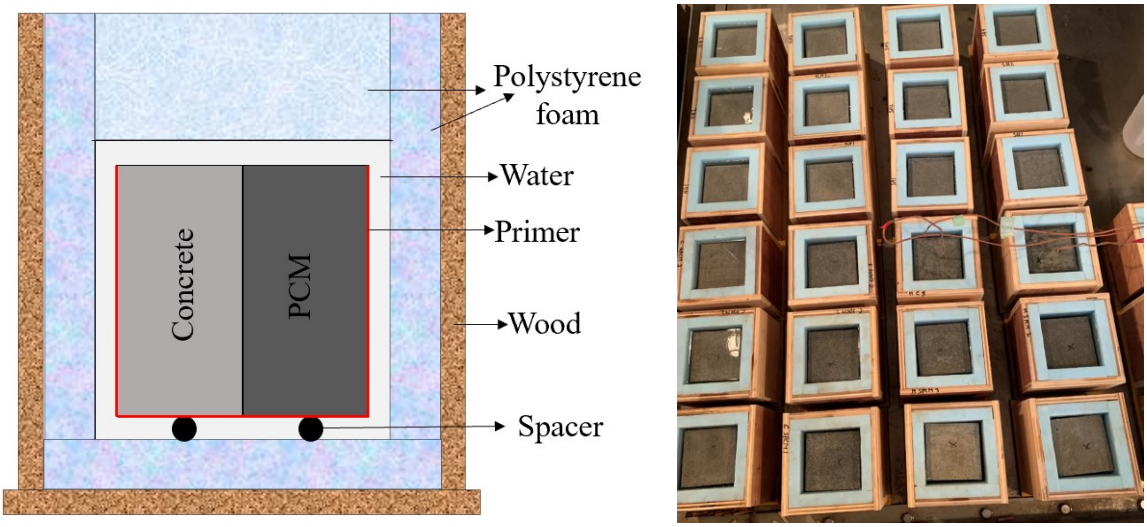

(a) Self-designed freeze thaw environment (b) Specimen setup in chamber

Figure 4-3 Freeze-thaw test set up

4.2.3.2 Elevated temperature

In the second series of experimentation, the influence of temperature was incorporated. In many regions, temperature fluctuates from ambient condition of 20°C to extreme temperature of 60°C. Durability of the concrete, repair material and its adhesive bonding to substrate concrete may be affected by this elevated temperature. In some region, concrete structures are also exposed to cyclic temperature instead of constant temperature. To investigate this affect in detail, composite specimen repaired with normal PCM and modified 5% silica PCM were exposed to four different temperature variation in the laboratory as presented in Figure 4.4(a-d). The first condition was the exposure of composite specimen at constant temperature of 60°C for 3 days, abbreviated as "T_{SD}" (short duration exposure). In the second condition, composite specimen was put in oven at constant 60 °C for 36 days to resemble long term exposure at constant temperature, abbreviated as "T_{MD}". Cyclic condition of the temperature were also adopted in this research work to represent real environmental condition. In the first cyclic condition, temperature change during day and night was considered by putting the composite specimen in oven at 60 °C for 12 hours and then at 30 °C for another 12 hours, abbreviated as "T_{DN}" (day and night variation). In second cyclic condition, seasonal variation of the temperature was considered by replacing four season of a year by one day in the laboratory. Composite specimens were exposed at 60 °C in oven for 24 hours to represent summer season, followed by immersed in water for 24 hours at 20°C to show rainy season, at 5°C for 24 hours to represent winter season and at ambient condition at 25°C for 24 hours to represent spring season. One cycle in seasonal variation completed in 4 days and the specimen were tested after 12 cycles. In all cases, the composite specimens were tested at room temperature.

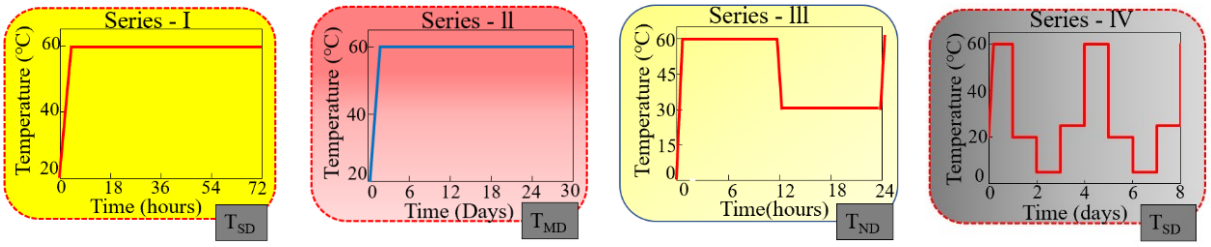

(a) (b) (c) (d)

Figure 4-4 Exposure condition used to investigate the effect of elevated temperature

4.2.3.3 Moisture content

To investigate the influence of moisture on the concrete-PCM interfacial bonding strength, composite specimen repaired with normal PCM and modified 5% silica PCM were exposed to wetting and drying cycles (W/D cycles) and continuous immersion in water at room temperature in the

laboratory. For one W/D cycles, the specimens were submerged in water for 2 days to get wetting condition and drying was conducted in ambient air exposure in the laboratory for 2 days. There is no standard test method available for the W/D cycles in the technical literature. Different researchers used different test method during wetting and drying cycles [29]. In this research work, the test was performed in wet state because of the sensitivity of PCM to the surrounding moisture after exposure of 0, 12 and 24 W/D cycles. For continuous wet condition, the specimens were submerged into water continuously. The specimens were taken out from water on testing day and test was conducted immediately in wet conditions. Test was performed after 0, 48 and 96 days of continuous immersion in water. The process of W/D cycles and continuous immersion in water are described in Figure 4.5.

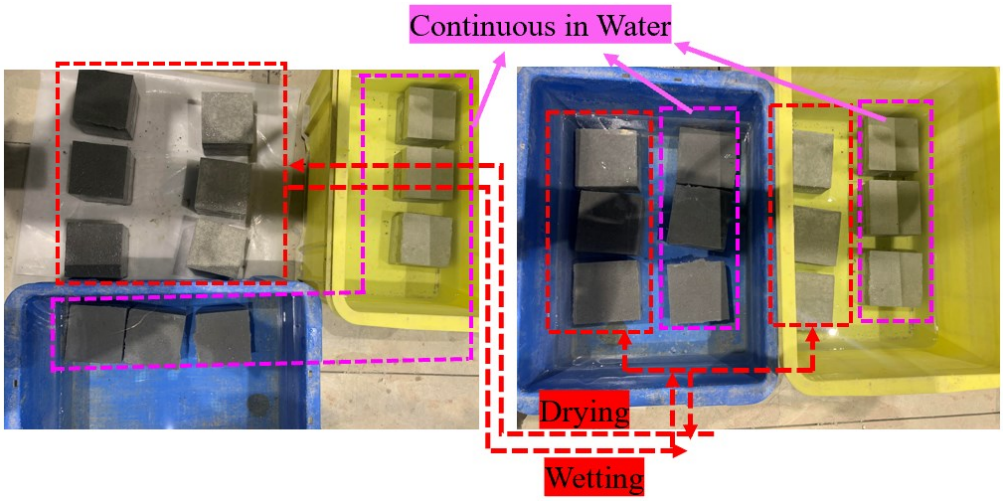

Figure 4-5 Exposure condition used for W/D cycles and continuous immersion in water

Table 4-3 Summary of exposure conditions, test performed and number of specimens.

Exposure condition	Specimen level			Test type	Overlay constituents	
					Normal PCM (N)	Modified 5% silica PCM (M)
	Freezing-thawing cycle (Series-I)	Type A	FTC0_WE	Splitting tensile	3	3
			FTC40_WE		3	3
			FTC70_WE		3	3
			FTC95_WE		3	3
			FTC120_WE		3	3
			FTC145_WE		3	3
		Type B	FTC6_NE		3	3
			FTC12_NE		3	3
			FTC20_NE		3	3
	Elevated temperature (Series-II)	0 days	T_{Con}	Bi-surface shear	3	3
		3 days	T_{SD}		3	3
		36 days	T_{MD}		3	3
		30 cycle	T_{DN}		3	3
		12 cycle	T_{SV}		3	3
	Moisture content (Series-III)	0	W/D cycle (No.)	Bi-surface shear	3	3
		12			3	3
		24			3	3
		0	Continuous immersion (days)		3	3
		48			3	3
		96			3	3

Note: "WE" represent with epoxy resin, "NE" represent without epoxy resin.

4.2.4 Testing procedure

4.2.4.1 Bulk specimens

Cylinder compressive strength of substrate concrete, normal PCM and modified 5% silica PCM was evaluated by conducting compressive strength test after 28 days of curing according to the standard test method ASTM C39 [31] with a universal testing machine (UTM) and found to be 41.57, 42.24 and 54.80 MPa, respectively. Compressive strength of the constituent overlay materials was also measured after 90 days of casting. No significant change in strength from the strengths at 28 days was observed for the case of normal PCM, but an increase of 17% strength was observed for modified 5% silica PCM. The tensile strength of monolithic concrete, normal PCM and modified 5% silica PCM were measured by splitting tensile test and found to 4.19, 3.57 and 3.47 MPa, respectively. In general, the tensile strength of concrete was measured by performing a split tensile test on cylindrical specimens following ASTM standards [31] and using Equation 4.2. In this research work, cubical specimens were tested specimens according to the process described by Li [32] or Rashid [33] and the tensile strength was measured using Equation 4.3.

4.2.4.2 Interfacial splitting tensile strength test

The splitting tensile test is widely used to evaluate tensile strength due to its ease of sample preparation, low variation in test results, and simple loading method. A splitting tensile prism test was conducted in this study, which assumes uniform tensile stress along the bond plane to evaluate the tensile strength of the concrete-PCM interface. Although cylindrical specimens were prescribed in ASTM C496 [33], it was proved by Li [32] that essentially uniform tensile stress in the splitting plane is produced in both the cylinder and square prism by using the finite element method. Before testing, two steel strips of size 200x12x6 mm were used at the top and bottom of the specimen to evenly distribute the load. This strip has an influence on the stress distribution during loading, and the stress conditions in the cylindrical and cubical specimens are shown in Figure 4.6. The size of the strip also affects the tensile strength of the specimen [32]. The corrected splitting tensile strength is calculated by incorporating the ratio of the width of the strip to the height of the specimen (β), as presented in Equation 4.3.

$$f_{st} = \frac{2P_u}{\pi A} \tag{4.2}$$

$$f_{st}(\beta) = \frac{2P_u}{\pi A}\left[(1-\beta^2)^{\frac{5}{3}} - 0.0115\right] \tag{4.3}$$

where f_{st} is the split tensile strength (MPa); $f_{st}(\beta)$ is the corrected split tensile strength considering the effect of the strip (MPa), P_u is the ultimate load (kN), A is the area of the specimen interface (m^2), and β is the ratio of the width of the strip to the height of the specimen.

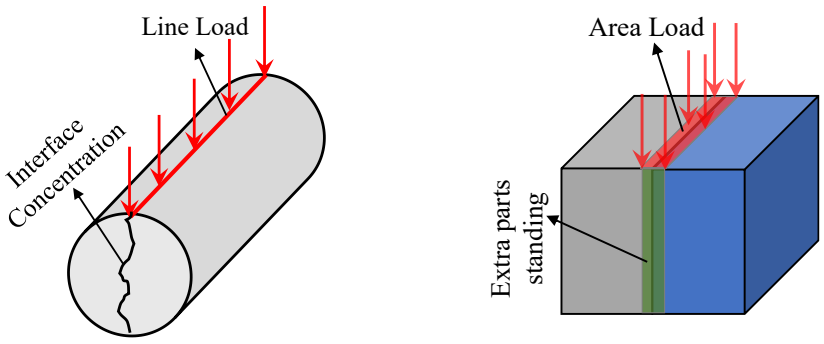

(a) Cylindrical specimen (b) Prism specimen

Figure 4-6 Difference in stress condition for cylindrical and prism specimens

4.2.4.3 Bi-surface shear strength test

Interfacial shear strength was evaluated by using bi-Surface shear strength test which was explained in detail by Momayez [10]. Considering the ease of specimen preparation, simple loading method, and many specimens, the bi-surface shear test was adopted in this research work. This

method is widely used for evaluation of interfacial shear strength as it gives less variation in results. The scheme of the test method used for the measurement of the interfacial shear strength of the composite is shown in Fig. 8, and it was evaluated by using Equation 4.4.

$$\tau_{max} = \frac{P_u}{2A} \tag{4.4}$$

where τ_{max} is the interfacial shear strength (MPa), P_u is the ultimate load (N) and A is the area of the connected interface (mm^2).

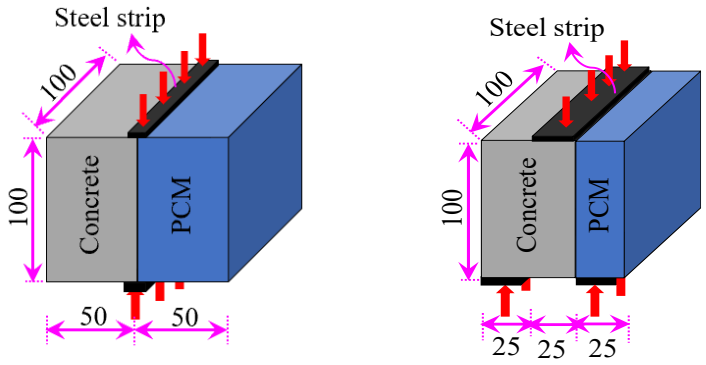

(a) Splitting tensile strength test (b) Bi-surface shear test

Figure 4-7 Schematic diagram of the test method used in this research work (unit: mm)

4.3 Test results and discussions

4.3.1 Series-I (Effect of freeze-thaw cycle on the interface)

4.3.1.1 Relative dynamic elastic modulus (RDEM)

It is known that the micro cracks generated inside the concrete or repair material under various pressure: hydraulic pressure [36], osmotic pressure [37], crystallization pressure [38], etc. during the exposure to freeze-thaw cycle. The elastic modulus of the components decreases with the occurrence of microcracks. Relative dynamic elastic modulus (RDEM) is one of the method used to quantify the extent of damage of cementitious material under freeze-thaw damage in which RDME of 100% denote no degradation, and RDME below 60% denote severe damage [30]. The measured RDME of normal PCM and modified 5% silica PCM composite specimens was calculated according to ASTM E 1876-09 [39] and presented in Figure 4.8. The damage progress in all the composite specimen with silica fume is less compared to without silica fume cases. This might result due to the facts of more hydrogen bond at the interface and fewer porosity caused with the inclusion of silica fume with PCM as a repair material.

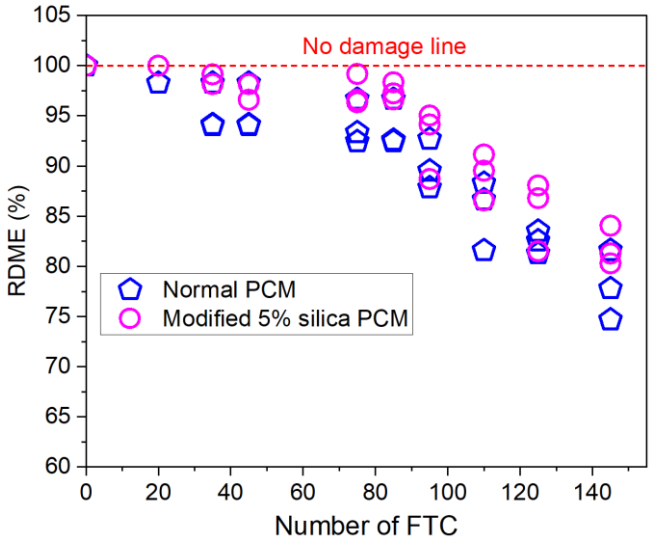

Figure 4-8 RDEM of composite specimens under FTC (Type A specimens)

4.3.1.2 Interfacial splitting tensile strength

Splitting prism tests on composite specimen were conducted to obtain the interfacial splitting tensile strength. The average strength of three specimens were considered as the interfacial splitting tensile strength under particular condition and presented in Figure 4.9(a-b) along with the standard deviation. In every particular condition, the data of the specimens were excluded for average calculation when the difference value between any measured value and the mean value calculated exceeds 20% of the mean value. The splitting tensile strength decreased slowly under increasing freeze-thaw cycles in exposure type A [Figure 4.9(a)], while that of exposure type B decreased quickly [Figure 4.9(b)]. In both exposure type, the earlier occurrence of a sharp decline of the interfacial tensile strength was observed in normal PCM composite specimens than that of modified PCM composite specimen, indicating a delay of degradation process under FTC in later case. In exposure type A, the reduction of the interfacial tensile strength of normal PCM composite specimen was 9.9%, 24.4%, 35.2%, 37.1% and 54.2% after 40, 70, 95, 120 and 145 freeze-thaw cycles, respectively of that of 0 cycle. In case of modified PCM composite specimen, the strength decrease percentage was 6.1%, 7.4%, 18.3%, 20.4% and 29.6% after 40, 70, 95, 120 and 145 freeze-thaw cycles, respectively of that of 0 cycle. In exposure type B, the interfacial strength of normal and modified composite specimen decreased by 46.7% and 18.7% after 20 freeze-thaw cycles, 16.1% and 10.5% after 12 freeze-thaw cycles, 15.8% and 3.2% after 6 freeze-thaw cycles, respectively of that of 0 cycle. In all cases, the reducing ratio of interfacial strength was higher in normal PCM specimens compared to modified PCM specimens, indicating positive influence of silica fume under FTC.

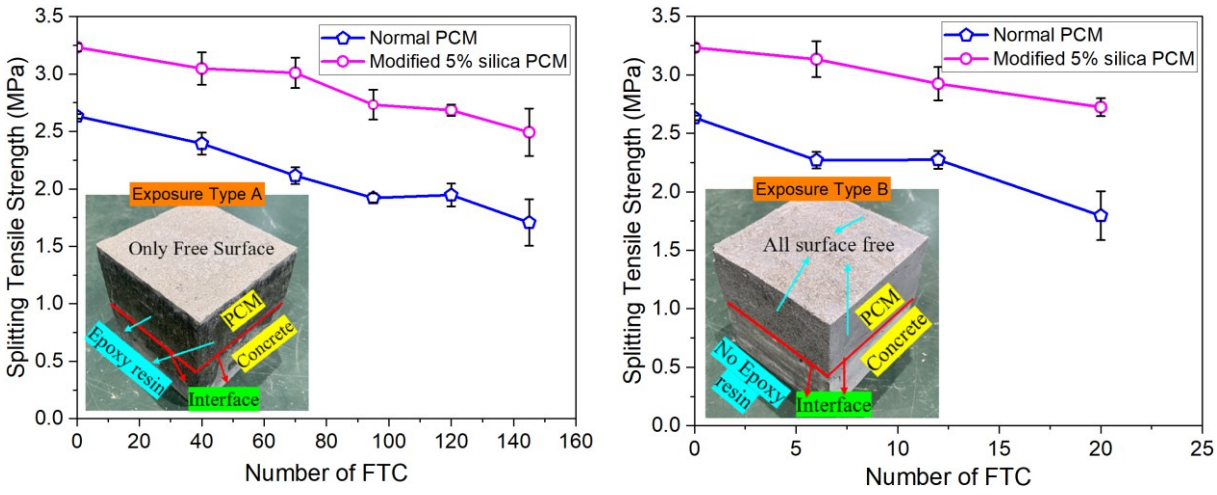

(a) Exposure type A (b) Exposure type B

Figure 4-9 Degradation of interfacial strength with different overlay constituents under FTC

The constituent of the overlay material attached to the substrate concrete influenced the interfacial bonding strength under FTC. With increasing number of FTC, the interfacial splitting tensile strength of composite specimen repaired with normal PCM decreased much quicker than those of composite specimen repaired with modified 5% silica PCM. The inclusion silica in the overlay material greatly increased the interfacial strength compared to without silica fume cases in both exposure type under FTC as presented in Figure 4.10(a-b). It is believed that the higher porosity at the interface increases water absorption due to wall effect and continuous freezing and thawing cause damage to the interface initiating micro cracks that increase with water absorption. The extreme fine particle size of silica fume in the fresh repairing material grew into the cavities and pores at the surface of substrate concrete resulting in a denser microstructure with higher intermolecular forces and mechanical interlocking. This will result decreasing the rate of water absorption and impact of different pressure release during FTC at the interface, thus decreasing the freeze-thaw damage. The repair material with inclusion of silica fume cause denser structure compared to without silica fume causing less water intrusion resulting less damage during FTC. In addition, the formation of more hydrogen bonds with strong binding force at the interface leads to acquiring good bond between substrate concrete and overlay mortar with silica fume inclusion, thus reduces the damage initiation under freeze-thaw environments. The experimental data of interfacial bonding strength obtained from

the loading test were further analyzed statistically using a one-way ANOVA to evaluate the influence of silica fume as a repair mortar under freeze-thaw environment and presented in Table 4.4.

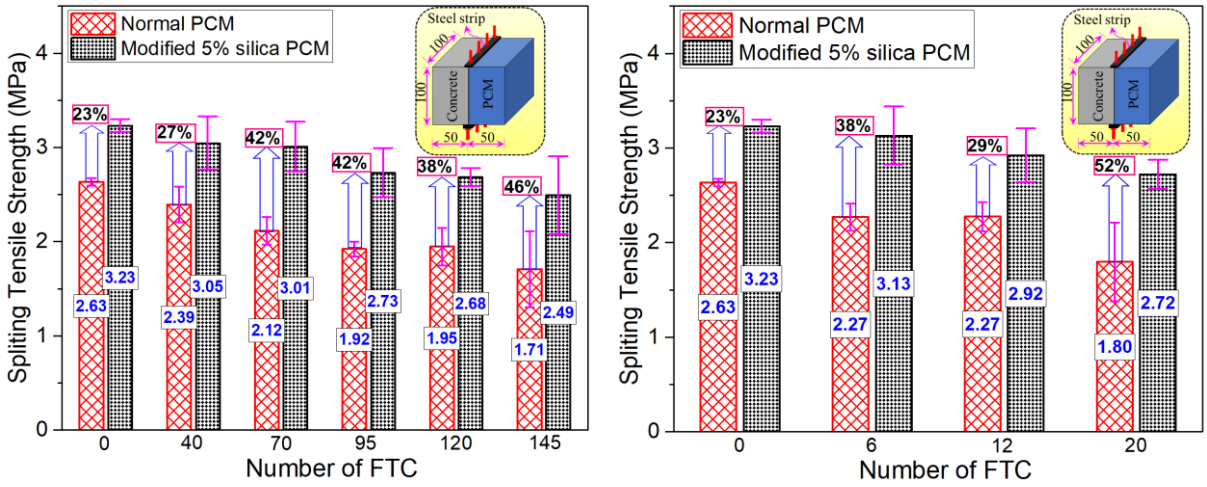

(a) Exposure type A (b) Exposure type B

Figure 4-10 Influence of silica fume on interfacial splitting tensile strength under FTC

Table 4-4 Statistical analysis of the influence of FTC on the interfacial splitting tensile strength

Factor		FTC No.	Splitting tensile strength (MPa)			*SS*	*DF*	*MS*	*F* value	F_x	Level of Significance
Type A	Normal PCM	0	2.63	2.67	2.60	2.03	1	2.03	36.71	$F_{0.1} = 3.46$ $F_{0.05} = 5.14$ $F_{0.01} = 10.92$	Highly Significant effect (a)
		40	2.61	2.29	2.28	0.89	16	0.06			
		70	2.13	1.96	2.26	--	--	--			
		95	1.83	1.94	1.99	--	--	--			
		120	1.25	1.87	2.01	--	--	--			
		145	1.25	1.87	2.01	--	--	--			
	Modified 5% silica PCM	0	3.26	3.28	3.15	1.06	1	1.06	10.26	$F_{0.1} = 3.46$ $F_{0.05} = 5.14$ $F_{0.01} = 10.92$	Significant effect (b)
		40	1.28	2.85	3.25	1.56	16	0.11			
		70	2.53	2.91	3.59	--	--	--			
		95	2.61	3.03	2.56	--	--	--			
		120	2.87	3.00	2.19	--	--	--			
		145	2.22	2.29	2.97	--	--	--			
Type B	Normal PCM	0	2.63	2.67	2.60	0.73	1	0.73	29.61	$F_{0.1} = 3.46$ $F_{0.05} = 5.14$ $F_{0.01} = 10.92$	Highly Significant effect (a)
		6	2.16	2.22	2.43	0.22	10	0.03			
		12	2.15	2.44	2.23	--	--	--			
		20	1.69	1.90	2.50	--	--	--			
	Modified 5% silica PCM	0	3.26	3.28	3.15	0.45	1	0.45	9.799	$F_{0.1} = 3.46$ $F_{0.05} = 5.14$ $F_{0.01} = 10.92$	Significant effect (b)
		6	3.30	2.78	3.31	0.46	10	0.05			
		12	3.27	2.87	2.63	--	--	--			
		20	2.81	2.55	2.81	--	--	--			

The influence of number of freeze-thaw cycle on the interface strength of modified 5% silica PCM-concrete and normal PCM-concrete was evaluated comparing the calculated *F*-value with critical F-value (F_x) obtained using *F* distribution at 1% ($F_{0.01}$), 5% ($F_{0.05}$) and 10% ($F_{0.1}$) significant level. The details calculation procedure and significant criterial was described in Chapter 3 (Section 3.2.6). The calculated F-value of the normal PCM specimens were obtained very high compared to modified 5% silica PCM specimens. Following the significant criteria as shown in Chapter 2 (Table 3.4) and comparing the calculated and critical values, it was confirmed that freeze-thaw environment have less effect on the interface of modified 5% silica PCM-concrete specimens compared to the interface of normal PCM-concrete that have highly significant effect under FTC. Conclusively, the experimental and statistical results imply that the inclusion of silica fume with PCM as a repair material is very important to achieve good interfacial bonding strength under freeze-thaw environments.

4.3.1.3 Fracture modes

Careful visual observation was made during and after the loading test of the composite specimen to identify the fracture modes and named according to the definition of fracture mode mentioned in Chapter 2 (Section 2.3.3.1). The fracture mode of all the composite specimens tested under FTC are presented in Figure 4.11(a-b). Pure interfacial adhesive (I) fracture mode was observed dominant in the composite specimens with normal PCM. At freeze-thaw cycles of 120 and 145, substrate concrete was distinctly separated from repairing mortar in all the tested specimens repaired with normal PCM. This finding reflects an increase of damage of the normal PCM-concrete interface under the freeze-thaw environments, leaded to more interface failure. By contrast, the specimens with 5% silica PCM mostly showed composite or mixed fracture mode such as (I-P), (I-C) or (C-P). Even at freeze-thaw cycles of 120 and 145, only one pure interface fracture (I) was observed. This exhibited that the inclusion of silica fume with PCM as a repair material effectively improve the resistance of interface fracture under freeze-thaw cycles. Silica fume optimizes the structure of the interface between substrate concrete and PCM with better durability by acquiring denser structure of the interfacial zone with more chemical bonding. Consequently, mixing silica fume with PCM improve the durability of the interfacial performance of concrete-PCM interface under harsh freeze-thaw environments

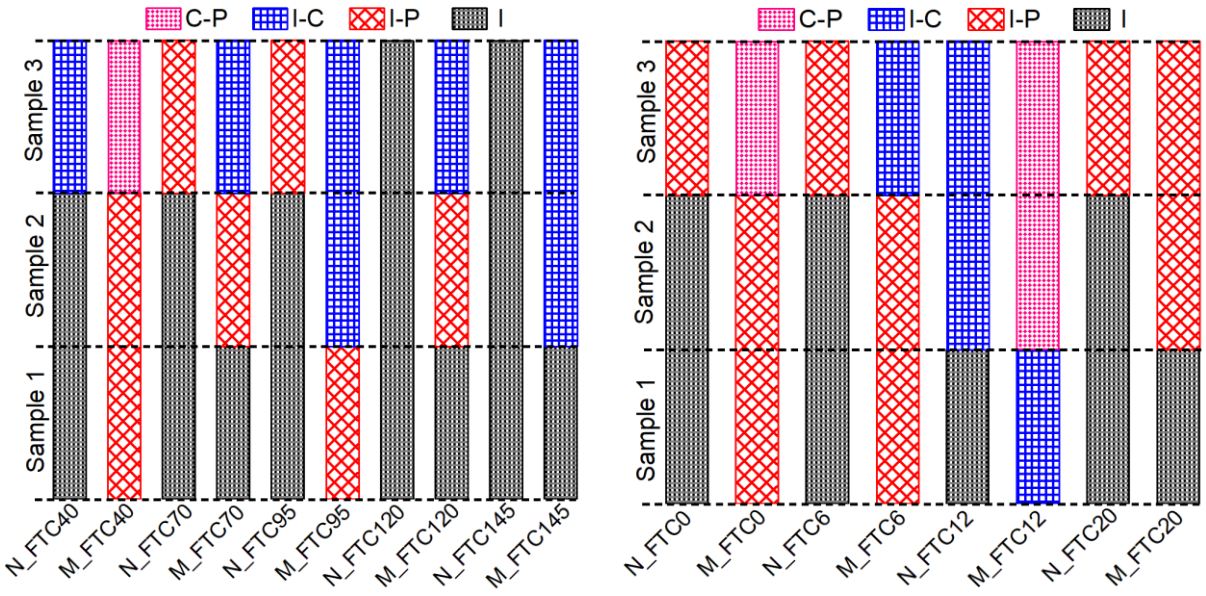

(a) Exposure type A (b) Exposure type B

Figure 4-11 Fracture mode of all the composite specimen tested under FTC

4.3.2 Series-II (Effect of elevated temperature on the interface)

4.3.2.1. Influence of elevated constant temperature

The composite specimens were exposed to a constant 60°C temperature for 3 days to study the influence of a short duration exposure and for 30 days to study the influence of a long time exposure.

The interfacial shear strength was evaluated by performing bi-surface shear strength test. After the exposure, the specimens were kept in the laboratory for some times to cool it down and tested at room temperature. The reduction in interfacial shear strength with exposure to constant temperature conditions were observed compared to without exposure cases (control specimens - T_{CON}), 18.91% and 8.22% during T_{SD} exposure and 21.76% and 16.6% during T_{MD} exposure for normal PCM and modified 5% silica PCM specimens, respectively. Higher strength reduction in normal PCM specimens might be due to the presence of higher porosity at the normal PCM-concrete interface than the modified PCM-concrete interface. During drying at high temperature, some of the fine pores collapsed resulting in larger pores and reduce the strength with an increase in porosity [40, 41]. In all exposure condition, the interfacial strength was also observed higher in modified PCM specimens compared to normal PCM specimen (35.26% after T_{SD} exposure and 27.3% after T_{MD} exposure) as presented in Figure 4.12(a). Denser microstructure with silica fume incorporation improves the structure of the interface with fewer porosity, thus reduce the influence of elevated temperature at the modified PCM-concrete interface and result higher interfacial strength than normal PCM specimens.

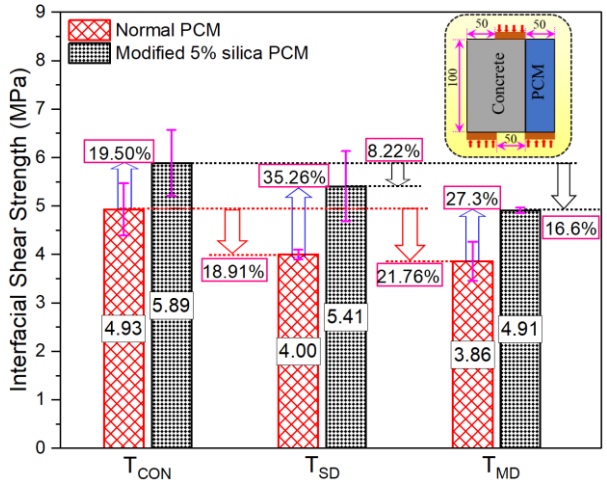

(a) Comparion of interfacial bond strength

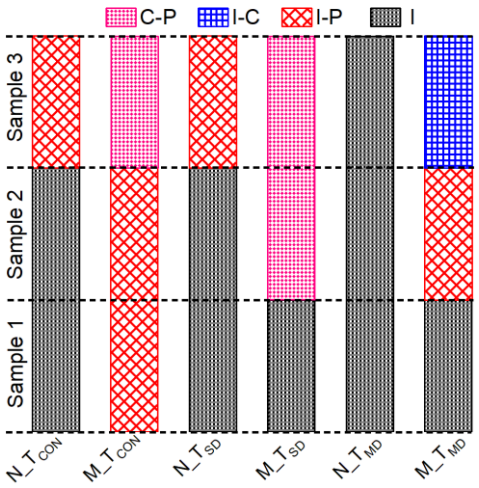

(b) Fracture mode

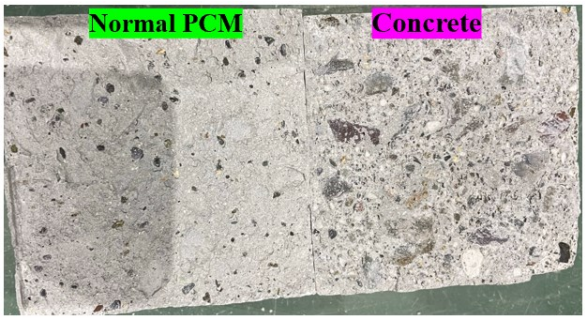

(c) Pure interface fracture (I) under T_{MD}

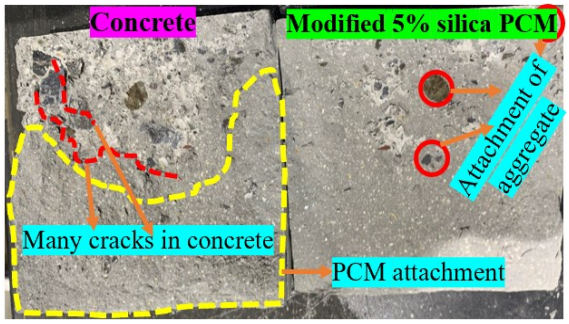

(d) Mixed mode fracture (C-P) under T_{SD}

Figure 4-12 Interfacial strength at elevated temperature (T_{SD} and T_{MD}) along with fracture mode

The behaviour of the composite specimens with silica fume inclusion under exposure to constant elevated temperature was also discussed in light of the fracture mode. The fracture mode of all the composite specimens evaluated after loading test under T_{SD} and T_{MD} along with control cases are presented in Figure 4.12(b). Adhesive pure interface (I) fracture mode was observed as major failure type in composite specimen repaired with normal PCM, both at control cases (tested before any exposure condition) and after exposure condition (T_{SD} and T_{MD}). Examples of adhesive pure interface (I) fracture mode of the composite specimens repaired with normal PCM is shown in Figure 4.12(c). The composite specimens repaired with 5% silica PCM exhibited only one pure interface fracture (I) mode under T_{SD} and T_{MD}, whereas control specimen (tested before any exposure condition) do not include any pure interface fractures. An examples of mixed fracture mode (I-P) of the composite specimens repaired with modified 5% silica PCM is shown in Figure 4.12(d). PCM attachment were found in almost whole substrate concrete surface which indicates the degradation of PCM more than

the degradation of adhesive interface as PCM is sensitive to high temperature. Higher number of specimens failure in composite or mixed mode fracture in modified PCM cases indicate higher adhesion of modified PCM overlay with substrate concrete with better durability under short and long duration exposure at elevated temperature.

4.3.2.2 Influence of temperature cycle

Real environmental condition was assumed considering cyclic temperature exposure by simulating the day-night and seasonal variation for the durability of the repaired system and provided in the laboratory in programmed oven. The temperature were set at 60°C for 12 hours and 30°C for another 12 hours for the day-night variation case (T_{DN}) and tested after 30 days of exposure. Interfacial strength reduction was observed under T_{DN} in both normal and modified PCM specimens compared to its corresponding control specimens tested before any exposure condition (T_{CON}) as presented in Figure 4.13(a). The percentage reduction of the interfacial strength of the exposure specimen (T_{DN}) compared to the control specimens were almost half for the case of 5% silica PCM than that of normal PCM specimens. The strength increases of about 42% in modified PCM cases compared normal PCM specimens under T_{DN} confirm the positive influence of the inclusion of silica fume with PCM as a repaired mortar. The fracture mode of all three normal PCM composite specimen tested after temperature exposure (T_{DN}) were observed pure interface fracture (I), whereas two out of three specimen with modified 5% silica PCM exhibited mixed (I-P) fracture mode as presented in Figure 4.13(b). Even though the PCM is very sensitive to high temperature [22, 42], the occurrence of pure interface fracture in normal PCM specimens [Figure 4.13(c)] indicates that the normal PCM-concrete interface is more vulnerable under cyclic temperature condition exposure. On contrast, in the pictural view of the fracture surface of the modified 5% silica PCM specimen, the PCM attachment on concrete side was observed as shown in Figure 4.13(d) that verify the degradation of PCM more than the adhesive interface at elevated temperature.

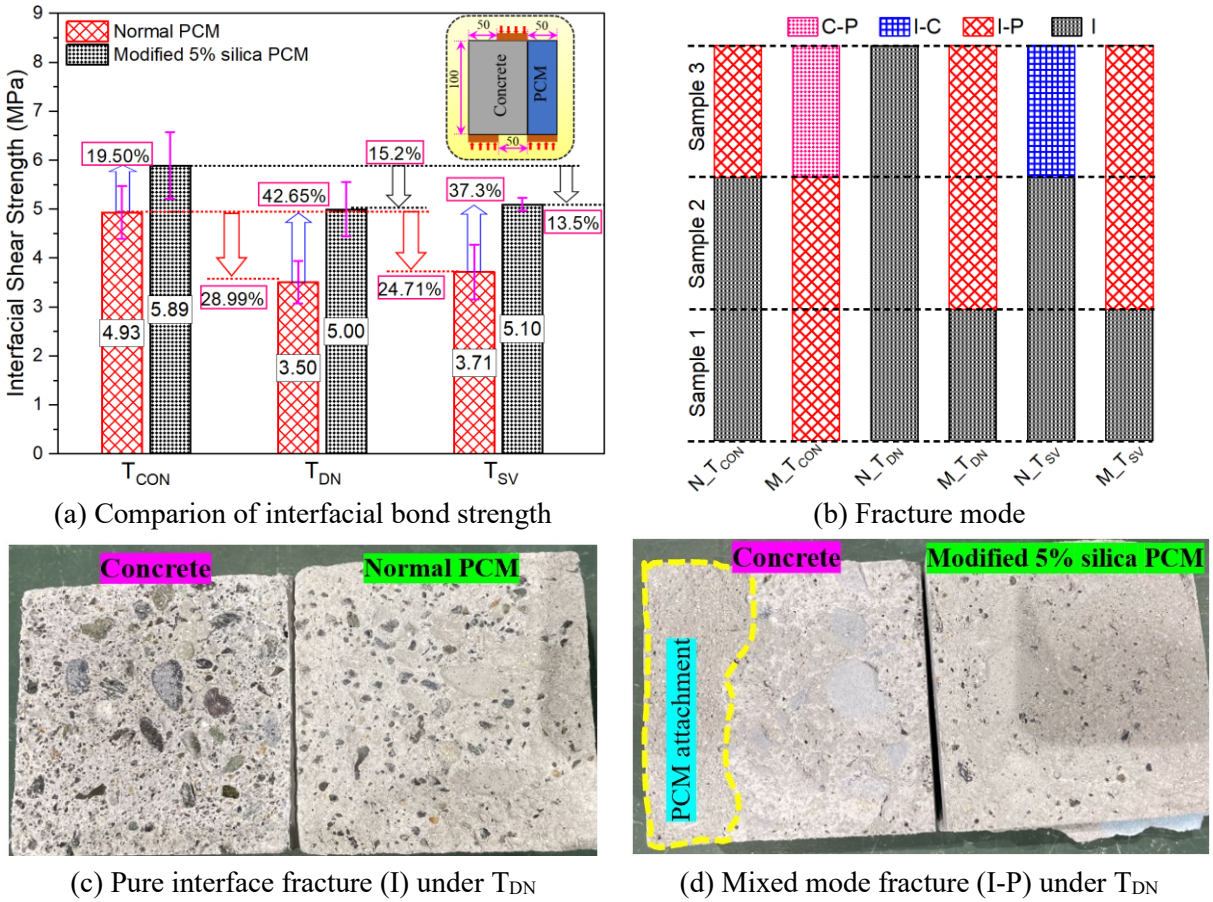

(a) Comparion of interfacial bond strength

(b) Fracture mode

(c) Pure interface fracture (I) under T_{DN}

(d) Mixed mode fracture (I-P) under T_{DN}

Figure 4-13 Interfacial strength under cyclic temperature exposure (T_{DN} and T_{SV}) with fracture mode

The temperature variation of four season (summer, rainy, winter and spring) was simulated by exposing the specimen in each environment for 24 hours in the laboratory. One cycle of the seasonal variation exposure condition (T_{SV}) was completed in four days and the mechanical loading test were performed to evaluate the bonding strength after 12 cycles of exposure (48 days). The strength reduction of 24.7% and 13.5% were observed under T_{SV} for normal PCM and modified 5% silica PCM, respectively compared to T_{CON} specimens as presented in Figure 4.13(a). The bond strength reduction was relatively low in the constant temperature exposure compared to the reduction in cyclic temperature condition exposure. The polymers in the PCM may degrade and cannot recover fully due to the cyclic temperature variation. Owing to cyclic condition, additional stress may generate at the interface and creates a condition of generating micro-cracks resulting significant reduction in the bonding strength. The outcome of higher interfacial strength (about 37%) as presented in Figure 4.13(a) and a smaller number of pure interface fracture (I) mode as presented in Figure 4.13(b) under T_{SV} in modified 5% silica PCM specimens suggested a positive influence of the inclusion of silica fume with PCM as a repaired mortar. This can be attributed by the formation of more hydrogen bond at the interface with strong binding force and by generating denser microstructure of the interface (micro-filler effect) due to incorporation of extremely fine and reactive silica fume with PCM. Conclusively, silica fume improves the durability of the composite specimen under cyclic temperature conditions.

4.3.3 Series-III (Effect of moisture content)

4.3.3.1. Wetting and drying cycles

The composite specimens were exposed to cyclic 2 days wetting followed by 2 days drying condition to study the influence of simultaneous wetting and drying (W/D) condition on the interfacial strength. One W/D cycle was completed in four days and the mechanical loading test were performed to evaluate the bonding strength after 0, 12 and 24 cycles of exposure. The interfacial strength reduction was observed with the increase of the W/D cycles both in normal and modified PCM specimens as presented in Figure 4.14(a).

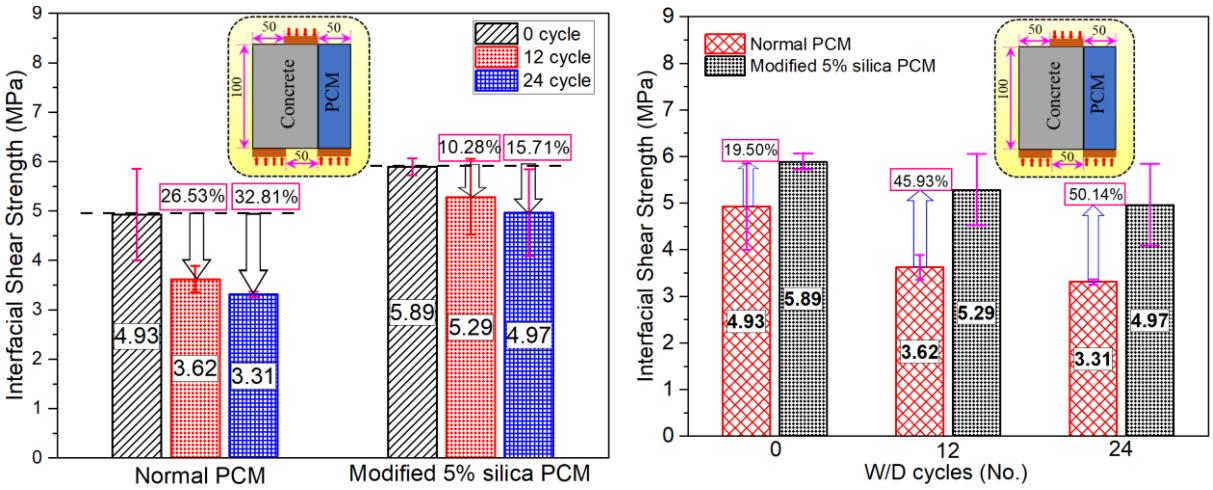

Figure 4-14 Bonding strength of the composite specimen under moisture content (W/D cycles)

The strength reduction might cause due to presence of moisture at interface. In W/D cycle condition, the presence of moisture at the interface exert water pressure causing micro cracks that deteriorates the interfacial bonding during continuous wetting and drying, resulting significant reduction in the bonding strength. The strength reduction was only about 15% in case of modified 5% silica PCM specimen, whereas it was more than 30% in case of normal PCM specimen compared to its corresponding control specimens tested before any exposure condition (0 cycle). To evaluate the influence of silica fume, the interfacial strength of the composite specimens with/without silica fume were compared under different W/D cycle exposure and presented in Figure 4.14(b). In all exposure states of W/D cycles, the modified 5% silica PCM specimens showed higher interfacial bonding strength compared to normal PCM specimens. The use of silica fume reduces the porosity of the

interface due to its extreme fineness, thus reduces moisture presence at the void space. This will cause less presence of moisture at the void space and reduce the impact of water pressure during continuous wetting and drying, thus decreasing the damage degradation under W/D cycles. In addition, the formation of more C-S-H with strong binding force with silica fume inclusion helps to acquire adequate bond between concrete substrate and repair material (as mentioned in Chapter 2 and Chapter 3), thus reduces the damage initiation and propagation along the interface under W/D cycles.

The behaviour of the composite specimens with/without silica fume inclusion under exposure to W/D cycles was also discussed in light of the fracture mode. The fracture mode of all the composite specimens tested after 0, 12 and 24 W/D cycles of exposure is presented in Figure 4.15(a-b). The acronym designation adopted are as follows: the first letter "N" or "M" refers to normal or modified 5% silica PCM followed by exposure condition and exposure duration. For example, N_W/D_12C refers to a composite specimen with normal PCM exposed under wetting and drying condition and tested after 12 cycle of exposure. The fracture modes of all normal PCM specimens was pure interface fractures (I) irrespective of the number of W/D cycles, whereas the specimen with 5% silica PCM exhibited only one pure interface fracture (I) and two cases of composite or mixed fracture mode, such as (I-P) or (I-C). A smaller number of pure interface fracture (I) in modified 5% silica PCM specimens compared to normal PCM specimens indicates higher adhesion of modified PCM overlay with substrate concrete with better durability.

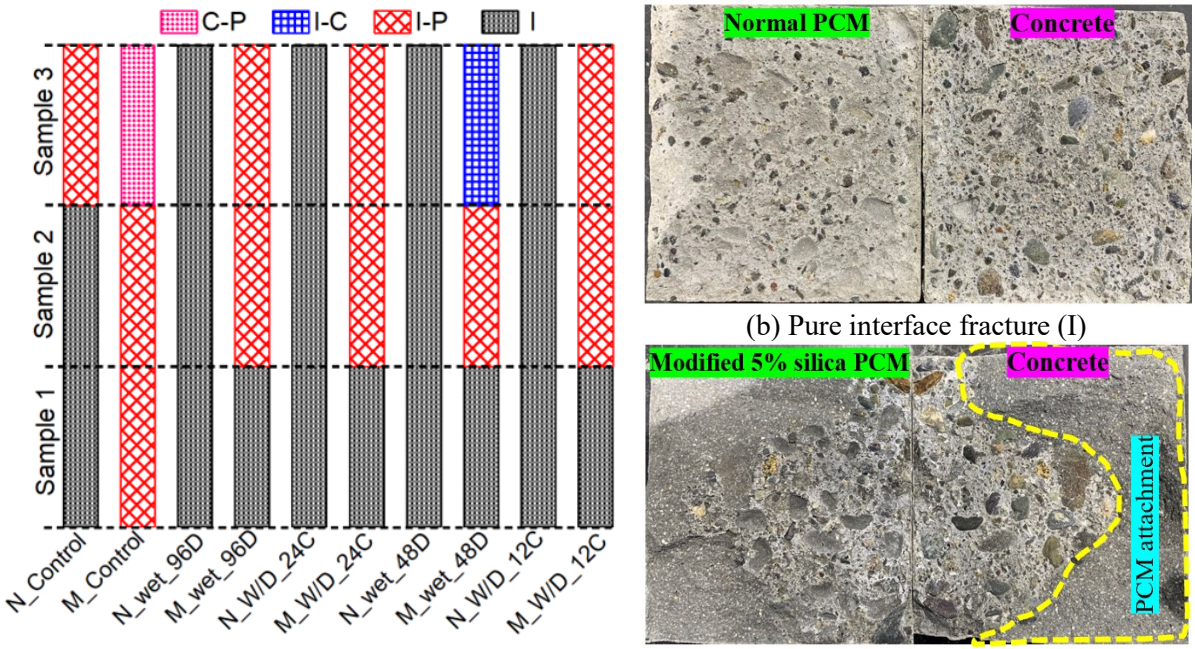

(a)

(b) Pure interface fracture (I)

(c) Mixed mode fracture (I-P)

Figure 4-15 Bonding strength of the composite specimen under moisture

Statistical analyses of the experimental data of interfacial bonding strength obtained from the loading test were performed using a one-way ANOVA to evaluate the influence of silica fume as a repair mortar under W/D cycles and presented in Table 4.5. The calculated F-value of the modified 5% silica PCM specimens (5.17) were obtained smaller compared to normal PCM specimens (14.92). Following the significant criteria mentioned in Chapter 2 (Table 3.4) and comparing the calculated and critical values, it was confirmed that the exposure condition of W/D cycle have less effect on the interface of modified 5% silica PCM-concrete interfacial strength compared to the interface of normal PCM-concrete that have highly significant effect under W/D cycle. Conclusively, the experimental and statistical results imply that the inclusion of silica fume with PCM as a repair material is very important to achieve good interfacial bonding strength under W/D cycle.

Table 4-5 Statistical analysis of the influence of moisture on the interfacial bonding strength

Factors and exposure conditions			Interfacial shear strength (MPa)			*SS*	*DF*	*MS*	*F* value	F_x	Level of Significance
W/D cycles	Normal PCM	0 cycle	5.60	4.27	6.05	5.98	1	5.98		$F_{0.1}$ = 3.46	Highly Significant effect (a)
		12 cycle	3.90	3.36	3.61	2.80	7	0.40	14.92	$F_{0.05}$ = 5.14	
		24 cycle	3.28	3.37	3.27	--	--	--		$F_{0.01}$ = 10.92	
	Modified 5% silica PCM	0 cycle	6.27	6.30	5.11	2.70	1	2.70		$F_{0.1}$ = 3.46	Significant effect (d)
		12 cycle	4.52	6.05	5.29	3.66	7	0.52	5.17	$F_{0.05}$ = 5.14	
		24 cycle	5.47	4.46	3.72	--	--	--		$F_{0.01}$ = 10.92	
Continuous immersion	Normal PCM	0 days	5.60	4.27	6.05	5.20	1	5.20		$F_{0.1}$ = 3.46	Significant effect (b)
		48 days	3.93	3.92	4.78	3.67	7	0.53	9.92	$F_{0.05}$ = 5.14	
		96 days	4.14	3.67	2.51	--	--	--		$F_{0.01}$ = 10.92	
	Modified 5% silica PCM	0 days	6.27	6.30	5.11	0.07	1	0.07		$F_{0.1}$ = 3.46	No or Very little effect (d)
		48 days	5.41	6.22	5.63	1.46	7	0.21	0.31	$F_{0.05}$ = 5.14	
		96 days	5.48	5.54	6.03	--	--	--		$F_{0.01}$ = 10.92	

4.3.3.2 Continuous immersion in water

The composite specimens were immersed in water to study the influence of continuous immersion in water on the interfacial strength. The mechanical loading test were performed to evaluate the bonding strength after 0, 48 and 96 days of exposure. The interfacial strength reduction of about 20% were observed after 96 days of exposure compared to control cases tested before any exposure condition (zero immersion day) of normal PCM specimens, whereas its effects was found marginal in case of modified PCM specimens, as presented in Figure 4.16(a).

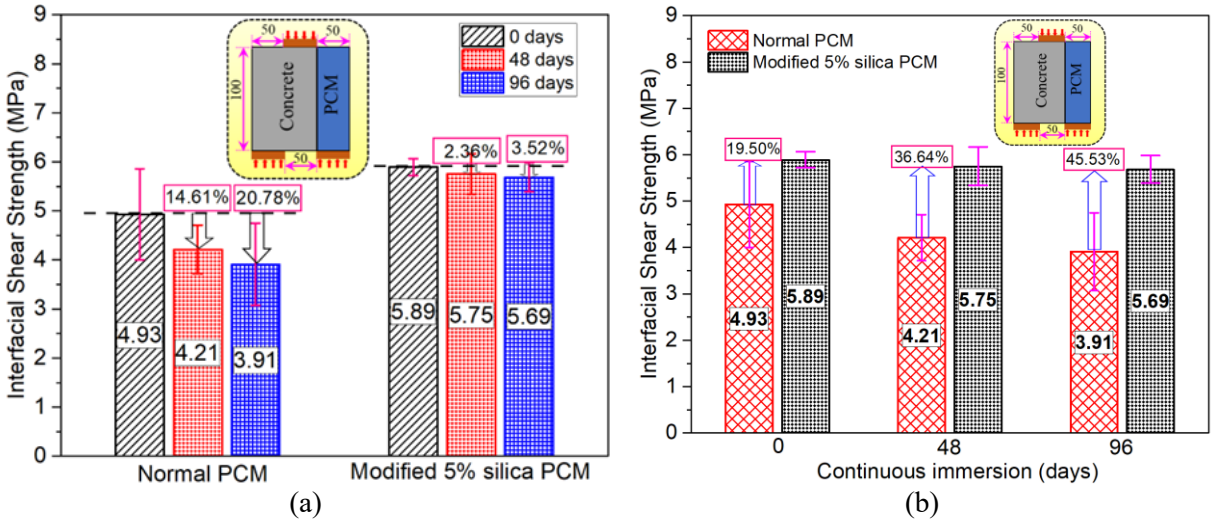

Figure 4-16 Bonding strength of the composite specimen under moisture (continuous wetting)

The presence of extra moisture at the interface of normal PCM specimens due to higher porosity loosen the cohesion of the polymers by swelling and dissolve the polymer films, resulting strength reduction [43]. The absorbed water in modified 5% silica PCM specimens is quite limited during continuous wetting due to lowering of porosity with silica fume inclusion, thus its effect on modified specimens is marginal. The effect on interfacial bonding strength in continuous immersion in water was lower compared to the W/D cycle strengths at the same age after the moisture exposure starts. Continuous immersion in water provides suitable environment for the hydration and curing of PAE PCM. In addition, in continuous immersion cases, presence of moisture at interface hydrates the concrete and presence of hydroxyl group in concrete makes hydrogen bond with the PCM and gives extra adhesion to the composite specimen [44].

The influence of silica fume was evaluated by comparing the outcome of the interfacial strength of the composite specimens with/without silica fume after 0, 48 and 96 days of continuous wetting, as presented in Figure 4.16(b). Higher interfacial bonding strength was observed in modified 5% silica PCM specimens compared to normal PCM specimens at all exposure states of continuous immersion. Statistical analyses of the experimental data using a one-way ANOVA presented in Table 4.5 confirmed that the exposure condition of continuous wetting have very little effect on the interface of modified 5% silica PCM-concrete interfacial strength compared to the interface of normal PCM-concrete that have significant effect. The influence of silica fume incorporation was also evaluated by comparing the fracture mode of the composite specimens with/without silica fume. The fracture mode of all the specimens tested under the exposure of continuous immersion is shown in Figure 4.15(a). As an example, the pictural view of the fracture surface after the loading test of the normal PCM and Modified 5% silica PCM specimen is shown in Figure 4.15(b) and Figure 4.15(c), respectively. A smaller number of pure interface fracture (I) in modified 5% silica PCM specimens compared to normal PCM specimens indicates higher adhesion of modified PCM overlay with substrate concrete. Continuous immersion in water provides suitable environment for the hydration and curing of silica fume modified PCM. In addition, free alkali after the hydration of cement reacts with the silica compound of silica fume under the water supply condition to form an additional C-S-H hydrates, resulting better bonding performance of the composite under continuous wetting condition. Conclusively, the inclusion of silica fume with PCM as a repair material is very important to achieve good interfacial bonding strength under continuous wetting.

4.4 Conclusions

The experimental study was conducted on the interface behavior between substrate concrete and two types of repairing mortars (normal PCM and modified 5% silica PCM). Different environmental condition, by considering freezing and thawing, elevated temperature fluctuation and moisture content were assumed in this experimental work. The influence of such exposure condition on the bonding strength of the composite specimens with/without silica fume was investigated and the following conclusions were drawn.

- The freeze-thaw cycles had significant negative influences on bonding behaviors of substrate concrete-PCM interface. The damage progress, occurrence of interface fracture and degradation of interfacial bonding strength under FTC significantly influenced by the constituents of the repairing mortar. The splitting tensile strength of normal PCM composite under FTC decreases more quickly than that of modified 5% silica PCM composite. Normal PCM composite causes earlier occurrences of the sharp decline and more decrease of interfacial strength than that of modified silica PCM specimens.
- Mixing silica fume with PCM significantly increase interfacial bonding strength, provides better adhesion with substrate concrete and improves the durability of the interfacial performance of concrete-PCM interface under harsh freeze-thaw environments
- The exposure of the composite specimens at elevated temperature (60°C) significantly reduces the interfacial bonding strength. Specimens repaired with normal PCM results more decrease of interface shear strength than that of modified PCM compared to its corresponding reference specimens under both short duration (3 days) and long duration (30 days) exposure at constant 60°C temperature. Earlier occurrence of interface fracture and a greater number of pure interface

fracture mode in normal PCM specimens compared to modified 5% PCM specimens indicates higher adhesion of modified PCM overlay with substrate concrete with better durability under short and long duration exposure at elevated temperature.

- The reduction of interfacial strength further increases under cyclic temperature conditions resulting more detrimental influence of the elevated temperature on the interfacial bonding strength. Mixing silica fume with PCM significantly increase interfacial bonding strength (about 40% compared to normal PCM cases), provides better adhesion with substrate concrete (occurrence of composite or mixed mode fracture instead of pure interface fracture that happened in normal PCM cases) and improves the durability of the interfacial performance of concrete-PCM interface under cyclic temperature conditions.
- The interfacial strength of normal PCM specimens significantly reduced under both wetting and drying condition and continuous immersion compared to the reference specimens. The interfacial strength of modified 5% silica PCM specimens reduced insignificantly under continuous immersion exposure and reduced moderately under wetting and drying, compared to reference specimens.
- The inclusion of silica fume significantly improves the interfacial bonding strength compared to without silica fume cases under the influence of moisture by wetting/drying and continuous immersion.
- The influence of moisture under continuous immersion results lower reduction of interfacial strength compared to the exposure under wetting and drying cycle at the same age after the moisture exposure starts for both the normal PCM and 5% silica PCM specimens.

In conclusion, the use of silica fume achieves adequate bond strength with concrete substrate, improves adhesion and durability under harsh environmental conditions. Considering ease in practical application, environmentally friendly nature, and ability to achieve adequate bond strength with concretes substrate (under environmental condition), this study can provide an indication to practitioner for engineering application of silica fume in polymer cement-based repair materials under harsh environment.

Reference

[1] Kim, J., Moon, J.H., Shim, J.W., Sim, J., Lee, H.G. and Zi, G. (2014). "Durability properties of a concrete with waste glass sludge exposed to freeze-and-thaw condition and deicing salt." *Construction and building materials*, *66*, 398-402.

[2] Song, Y.P. and Ji, X.D. (2006). "Analysis on reliability of concrete under freezing thawing action and evaluation of residual life." *Journal of Hydraulic Engineering, 37*(3), 259-263.

[3] Jiang, L., Niu, D., Yuan, L. and Fei, Q. (2015). "Durability of concrete under sulfate attack exposed to freeze–thaw cycles." *Cold Regions Science and Technology*, *112*, 112-117.

[4] Hamoush, S. and Picornell,D. M. (2011). "Freezing and thawing durability of very high strength concrete." American Journal of Engineering and Applied Sciences 4(1): 42–51.

[5] Tuyan, M., Mardani,A. and Ramyar, K. (2014). "Freeze–thaw resistance, mechanical and transport properties of self-consolidating concrete incorporating coarse recycled concrete aggregate." Materials & Design 53: 983–991.

[6] Song, W.L., Li, X.F. and Ma, K.F. (2010)/ "The effect of freeze-thaw cycles on mechanical properties of concrete," *Advanced Materials Research*, 163-167, 3429–3432.

[7] Shang, H. and Song, Y. (2008). "Behavior of air-entrained concrete under the compression with constant confined stress after freeze-thaw cycles." *Cement and Concrete Composites*, 30(9), 854–860.

[8] Gong, F., Sicat, E., Zhang, D. and Ueda, T. (2015). "Stress analysis for concrete materials under multiple freeze-thaw cycles." *Journal of Advanced Concrete Technology, 13*(3), 124-134.

[9] Hasan, M., Ueda, T. and Sato, Y. (2008). "Stress-strain relationship of frost-damaged concrete subjected to fatigue loading." *Journal of Materials in Civil Engineering, 20*(1), 37-45.

[10] Nili, M., Azarioon, A. and Hosseinian, S. M. (2017). "Novel internal-deterioration model of concrete exposed to freezethaw cycles." *Journal of Materials in Civil Engineering, 29*(9), 04017132.

[11] Qian, Y., Zhang, D., and Ueda, T. (2016). "Interfacial Tensile Bond between Substrate Concrete and Repairing Mortar under Freeze-Thaw Cycles." Journal of Advanced Concrete Technology, 14; 421-432.

[12] Jun, T., Xiaowei, W., Yu, Z., Shaowei, H., Wei, R., Yinfei, D., Wenwei, W., Can, S., Jie, M. and Yuxiao, Y. (2019). "Investigation of damage behaviors of ECC-to-concrete interface and damage prediction model under salt freeze-thaw cycles." Construction and Building Materials 226; 238–249.

[13] Ali, S. and Reza, K.K. (2017). "Bonding durability of polymer-modified concrete repair overlays under freeze–thaw conditions." Magazine of Concrete Research, 69(24), 1268–1275.

[14] Al-Jabri, K.S., Hago, A.W., Al-Nuaimi, A.S. and Al-Saidy, A.H. (2005). "Concrete blocks for thermal insulation in hot climate. Cement and Concrete Research; 35(8):1472-9.

[15] Al-Gahtani, A.S.R. and AI-Mussallam, A.A. (1995). "Performance of repair materials exposed to fluctuation of temperature. Journal of Materials in Civil Engineering;7:9-18.

[16] Henry, M., Darma, I. S. and Sugiyama, T. (2014). "Analysis of the effect of heating and re-curing on the microstructure of high strength concrete using X-ray CT," *Construction and Building Materials*, 67;37–46.

[17] Luo, X., Sun, W. and Chan, Y. N. (2012). "Residual compressive strength and microstructure of high performance concrete after exposure to high temperature." *Materials and Structures*, 33(5), 294–298.

[18] Akca, A. H. and Ozyurt, N. (2018). "Effects of re-curing on micro- ¨structure of concrete after high temperature exposure," *Construction and Building Materials*, 168, 431–441.

[19] Chang, Y. F., Chen,Y. H., Sheu, M. S. and Yao, G. C. (2006). "Residual stress–strain relationship for concrete after exposure to high temperatures," *Cement and Concrete Research*, 36(10), 1999–2005.

[20] Chen, B., Li, C. and Chen, L. (2009). "Experimental study of mechanical properties of normal-strength concrete exposed to high temperatures at an early age," *Fire Safety Journal*, 44(7), 997–1002.

[21] Zhai, Y., Deng, Z., Li, N. and Xu, R. (2014). "Study on compressive mechanical capabilities of concrete after high temperature exposure and thermo-damage constitutive model," *Construction and Building Materials*, 68(3), 777–782.
[22] Ries, M. L. (2012). "Effect of Temperature on the Mechanical Properties of Polymer Mortars." Materials Research; 15(4): 645-649
[23] Hassan, K.E., Robery, P.C and Al-Alawi, L. (2009). "Effect of hot-dry curing environment on the intrinsic properties of repair materials." Cement and Concrete Composites;22(6):453-458
[24]Tamon, U., Rashid, K., Ye, Q., & Dawei, Z. (2017). Effects of temperature and moisture on concrete-PCM interface performance. *Procedia Engineering*, *171*, 71-79.
[25]Rashid, K., Ueda, T., Zhang, D., Miyaguchi, K. and Nakai, H. (2015). "Experimental and analytical investigations on the behavior of interface between concrete and polymer cement mortar under hygrothermal conditions. Construction and Building Materials;94:414-25.
[26] Rashid, K., Ueda, T., Zhang, D. and Miyaguchi, K. (2015). "Study on influence of temperature on bond integrity between polymer cement mortar and concrete." International Conference on Advances in Construction Materials, Whistler, Canada; 2015
[27] Hassan, K.E, Brooks, J.J and Al-Alawi, L. (2001). "Compatibility of repair mortars with concrete in a hot-dry environment. Cement and Concrete Composites;23(1):93-101.
[28] Park, D., Ahn, J., Oh, S., Song, H. and Noguchi T. (2009). "Drying effect of polymer-modified cement for patch repaired mortar on constraint stress." Construction and Building Materials;23(1):434-47.
[29] Ohama, Y. (1995). "Handbook of polymer-modified concrete and mortars-properties and process technology." New Jersy, Noyes Publications.
[30] ASTM C666-03. (2008). "*Standard test method for resistance of concrete to rapid freezing and thawing.*" ASTM, Philadelphia, PA.
[31] ASTM C 39-03. (2003). "Standard test method for compressive strength of cylindrical concrete specimens." USA.
[32] Li, G., Xie, H. and Xiong, G. (2001). "Transition zone studies of new-to-old concrete with different binders." *Cement and Concrete Composites.*, 23, 381–387.
[33] Rashid, K., Ueda, T. and Zhang, D., (2016). "Study on Shear Behavior of Concrete-polymer Cement Mortar at Elevated Temperature." Civil Engineering dimensions, 18(2), 93-102.
[34] ASTM C496, (1996). "*Standard test method for splitting tensile strength of cylindrical concrete specimens*." ASTM, Philadelphia, PA.
[35] Rocco, C., Guinea, G.V., Planas, J. and Elices, M. (1999). "Size effect and boundary conditions in the Brazilian test: theoretical analysis." Materials and Structures, 32(6):437-44.
[36] Powers, T. C. (1945). "*A working hypothesis for further studies of frost resistance of concrete.*" Portland Cement Association, Research Laboratory, 28p.
[37] Powers, T. C. and Helmuth, R. (1953). "*Theory of volume changes in hardened portland-cement paste during freezing*." Portland Cement Association, Research Laboratory, 12p.
[38] Scherer, G. W. and Valenza, J. J. (2005). "Mechanisms of frost damage." *Materials Science of Concrete VII*, American Ceramic Society, 209-246.
[39] ASTM E1876-09, (2009). "*Standard test method for dynamic Young's modulus, shear modulus, and Poisson's ratio by impulse excitation of vibration*." ASTM, Philadelphia, PA.
[40] Galle C. (2001). "Effect of drying on cement-based materials pore structure as identified by mercury intrusion porosimetry: A comparative study between oven-, vacuum-, and freeze-drying." Cement and Concrete Research. 31(10):1467-77.
[41] Bazant, P. and Kaplan, F. M. (1988)." Effect of Temperature and Humidity on fracture Energy of Concrete." ACI Material Journal, 262-71.
[42] Biswas, M. and Kelsey, R.G. (1991). "Failure model of polymer Mortar." Journal of Engineering Mechanics, 117(5):1088–104.
[43] Knapen, E and Gemert, D.V. (2009). "Effect of under water storage on bridge formation by water-soluble polymers in cement mortars." Construction and Building Materials, 23(11):3420-5.
[44] Chen, C.H., Huang, R. and Wu, J.K. (2006). "Influence of soaking and polymerization conditions on the properties of polymer concrete." Construction and Building Materials. 20(9):706-12.

Chapter 5
PERFORMANCE OF PCM STRENGTHENED RC BEAM WITH/WITHOUT SILICA FUME AS REPAIR MATERIAL

5.1 Introduction

Currently, there is a tremendous demand of strengthening or upgradation of existing RC structures due to ageing as well as increase in service loads that traditionally been achieved by enlarging the member sections using external bonding [1-3] or cementitious material [4-8]. In the last several decades, the use of PCM become a promising candidate as a cementitious matrix material of the strengthening layer because of its superior properties over ordinary concrete/cement mortar. In PCM retrofitting methods, the strengthening bars are fixed underneath the RC members followed by spraying/troweling of PCM as the use of PCM alone cannot perform efficiently due to its low tensile strength. The PCM overlaid to the tension side surface of reinforced concrete RC structure often performs to upgrade the flexural capacity and stiffness [9-10] and reduce deformation and alleviate stress of the repaired structures [11]. An improvement in fatigue resistance were also observed in laboratory test by using this method of strengthening [12]. Despite an increase in load carrying capacity of the PCM strengthened RC beams, experimental observation has shown the occurrence of different premature debonding failure modes like concrete cover separation, peeling off in the constant moment zone, peeling off in the shear flexure and overlay end zone which led to not fully utilization of its capacity and hinders the worldwide application of this method [9-10, 13]. Therefore, from the perspective of practical application of PCM overlaying method, the processes and procedures of this method should be improved to reduce the occurrence of premature debonding failure as well as to increase the load carrying capacity of the strengthened structures. As a possible means silica fume is intending to use with PCM as a repair mortar. It was concluded form the material level test mentioned in the previous chapters that the inclusion of silica fume with PCM as a repair material significantly improve the concrete-PCM interfacial bonding strength and durability. For a successful strengthening techniques, an improvement in the performance level concerning load carrying capacity and failure modes should also be achieved at material level.

To understand the performance of PCM strengthened members with or without silica fume at material level, experiments were conducted on RC beams with the aim to use silica fume in practical PCM overlaying method. The primary focus of this work is to enhance the concrete-PCM interfacial bond by using silica fume with PCM as a repair material to prevent premature debonding failure which was reported in the technical literature as one of the major failure mode of PCM strengthened RC beams [9-10, 13-14] and increase the serviceability of the deteriorated structures. In the past research, it was mentioned that the use of cementitious material alone may not be efficient unless a very thick layer of overlay (not preferable in practice) applied for the structural strengthening of existing RC members [15-16]. Considering this issue, the flexural strengthening performance of PCM strengthened RC beams with or without silica fume was investigated using three types of commonly used tensile strengthening bar (conventional reinforcement, CFRP strand sheet and CFRP grid). Conventional material such as steel is readily available and cost effective material, but its higher tensile stiffness may cause higher stress concentrating generating interfacial cracks. On the other hand, CFRP strand sheet and CFRP grid has becomes a highly attractive alternatives to the traditional overlaying bar due to its superior properties concerning high strength-to-weight ratio and highly durable nature [17-20]. In this research work, an efforts have been made to use modified 5% silica PCM together with tensile reinforcement for structural strengthening purpose to validate the positive influence of modified 5% silica PCM as an excellent matrix and bonding agent. The effectiveness of the conventional rebar, CFRP strand sheet and CFRP grid as a strengthening overlay bar also discussed in the viewpoint of load carrying capacity and failure modes.

Considering the above background, detailed experiments were designed to evaluate the behavior of PCM strengthened RC beams with or without silica fume as a repair material. Total 14 RC beams were cast and strengthened with two type of conventional rebar (D6 and D10), three types of CFRP grid with changing tensile stiffness (low, medium, and high) and adding different amount of CFRP

strand sheet by changing its width (50mm and 150mm) at soffit of beams and covered by troweling with normal and modified 5% silica PCM. The performance of PCM strengthened beams using particular strengthening bars with or without silica fume were compared under different heads, viz. failure modes, load deflection relationship, ultimate load, debonding load and, strain value and strain distribution of the strengthening bar along the beam. The ultimate load of strengthened beams considering perfect bond between substrate concrete-overlay material were also calculated and compared with the experiment results.

5.2 Experimental methodology

5.2.1 Material properties

In this experimental work, ready mixed concrete with target compressive strength of 40 MPa supplied by a local concrete company was used to cast all the un-strengthened RC beams at the same batch to minimize the experimental scatter. Five cylindrical specimens (ϕ150 mm×300 mm) were used to determine the compressive strength of the concrete. The tensile steel bars of 16mm dia bar while compression and shear reinforcement of 6mm dia bar and 10mm dia bar respectively were used to prepared reinforced RC beams. The properties of all the steel rebars used in this research work are presented in Table 5.1. For the flexural strengthening of RC beams, normal PCM or modified 5% silica PCM were used as a cementitious matrix to impregnate overlay reinforcement to form an external overlay. PCM containing poly acrylic ester (PAE) [Figure 5.1(a)] having same properties as reported in detail in Chapter 2 (Section 2.2.2) and same silica fume [Figure 5.1(b)] as reported in detail in Chapter 2 (Section 2.2.3) was used to prepare overlaying cementitious matrix. As an overlaying reinforcement, three types of commonly used tensile strengthening bar were used. Steel rebar of grade SD295A (D6 and D10) having mechanical properties as mentioned in Table 5.1 were used as one of the types of overlaying reinforcement.

(a) PCM (b) Silica fume (c) CFRP grid (d) CFRP strand sheet

Figure 5-1 Overlaying material used in this experimental work

Commercially available CFRP grid made up of untwisted yarns of continuous carbon fibers with thermoset epoxy resin impregnation and having nominal dimensions of 50 mm × 50 mm, as shown in figure 5.1(c) were used as other types of overlaying reinforcement. Three kinds of CFRP grids with different stiffness (low, medium and high) were used in the experimental program, which are designated as FTG-CR4, FTG-CR6 and FTG-CR8, according to the product datasheet provided by the manufacturer (Nippon Steel Co., Ltd, Japan). The mechanical properties of three types of CFRP grid used in this experimental program is tabulated in Table 5.2. Strand sheet made up with high tensile strength carbon fiber individually impregnated with resin [Figure 5.1(d)] were also used as an overlaying reinforcement, which are designated as FSS-HT-600 in the product datasheet provided by the manufacturer (Nippon Steel Co., Ltd, Japan). The used CFRP strand sheet in this research work has a nominal thickness of 0.333 mm and mechanical propertied as tabulated in table 5.2. It was used in two different amount by changing its width (50mm and 150mm).

Table 5-1 Properties of steel reinforcement

Steel reinforcement diameter	Area (mm^2)	Yield strength (MPa)	Elastic modulus (MPa)
D6	56.10	329	200000
D10	142.5	366	200000
D16	402.12	398	200000

Table 5-2 Properties of CFRP grid and CFRP strand sheet

Properties	CFRP grid			CFRP Strand Sheet	
	FTG-CR4	FTG-CR6	FTG-CR8	50mm width	150mm width
Area (mm^2)	13.2	35	52.8	16.65	49.95
Tensile strength (MPa)	1400	1400	1400	3400	3400
Elastic modulus (MPa)	110000	110000	110000	245000	245000

5.2.2 Details of the specimens

A total of 14 simply-supported RC beams with dimensions of 150x150x1440 mm having shear span ration of 3.5 were prepared and tested under four-point bending loading, as illustrated in Figure 5.2(a). Two rebars of diameter 6mm and 16mm were used as compression and tension reinforcement respectively. The concrete cover thickness was kept 25mm in every direction. The rebar of diameter 10mm were used as shear stirrups with 80mm spacing. The PCM was overlayed having a thickness of 20mm and a bond length of 1040 mm leaving 50mm free space from the supports as illustrated in Figure 5.2(a-b). The configuration of different types and amount of tensile strengthening bar with different cementitious matrix used in this research work is presented in figure 5.1(b). Seven different configuration of strengthening reinforcement were employed and two beams were cast with each strengthening reinforcement configuration, one was with normal PCM mortar and the other one was using modified 5% silica PCM to understand the influence of silica fume. In addition, several strain gauge were attached at different position of the strengthening bar as presented in Figure 5.1(c) to monitor the strain response of the reinforcing bar upon loading.

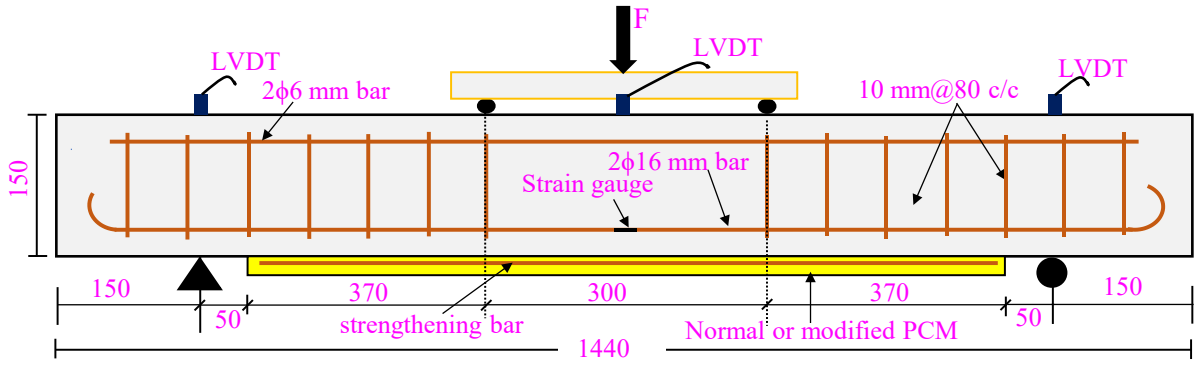

(a) Testing arrangement of four-point loading test

(b) cross sectional area of strengthened beams with different reinforcement in overlay

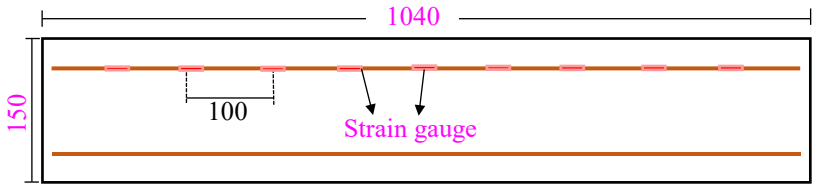

(c) layout of strain gauge attached at the overlay reinforcement

Figure 5-2 Detail of overlay strengthened beams with loading set-up (unit: mm)

5.2.3 Specimen preparation

The steel cage were prepared beforehand by tiring tensile, compression and shear reinforcement as shown in Figure 5.3(a). The tension reinforcements were bent at the ends to prevent failure near support end. At the center of each tension reinforcements, two steel strain gages were attached (diametrically opposite on the ribs) and covered with water resistant tapes to avoid damage during casting and inside the beam. Wooden molds were prepared for casting RC beams of size 150x150x1440 mm as shown in Figure 5.3(b). At the bottom of the molds, some amount of retarder were spread after mixing with water to prepare surface roughness and the prepared steel cage were placed inside of the wooden (tension reinforcements were on bottom) to expose the tension surface for surface preparation and casting of PCM layer later. Spacing of the steel cage from bottom was maintained by providing two spacers of height of 25 mm. Ready mixed concrete were placed in the wooden mold with steel cage to prepare RC beams. Once the concrete were cast in all molds, it was compacted and covered with water-soaked mattress and polythene sheet to avoid evaporation of moisture. Prior to demolding, the bottom layer of the mold were removed first and concrete surface was exposed to environment after 24 of casting. Due to use of retarder, the exposed concrete surface was not fully hard. The soft concrete surface was then sprayed with a strong jet of water until coarse aggregates were exposed to resemble rough substrate concrete surface as shown in Figure 5.3(c). After 48 hours of casting, all the beams were demolded and concrete was cured in wet condition by covering with water-soaked mattress and polythene sheet for 28 days. In every 7 days, water was sprinkled on the beam for proper curing.

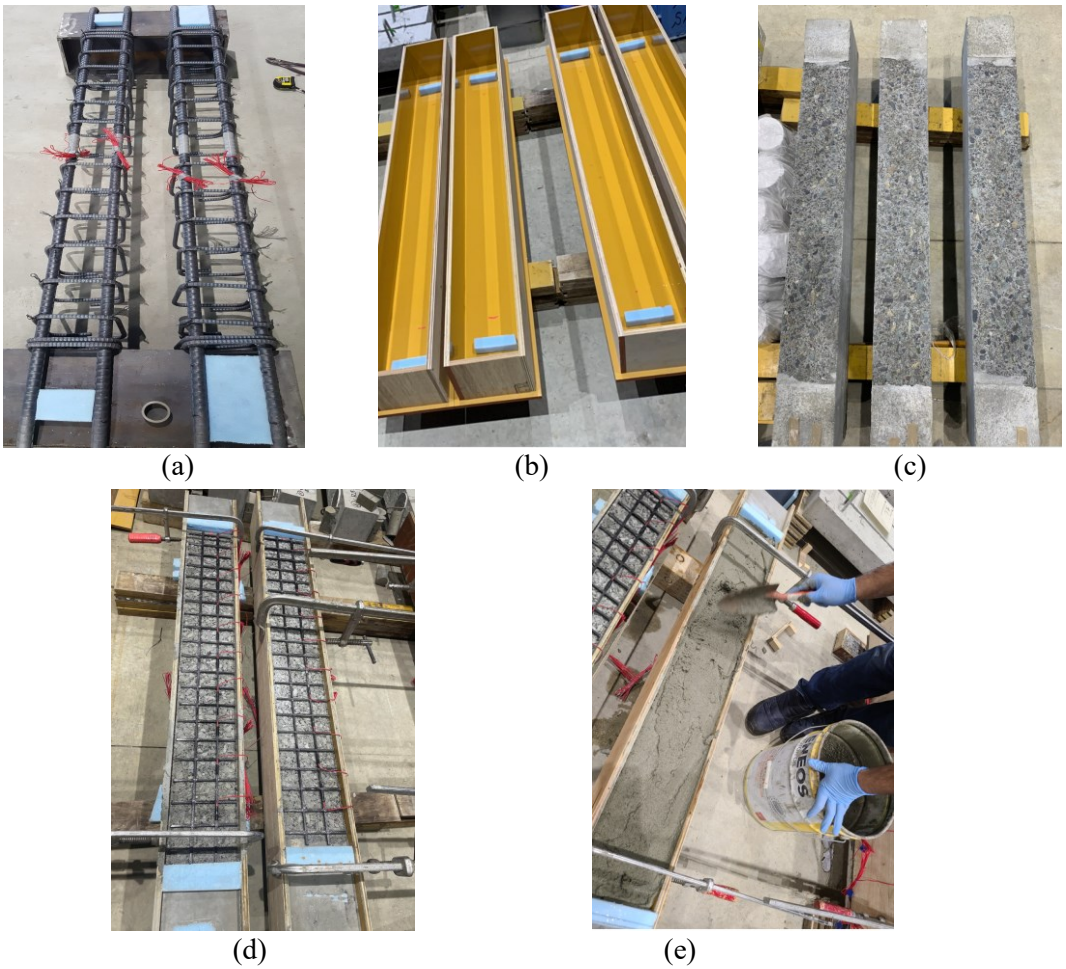

(a) (b) (c)

(d) (e)

Figure 5-3 Preparation of specimens for member level testing; (a) preparation of steel cage and strain gauge attachment, (b) wooden molds with retarder at bottom (c) Rough surface of the tensile face of the RC beam, (c) rough surface with formwork and reinforcement (as an example, CFRP grid) for overlay, (d) troweling of the PCM

To prepare the strengthened RC beams, rough surface of the cured concrete specimens were exposed and fix the overlaying reinforcement (steel rebar and CFRP grid) as shown in Figure 5.3(d). Screws and wire mess were used to anchored overlaying reinforcement to the treated substrate concrete surface. To maintain the thickness and bond length of the PCM overlay, mold of size 20*150*1040 mm were placed over rough surface of RC beam, prior of PCM casting. In preparing strengthened RC beams using CFRP strand sheet, the overlaying reinforcing bar were not fix directly to the treated concrete surface. Rather, PCM coating (about 5 mm) were cast first over the rough concrete surface and then CFRP grid was pressed with roller followed by pouring of second layer of PCM to make overlay thickness of 20mm. Before casting of PCM layer, the rough surface of the concrete was pre-wetted for 24 hours. Just before casting of repair material, the surface water was removed using clothes/tissues to provide saturated concrete substrate with dry surface for adequate bonding and PCM was trowelled as shown in Figure 5.3(e). Later, it was covered with plastic and mattress sheet to preserve the moisture condition. Methodology of strengthened RC beams preparation for member level testing is explained in Figure 5.3(a-e). After 24 hours, formworks were demolded and it was cured in wet condition for about one week to facilitate the hydration to took place followed by dry curing of 21 days to facilitate polymer film formation. Summary of all the beam specimens tested at member level is presented in Table 5.3. The tensile stiffness in newton (N) was calculated using area and elastic modulus of the reinforcing bar. The acronym designation adopted of each specimens are as follows: the first letter "N" or "M" refers to normal or modified 5% silica PCM followed by different types and amount of strengthening reinforcement.

Table 5-3 Summary of specimens for member level testing

Specimens	Strengthening bar		Area (mm^2)	Tensile stiffness (N)	Overlay constituents
	Types	Specification			
N_Rebar_D6	Steel rebar	2@6D	56.6	11320	N
M_Rebar_D6					M
N_Rebar_D10		2@10D	141.5	28300	N
M_Rebar_D10					M
N_CFRP Grid_CR4	CFRP Grid	FTG-CR4 (low stiffness)	13.2	1320	N
M_CFRP Grid_CR4					M
N_CFRP Grid_CR6		FTG-CR6 (medium stiffness)	35	3500	N
M_CFRP Grid_CR6					M
N_CFRP Grid_CR8		FTG-CR8 (High stiffness)	52.8	5280	N
M_CFRP Grid_CR8					M
N_CFRP Strand (50mm)	CFRP strand sheet	FSS-HT-600 (50 mm width)	49.95	4895	N
M_CFRP Strand (50mm)					M
N_CFRP Strand (150mm)		FSS-HT-600 (150mm width)	19.98	12238	N
M_CFRP Strand (150mm)					M

5.2.4 Instrumentation and testing procedure

Monotonic four point bending test was carried out on each specimen with a clear span of 1140 mm between two supports. The support points were set at a distance of 150 mm from the ends of the RC beam and the loading points were set at a distance of 420 mm from the support point to maintain shear span ratio of 3.5. The distance of support to the overlay end was 50 mm. The constant moment zone length was 300 mm, which was maintained using steel spreader connected with a hydraulic actuator of capacity 1000 kN. Four linear variable differential transducer (LVDT) were employed (two of them were aligned with supports and two were placed at center of beam) to measure mid-span deflection during loading. Steel strain gages were attached at the middle section of tensile reinforcement in concrete part and at a distance of 100 mm apart from 120mm away of overlay end in overlaying bar [Figure 5.5(c)] to record the strain values, which might give valuable information about strain distribution. These strain distributions might be helpful in understanding the debonding phenomenon, if it happens. The data of the strain gauges, LVDT and the load cell were recorded using data logger connected with computer (data acquisition system). The experiment setup used in the laboratory for the four point bending test is presented in Figure 5.4.

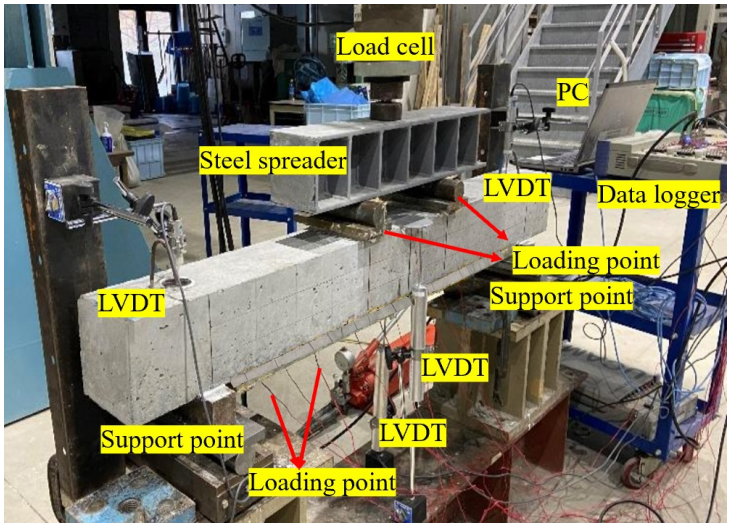

Figure 5-4 Experimental setup for four point bending test

5.3 Experimental results and discussion

The experimental data obtained from the four point bending test were analyzed further and the influence of the inclusion of silica fume with PCM as a repair material were discussed in the following section, comparing the performance of all the PCM strengthened beam in terms of the crack pattern, failure mode, ultimate load, debonding load, load-deflection curves, strain profiles of main steel bar and strengthening reinforcing bars.

5.3.1. Crack patterns and failure modes

In overlaying, most common failure reported in the technical literature is the debonding failure before the reaching to the flexural capacity [21-22]. Debonding failure has been categorized in several types and named according to the process described by other researchers [23-25]. Besides, classical failure of beam (tension failure of reinforcement in the tension zone either in concrete layer or overlay layer and crushing of concrete in compression zone) were also observed. In this research work, the failure modes were named seeing the crack distribution along the beam and observing the strain value at tensile and strengthening reinforcement. The failure situation for all the strengthened RC beam tested in this work is presented in Figure 5.5(a-c) and discussed herewith.

5.3.1.1 Beam strengthened with steel rebar

The crack patterns and failure modes of RC beams strengthened with different amount of steel bar and PCM matrix is illustrated in Figure 5.5(a). In specimens with D6 strengthening bar, the failure mode was characterized by yielding of tensile rebar (both in concrete and PCM layer) followed by concrete crushing representing flexural failure in both normal PCM and modified PCM specimen. Though partial separation of PCM overlay was observed up to 24 mm from the overlay end in normal PCM strengthened beam, but it did not propagate further and beam failed with no debonding at the interface. In specimens with D10 strengthening bar, partial separation of overlay layer at the end with critical diagonal crack was observed in normal PCM strengthened beam representing bond failure. The occurrence of sudden drop of the strain value in the strengthening bar before the yielding of main steel bar confirm the bond failure. In modified PCM strengthened beam, sudden drop of the strain value in the strengthening bar was not observed representing no bond failure, but the failure was characterized by concrete cover separation due to high stress concentration at the overlay end and due to critical diagonal crack in shear-flexure zone. In all cases, the crack numbers in strengthened beam with modified PCM were more than those observed in strengthened beam with normal PCM. Overall, it seems that the use of silica fume with PCM as a repair material improves interfacial bonding.

5.3.1.2 Beam strengthened with CFRP grid

Figure 5.5(b) illustrated the crack patterns and failure modes of RC beams strengthened with different amount of CFRP grid and PCM matrix. Both normal and modified PCM strengthened beam

with CFRP grid having low stiffness (CR4) failed due to concrete crushing followed by the rupture of CFRP grids and without any debonding. Cracks were first initiated in tensile surface of the constant moment zone and then propagated toward compression zone which widened further with the increase in load. Cracks also appear in flexural-shear zone and propagated in inclined direction towards loading points. Eventually, concrete was crushed and CFRP grid was ruptured at the ultimate states. The possibility of the debonding failure increased with the increase of the strengthening reinforcement area due to high stress concentrations.

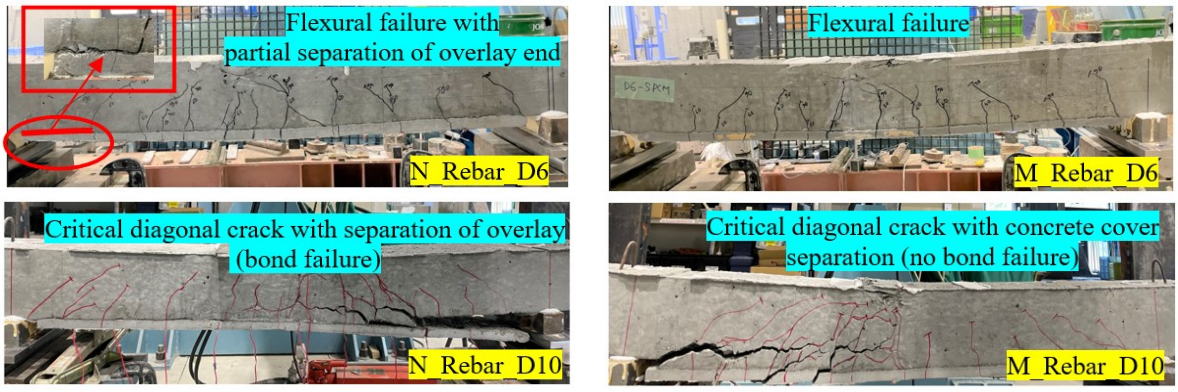

(a) Beam strengthened with steel rebar

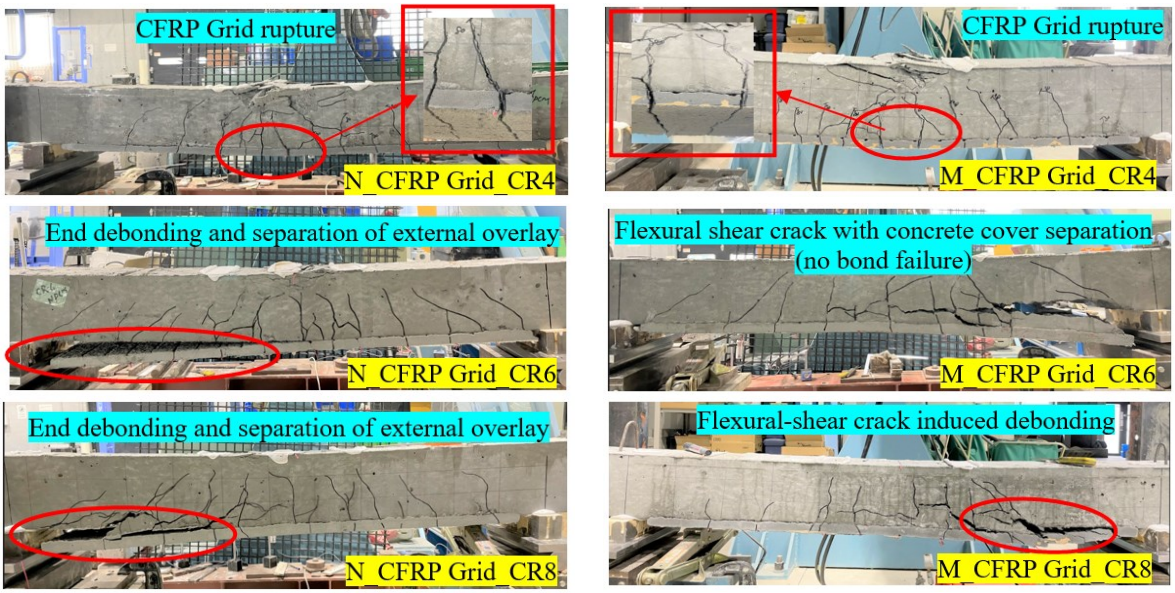

(b) Beam strengthened with CFRP grid

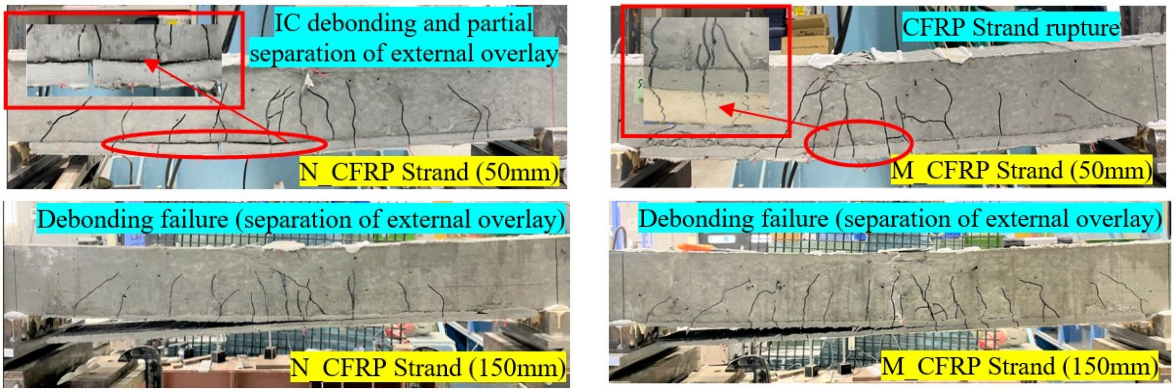

(c) Beam strengthened with CFRP strand sheet

Figure 5-5 Observed crack pattern and failure mode of the strengthened RC beam

With the increase of the stiffness of the CFRP grid (CR6 and CR8), debonding failure were likely to happened in normal PCM strengthened beam. Though bond separation of PCM overlay was observed in normal PCM strengthened beam, but no bond failure was observed in modified 5% silica PCM strengthened beam, rather concrete cover separation occurred in the post peak region due to high stress concentration (CR6) and flexural-shear crack induced debonding due to critical diagonal crack in the shear-flexure zone (CR8) in the latter case. The strain value of the main steel bar at the time of sudden drop of the load value were 1106μ and 6980μ in case of the strengthened beam with CR6, and 1857μ and 4429μ in case of the strengthened beam with CR8 for normal PCM and modified PCM specimen, respectively. It reflect that the main steel rebar of the modified PCM strengthened beam already yielded at the time of debonding, representing more stress transfer from the concrete part to the overlay part and the occurrence of debonding failure in the post peak region. The occurrence of the bond failure in modified PCM strengthened beam was reduced probably because of the relatively stronger bond achieved between the cementitious mortar and the concrete substrate with the silica fume inclusion.

5.3.1.3 Beam strengthened with CFRP strand sheet

The illustration of crack pattern and failure mode of strengthened beam with CFRP strand sheet is presented in Figure 5.5(c). The number of cracks were more in modified PCM specimens then in normal PCM specimens. In using CFRP strand sheet of width 150mm, separation of overlay ends was observed along the strengthening reinforcement in both normal PCM and modified PCM specimen due to very high stress concentration at the ends. The strain value of the main rebar at the time of debonding was 538μ and 1292μ (not reach the yielding strain – 2000μ) for the normal PCM and modified PCM strengthened beam, respectively. The failure mode of the normal PCM strengthened beam with 50mm width strand sheet was characterized as intermediate crack (IC) induced debonding, whereas the use of reduced strand sheet width (50mm) shifted the failure mode of the modified 5% silica PCM strengthened beam to concrete crushing followed by the rupture of CFRP strand sheet (without any debonding). The use of modified silica PCM seemed to be the most efficient solution in achieving the composite action of the strengthening system and avoiding the debonding failure. Conclusively, the inclusion of silica fume with PCM results a promising cementitious matrix for overlay which can be used together with the tensile strengthening reinforcement for practical strengthening applications.

5.3.2 Load-displacement behavior

The experimental load deflection curves at the mid span of the tested strengthened beams with different types and amount of strengthening reinforcement is presented in Figure 5.6(a-c). To understand the influence of silica fume inclusion with PCM, load-displacement curve of the strengthened beam with normal PCM matrix and modified PCM matrix were plotted together having particular same amount of strengthening reinforcement. The ductility level were decreased with the increase of the amount of strengthening reinforcement. Strengthened beam of both normal and modified PCM matrix having “rebar_D6” [Figure 5.6(a)] and “CFRP grid_CR4” [Figure 5.6(b)] specification showed ductile behavior and the failure observed were flexural failure. But for beam specification of “rebar_D10” [Figure 5.6(a)] shows sudden drop of the load and failure mode shifted from flexural to debonding failure. Sudden drop of the load was observed earlier in beam having specification “N_Rebar_D10” compared to “M_Rebar_D10” representing earlier occurrence of debonding and less ductile behavior in former case. The initial stiffness of all strengthened beams remained unchanged until onset of cracking. The stiffness was found increasing with the increase of the amount of strengthening reinforcement. The stiffness was observed lower in the beam strengthened with the modified PCM matrix compared to its corresponding normal PCM strengthened beams. Earlier occurrence of the sudden drop of the load value were also observed in normal PCM strengthened beam with CFRP grid (CR6 and CR8) as presented in Figure 5.6(b) and with CFRP strand sheet (150mm case) as presented in Figure 5.6(c) compared to its corresponding modified PCM strengthened beam, representing a delay of debonding in later case. The load displacement diagram of modified PCM strengthened beam with CFRP grid (CR6) as presented in Figure 5.6(b) and with CFRP strand sheet (50mm case) as presented in Figure 5.6(c) showed gradual decrease of the load instead of sudden drop that occurred in corresponding normal PCM strengthened beam, indicating an

increase of ductile behavior with silica fume inclusion. The decrease of the stiffness occurred gently in the post peak region of modified PCM strengthened beam with CFRP grid (CR6) [Figure 5.6(b)] and with CFRP strand sheet (50mm case) [Figure 5.6(c)]. This indicated that the overlay matrix with silica fume inclusion still provide a portion of load-carrying capacity during the post-cracking stage, that subsequently delayed the steel yielding in the beam strengthened with the modified silica PCM.

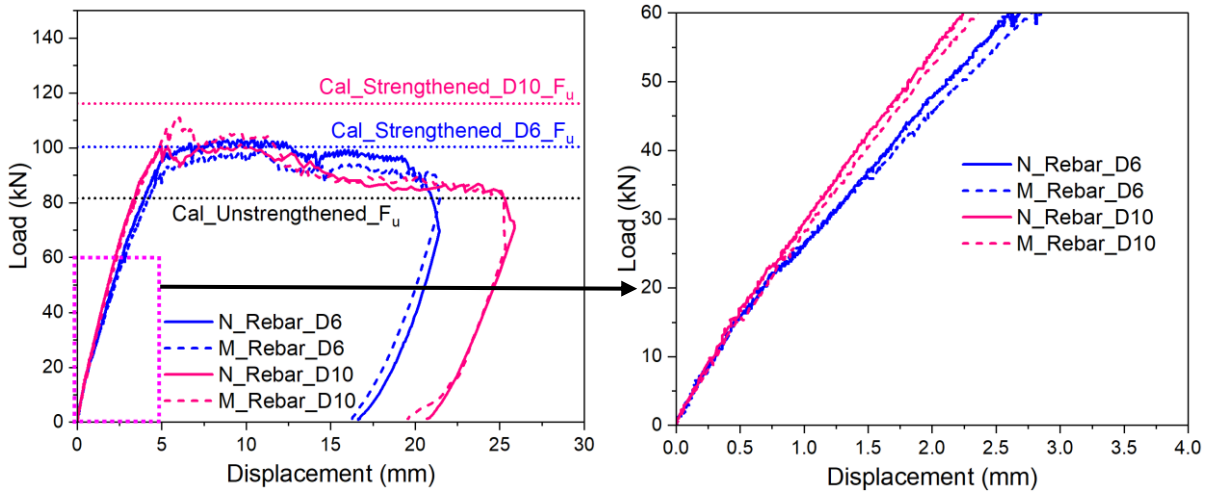

(a) Strengthned beam with steel rebar

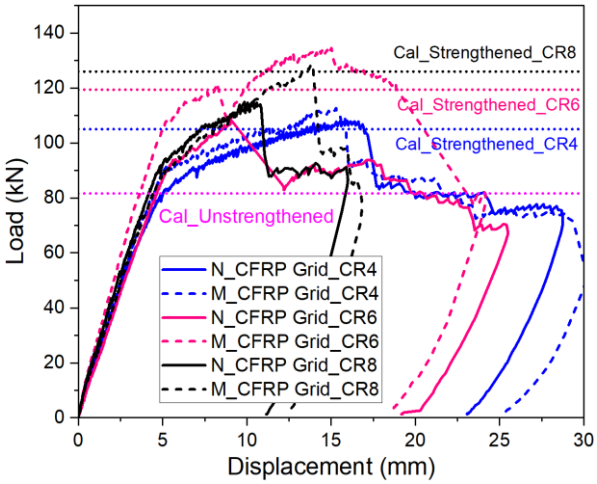

(b) Strengthned beam with CFRP grid

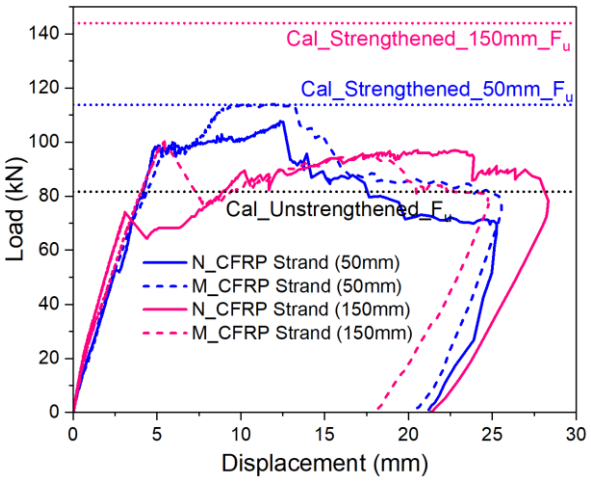

(c) Strengthned beam with CFRP strand sheet

Figure 5-6 Comparison of load-displacement diagram and ultimate displacement of all the strengthened RC beam

To understand the influence of silica fume in term of ductility, the displacement at the peak load of the normal and modified PCM strengthened beam were compared and presented in Figure 5.7. No significant differences were observed in beam "rebar_D6" and "CFRP grid_CR4" due to occurrence of flexural failure in both normal and modified PCM strengthened beam. In all other cases, significant increase of the displacement at peak load in modified PCM strengthened beams compared to normal PCM strengthened beam were observed as shown in Figure 5.6(d). An increase of about 65% and 33% were observed in beam "M_CFRP grid_CR6" and "M_CFRP grid_CR8", respectively compared to its corresponding normal PCM case. The beams strengthened with modified PCM matrix always exhibited better ultimate flexural deformation than their normal PCM counterparts, leading to a more ductile failure. Conclusively, the incorporation of silica fume significantly improves the ductile behavior of the strengthened beam as well as it results into a promising PCM cementitious matrix which can be used together with the strengthening reinforcement (especially CFRP grid) for practical strengthening applications.

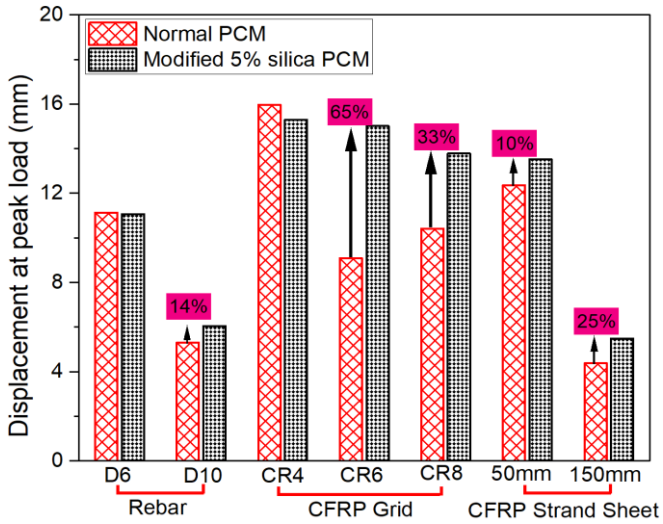

Figure 5-7 Influence of silica fume on the displacement at peak load

5.3.3 Load carrying capacity

The influence of silica fume is evaluated comparing the peak load and debonding load of the strengthened beam with or without silica fume obtained from the experimental results of the static loading test and discussed in the following subsection.

5.3.3.1 Peak load

The peak load describes the capacity of the structural member along with failure behavior, thus the performance of the strengthened beam tested in this research work is discussed considering peak load. Figure 5.8(a) showed the experimental results of peak load of all the strengthened beam along with the calculated result of unstrengthened beam. The peak load of all the strengthened beams was found higher than the peak load of the unstrengthened beam. Higher peak load of modified PCM strengthened beam was observed compared to the normal PCM strengthened beam in all cases except for flexural failure governs ("Rebar_D6" and "CFRP grid_CR4") beam. An increased peak load of about 25% and 12% were observed in beam "M_CFRP grid_CR6" and "M_CFRP grid_CR8", respectively compared to its corresponding normal PCM case. The percentage increase in the peak load of all the strengthened beams from unstrengthen beam is presented in Figure 5.8(b). The increase percentage was higher in modified PCM matrix strengthened beam than in normal PCM matrix strengthened beam, representing higher bond force transfer between the strengthening layer and the substrate concrete in former case. This confirmed that the inclusion of silica fume with PCM as a repair material significantly improved the performance of the strengthened beam.

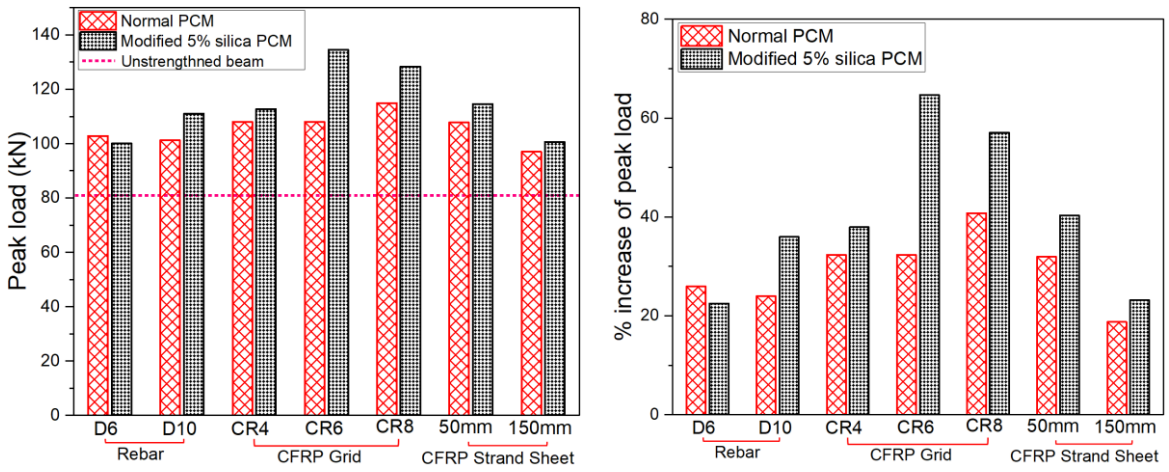

(a) comparison of peak load (b) Peak load change compared to reference beam

Figure 5-8 Influence of silica fume on the percentage increases in peak load

5.3.3.2 Debonding load

Debonding is the most common failure mode in the strengthened beams which is also observed in this research work. Sudden drop of the load value and strain value at the strengthening reinforcement were considered a criteria to choose the load as debonding load. The occurrence of the debonding failure stopped the load transfer from beam section to the overlaid layer, thus strain value of the strengthening reinforcement significantly dropped. Figure 5.9(a) showed the load of all the strengthened beam along with the calculated result of unstrengthened beam. The debonding load of all the strengthened beams is found higher than the peak load of the unstrengthened beam except for beam "N_CFRP strand (150mm)" in which debonding happened even before reaching the capacity of unstrengthened beam. Higher debonding load was observed in the modified PCM strengthened beam compared to the normal PCM strengthened beam in all cases. This confirms the positive influence of silica fume inclusion to delay the occurrence of debonding in strengthened beam. To understand it more precisely, the strain value of the main tensile steel bar at the debonding load were observed and presented in Figure 5.9(b). In all cases, higher strain value were observed in modified PCM strengthened beam compared to normal PCM strengthened beam, suggesting a high possibility of more load transfer from the concrete beam section to the overlaid layer in former cases. Conclusively, the inclusion of silica fume with PCM overlay delay the occurrence of debonding failure and improve the overall performance of the strengthened beam.

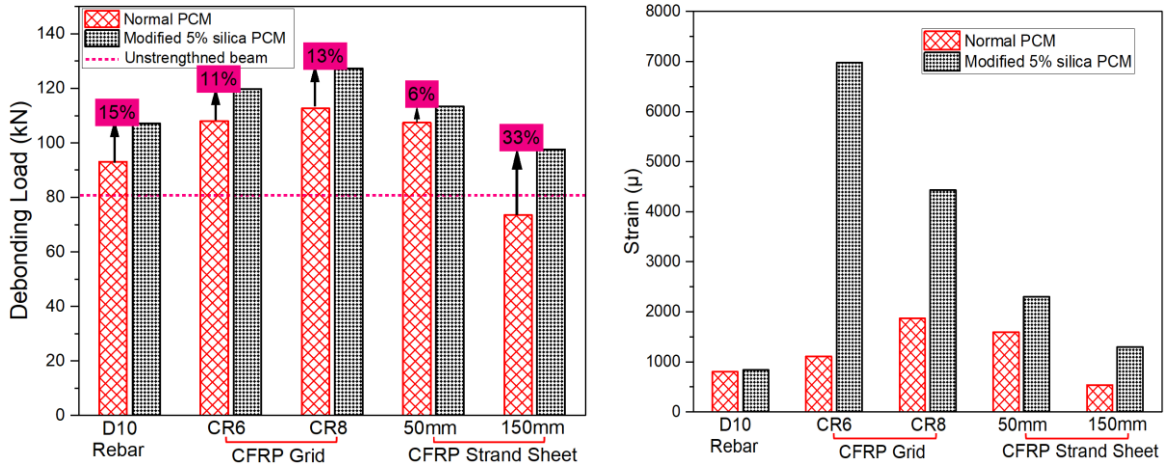

(a) Comparison of debonding load (b) Main steel bar strain at debonding load

Figure 5-9 Influence of silica fume to delay the occurrence of debonding

5.3.4 Strain measurements

One of the most efficient and effective way to describe the interaction among substrate concrete, cementitious matrix and strengthening reinforcement is the strain value in longitudinal steel reinforcement or the strain distribution of the strengthening reinforcement along the beam. The strain value at both longitudinal steel bar and strengthening reinforcement provide More insightful information which could not be revealed from the load-deflection behavior and failure mode at the ultimate state. The performance evaluation of the strengthened beam with silica fume inclusion is discussed in the following section in terms of the strain profiles of main steel bar and strengthening reinforcing bars.

5.3.4.1 Longitudinal steel bar strain value

The applied load versus the strain responses of the tensile steel bar at the midspan section for all tested strengthened beams are shown in Figure 5.10(a-c). It should be noted that the yielding strain of the steel bar was about 2000μ. In all cases, the load-strain response exhibited three stage. The two turning points corresponded to initial cracking load or yielding/debonding load. It is seen that the longitudinal steel bar strains in the modified PCM strengthened beam were effectively reduced compared to those in the normal PCM strengthened beams except for some cases, representing the possibilities of higher load transfer from the concrete layer to the overlay layer in former cases.

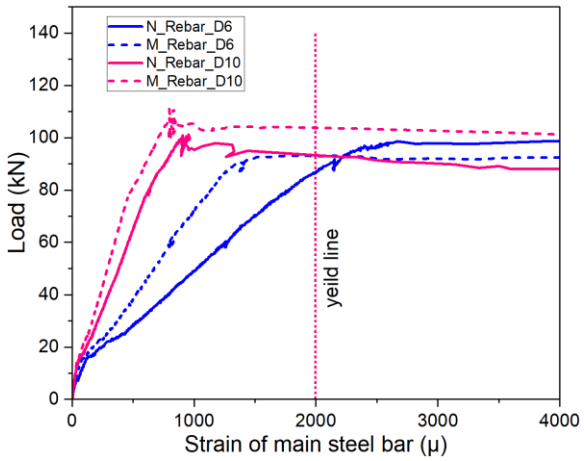

(a) Steel rebar as strengthning reinforcement

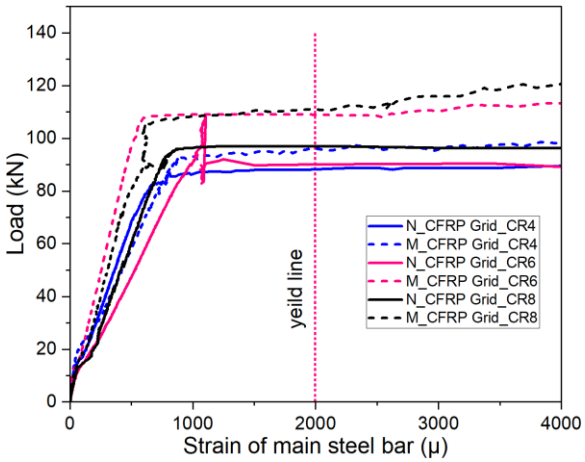

(b) CFRP grid as strengthning reinforcement

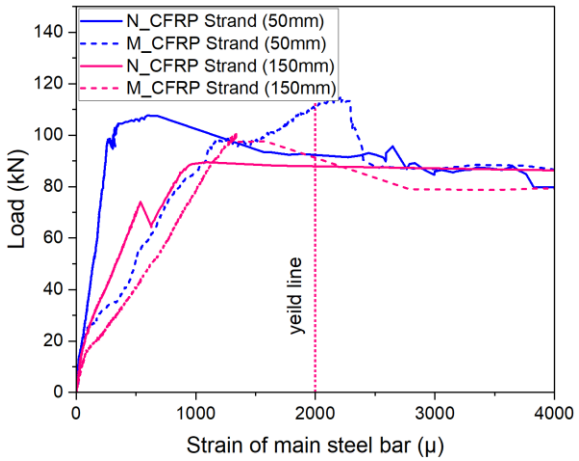

(c) CFRP strand sheet as strengthning reinforcement

Figure 5-10 Load-strain responses of the tensile steel bars at the midspan section

5.3.4.2 Strain distribution of strengthening bar

The strain distribution of the different types of strengthening reinforcement along the beam is presented in Figure 5.11(a-c). The origin of the x-axis in these figures represent the mid-section of the strengthened beam. One from each types of strengthening reinforcement were chosen as an example covering all types of failure mode observed, to compare the strain distribution of the modified PCM and normal PCM strengthened beam. The strains in the main tensile steel bar were less compared to the strengthening reinforcement due to their location closer to the neutral axis. In normal PCM strengthened beam with D6 as strengthening bar, a sudden increase of strain distributions within a certain span length in constant moment zone was seen as presented in Figure 5.11(a), implying the abrupt occurrence of local interface debonding within this length, or widening of a major flexural or flexural/shear crack. The strain value of the strengthening bar showed gradual decreasing tendency in the post peak region, representing the possibility of flexural failure due to widening of a major flexural or flexural/shear crack with further increase of the loading. In contrast, the strain distribution of the strengthening bar (D6) of the strengthened beam with modified PCM was apparently linear with some zigzags due to the cracking, such a sudden increase of strain distribution was not observed as presented in Figure 5.11(a). This suggests an excellent composite action between strengthening and concrete layer in using modified 5% silica PCM matrix. The strain distribution of the strengthening bar of modified PCM strengthened beam with CFRP grid (CR6) as presented in Figure 5.11(b) and with CFRP strand sheet (50mm case) as presented in Figure 5.11(c) were smoother compared to those corresponding beams with normal PCM matrix. No sudden increase/decrease of strain value was observed in the strengthening bar with modified PCM matrix since debonding does not happen, as

presented in Figure 5.11(b-c). On the other hand, sudden increase of the strain value in shear-flexure zone at load level of $0.9F_u$ [Figure 5.11(b)] and sudden dropping of the strain value just after the peak (debonding) load [Figure 5.6(c)] was observed for the strengthened beam with normal PCM matrix, representing the occurrence of debonding failure. This phenomenon suggests that the inclusion of silica fume in PCM helped a more uniform shear stress transfer at the interface between the strengthening layer and the substrate RC beam. In all cases, the strain values of strengthening reinforcement at any particular load level was higher in modified PCM cases, indicating the possibility of more load transfer from the concrete part to overlay part. Conclusively, the inclusion of silica fume significantly improve the bond performance of the strengthened structure.

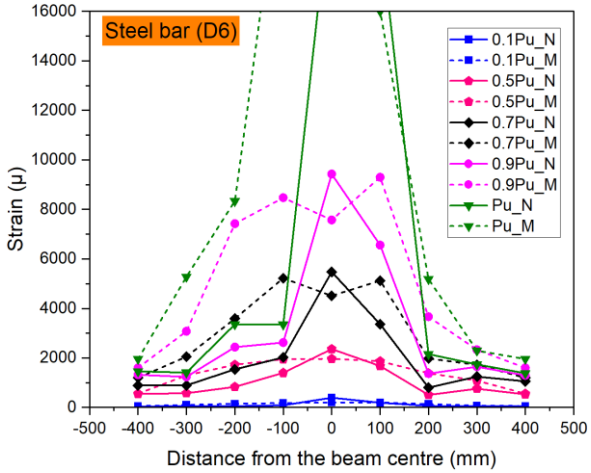

(a) Steel rebar as strengthning reinforcement

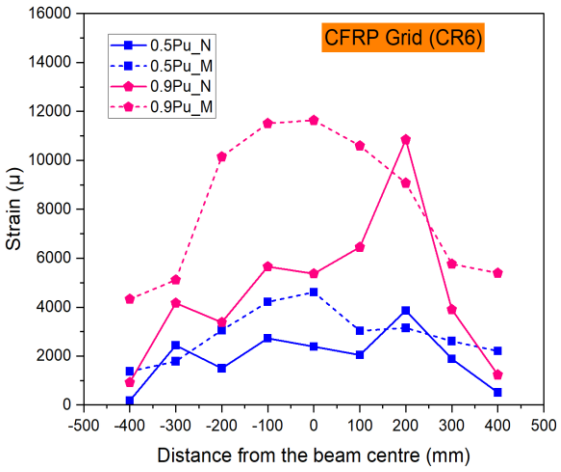

(b) CFRP grid as strengthning reinforcement

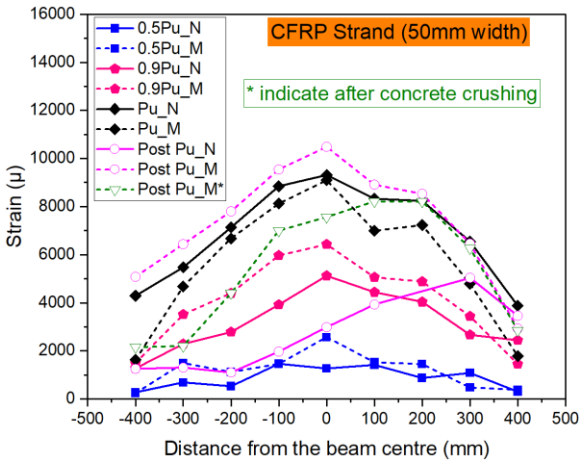

(c) CFRP strand sheet as strengthning reinforcement

Figure 5-11 Strain distributions of the strengthening reinforcement at different loading levels.

5.3.5 Flexural capacity analysis

The flexural capacity of the strengthened RC beam with PCM overlay is evaluated on the basis of conventional procedure recommended by the ACI 318 Code [26] and considering perfect bond between concrete and PCM. Following assumption were made; (1) plane cross-sections remain plane during the loading process; (2) the tensile strength of concrete was ignored; (3) the strain of compression concrete was taken as 3500μ (4) the tensile force of the overlaying layer was determined by combining the tensile forces of both strengthening reinforcement and cementitious matrix. The equivalent cross-section diagram along with strain and stress variation along the depth of the beam is shown in Figure 5.12. The detailed explanation of the value of the notations and the properties of the materials were mentioned in Section 5.2.1 and Section 5.2.2, which are used in the flexural capacity calculation. The ultimate moment strength was calculated using a rectangular stress block (using α_1 =0.67) acting over a depth $0.8x_0$. The neutral axis depth (x_0) was calculated from the equilibrium of

internal forces and the strain value in the compression, tensile and strengthening bar were determined from ε_c by the linear strain distribution. Finally, the moment for ultimate stage was taken about an axis and corresponding required load was calculated.

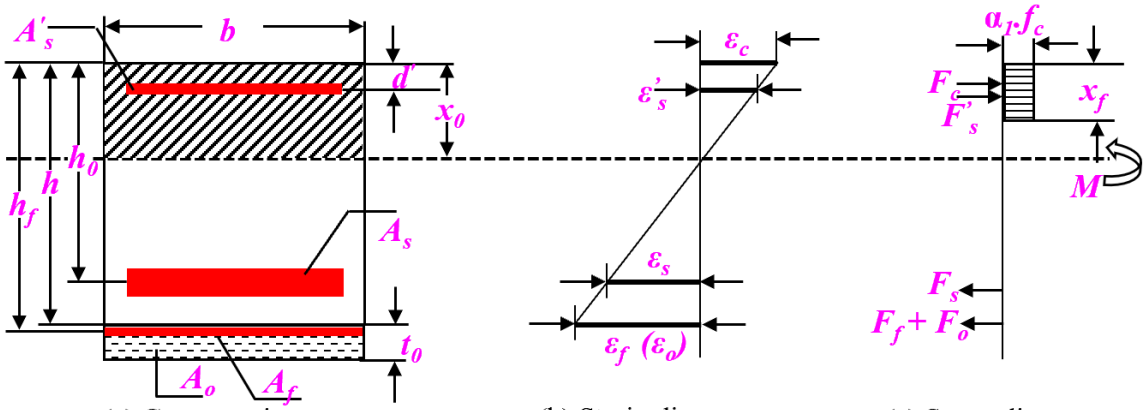

(a) Cross-section (b) Strain diagram (c) Stress diagram

Figure 5-12 Stress and strain distributions of the strengthened RC beam

The calculation result of peak load of all the strengthened beam is shown in Table 5.4 and compared with the corresponding experimental results. The calculated flexural capacity of all the normal PCM strengthened RC beam was overestimated mainly because of the occurrence of debonding at the interface, except for the beam "Rebar_D6" and "CFRP grid_CR4" that results close calculated and experimental value. This indicates that if no debonding occurs, the ultimate flexure strength of strengthened beam can be predicted based on the conventional procedure. In case of modified PCM strengthened beam, the calculated flexural capacity was found close to the experimental result or underestimated, except for the CFRP strand sheet (150mm case) due to the occurrence of debonding failure. The underestimation might be due to shear deformation after the occurrence of diagonal cracking of concrete. This diagonal cracking might results dowel action on the external strengthening layer, reducing the tensile rupture strain of the strengthening reinforcement. In cases, the shear deformation is high, there is a possibility of mixed-mode failure which is considered more significant in case of cement-bonded strengthening reinforcement system because of high bending stiffness [27].

Table 5-4 Comparison between calculation and experiment results

Specimens	Normal PCM			Modified 5% silica PCM		
	$F_{u,exp}$ (kN)	$F_{u,cal}$ (kN)	$\frac{F_{u,exp}}{F_{u,cal}}$	$F_{u,exp}$ (kN)	$F_{u,cal}$ (kN)	$\frac{F_{u,exp}}{F_{u,cal}}$
Rebar_D6	102.83	100.33	1.02	99.99	100.33	1.00
Rebar_D10	101.21	116.15	0.87	111	116.15	0.96
CFRP Grid_CR4	108.06	105.02	1.03	112.63	105.02	1.07
CFRP Grid_CR6	108.06	119.39	0.91	134.51	119.39	1.13
CFRP Grid_CR8	114.92	125.99	0.91	128.3	125.99	1.02
CFRP Strand (50mm)	107.74	113.75	0.95	114.59	113.75	1.01
CFRP Strand (50mm)	96.96	130.15	0.74	100.55	130.15	0.77

5.4 Conclusions

In this research work, the performance of the PCM overlaying method with the inclusion of silica fume was investigated at member level by conducting loading test of strengthened RC beams. Numbers of beams were prepared and tested at four point bending up to failure. Two types of matrix materials (normal PCM vs. modified 5% silica PCM) and seven different levels of the strengthening reinforcement served as the test variables. The test results were carefully observed and compared in terms of the crack patterns, failure modes, load-deflection responses, strain measurements in tensile steel bars and strengthening reinforcement and the following conclusions were drawn;

- The load carrying capacity of all the strengthened beams using PCM overlaying method increases significantly compared to the unstrengthen beam. The inclusion of silica fume in PCM further increases the load carrying capacity of the strengthened beam in comparison with normal PCM cementitious matrix.
- Compared to normal PCM mortar, however, use of modified 5% silica PCM mortar led to more ductile failure and dispersed more uniformly the shear stress transfer at the interface between the strengthening layer and the substrate concrete.
- Ductility level of the strengthened beam reduces with the increase in strengthening reinforcement area. More reduction occurs in normal PCM strengthened beam than in modified PCM strengthened beam.
- The inclusion of silica fume with PCM overlay delays the occurrence of the debonding failure and improve the overall performance of the strengthened beam. The occurrence of the bond failure in modified PCM strengthened beam reduces probably because of the relatively stronger bond achieved between the cementitious mortar and the concrete substrate with the silica fume inclusion.
- The use of larger amount of strengthening reinforcement having very high tensile stiffness triggers the occurrence of debonding failure. Special design check is necessary to select the appropriate amount of strengthening reinforcement. Further experimentation is necessary to choose appropriate amount of strengthening reinforcement, but there is a high possibility of getting better structural performance maintaining the reinforcement amount (area X tensile strength) ratio of the strengthening reinforcement and main steel bar within 0.5.
- In spite of the existence of a certain level of debonding, the flexural capacity of the modified PCM strengthened RC beams can be predicted with acceptable accuracy based on conventional procedure (sectional analysis) considering perfect bond between the cementitious mortar and the concrete substrate. However, in case of normal PCM strengthened RC beam, this method overestimate the flexural capacity due to earlier occurrence of the debonding at the interface.

In summary, the incorporation of silica fume with PCM can effectively improve the technical performance of the strengthened RC beam. Modified PCM mortar helps in improving the ultimate bending moment and enhancing the performance of the bonding surface, this reflecting a good repair effect.

References

[1] Saeed, A., Ayub, E., Rana, F. T., Muhammad, Z. and Saad, B. T. (2021). "Experimental investigation and strength model of RC deep beams externally bonded by CFRP." *Advances in Structural Engineering*, *24(16)*, 3645-3657.

[2] Alagu, S. P., Harik, I. E. and Choo, C.C. (2003). "Flexural behavior of R/C beams strengthened with carbon fiber-reinforced polymer plates and steel." Journal of Composites for Construction, 7(4), 292-301.

[3] Ashour, A.F., El-Refaie, S.A. and Garrity, S.W. (2004). "Flexural strengthening of RC continuous beams using CFRP laminates," Cement Concrete Composites, 26 (7); 765-775

[4] Kurtz, S. and Balaguru, P. (2001). "Comparison of inorganic and organic matrices for strengthening of RC beams with carbon sheets." Journal of Structural Engineering, 127(1):35–42.

[5] Toutanji, H., Zhao, L. and Zhang, Y. (2006). "Flexural behavior of reinforced concrete beams externally strengthened with CFRP sheets bonded with an inorganic matrix." Engineering Structure, 28(4):557–66.

[6] Hashemi, S. and Al-Mahaidi, R. (2010). "Investigation of bond strength and flexural behaviour of FRP-strengthened reinforced concrete beams using cement-based adhesives." Australian Journal of Structural Engineering, 11(2):129–39.

[7] Hashemi, S. and Al-Mahaidi, R. (2012). "Flexural performance of CFRP textile-retrofitted RC beams using cement-based adhesives at high temperature." Construction and Building Material, 28(1):791–7.

[8] Dai, J.G., Munir, S. and Ding, Z. (2014). "Comparative study of different cement-based inorganic pastes towards the development of FRIP strengthening technology." Journal of Composites for Constructions, 2014;18(3).

[9] Zhang, D., Ueda, T. and Furuuchi, H. (2012). "Concrete cover separation failure of overlay-strengthened reinforced concrete beams." Construction and Building Materials, 26(1):735-45.

[10] Zhang, D., Ueda, T and Furuuchi, H. (2011). "Intermediate Crack Debonding of Polymer Cement Mortar Overlay-Strengthened RC Beam." Journal of Materials in Civil Engineering. 23(6):857-65.

[11] Benjeddou, O., Ouezdou, M. B. and Bedday, A. (2007). "Damaged RC beams repaired by bonding of CFRP laminates." Construction and Building Materials, 21(6):1301-10.

[12]Satoh, K., Hizukuri, M., Hida, K., and Hikichi, K. (2000). "Strengthening effect of strengthened RC slab of highway bridge using polymer cement mortar shot bottom side thickening method." Proceeding of Japan Concrete Institute, 22(1), 517–522.

[13] Satoh, K. and Kodama, K., (2005). "Central peeling failure behavior of polymer cement mortar retrofitting of reinforced concrete beam." *Journal of Materials in Civil Engineering*, 17(2), 126-136.

[14] Rashid, K., Ueda, T. and Zhang, D. (2016). "Study on Shear Behavior of Concrete-polymer Cement Mortar at Elevated Temperature." Civil Engineering Dimension, vol. 18: 93–102.

[15] Martinola, G., Meda, A., Plizzari, G. A. and Rinaldi, Z. (2010). "Strengthening and repair of RC beams with fiber reinforced concrete." Cement Concrete Composites, 32(9):731–9.

[16] Shin, S. K., Kim, K. and Lim, Y. M. (2011). "Strengthening effects of DFRCC layers applied to RC flexural members." Cement Concrete Composites, 33(2):328–33.

[17] Zheng, Y. Z, Wang, W. W. and Brigham, J. C. (2016). "Flexural behaviour of reinforced concrete beams strengthened with a composite reinforcement layer: BFRP grid and ECC." Construction and Building Material, 115:424–37

[18] Kobayashi, A., Hidekuma, Y. and Saito, M. (2009). "Application of the FRP for Construction as High Durability Materials in Japan." Proceeding of US-Japan Workshop on Life Cycle Assessment of Sustainable Infrastructure Materials, Japan.

[19] Kobayashi, A., Sato, Y. and Takahashi, Y. (2009). "Basic Characteristics of FRP Strand Sheet and Flexural Behavior of RC Beams Strengthened with FRP Strand Sheet." Proceeding of Asia-Pacific conference on FRP in Structures (APFIS), Seoul Korea.

[20] Pardeep, K., Shashank, B. and Bishwajeet, B. (2020). "Influence of CFRP Strand Sheet on Flexural Strengthening of Reinforced Concrete Beam," Journal of Advanced Concrete Technology, 18, 778-793.

[21] Smith, S. T and Teng, J. G. (2002). "FRP-strengthened RC beams-II: Assessment of debonding strength models," *Engineering Structures.*, 24, 397–417.
[22] Garden, H. N., Quantrill, R. J., Hollaway, L. C., Thorne, A. M. and Parke, G. A. R. (1998). "Experimental study of the anchorage length of carbon fibre composite plates used to strengthen reinforced concrete beams," *Construction and Building Materials*, 12, 203–219.
[23] Teng, J. G. and Yao, J. (2007). "Plate end debonding in FRP-plated RC beams—II: Strength model." Engineering Structures. 29(10):2472-86.
[24] Yao, J., and Teng, J. G. (2007). "Plate end debonding in FRP-plated RC beams—I: Experiments." Engineering Structures. 29(10):2457-71.
[25] Smith, S. T. and Teng, J. (2001). "Interfacial stresses in plated beams." Engineering structures. 23(7), 857-71
[26] ACI Committee 318. (1995). "Building Code Requirements for Reinforced Concrete and Commentary (ACI 318 95/ ACI 318-R95)," American Concrete Institute, Detroit, 371.
[27] Yu, H., Bai, Y. L., Dai, J. G. and Gao, W. Y. (2017). "Finite element modeling for debonding of FRP-to-concrete interfaces subjected to mix-mode loading." Polymers, 9(9). No. 438.

Chapter 6
CONCLUSIONS AND RECOMMENDATIONS

6.1 Conclusions

Among the issues that still need to be taken up in PCM strengthening method of RC members, the debonding issues were addressed in this research. Extensive experimentations were carried out at micro and material level in order to observe the effectiveness of using 5% silica fume with PCM to improve the bonding behaviour of substrate concrete and overlay layer. Meanwhile, PCM overlay strengthened beams with different cross-section area of the strengthening bar and with the inclusion of silica fume in PCM were tested under monotonic flexure loading. Several conclusions were extracted from the experimental results and described with respect to behavior at micro level (Chapter 2), material level (Chapter 2 to Chapter 4) and member level (chapter 5), respectively.

6.1.1 Micro level testing

For evaluating the effectiveness of modified 5% silica PCM as a repair material (qualitatively and quantitively) in forming a chemical connection at the interface, microstructural analysis was performed. The following conclusions were extracted after conducting microstructural analysis using different microscopic test (SEM-EDS, XRD and TG-DTA).

- XRD and TG-DTA microscopic test can be used to investigate the formation of chemical connection at the interface, both qualitatively and quantitively.
- The incorporation of silica fume with PCM as a repair material significantly reduces the presence of harmful $Ca(OH)_2$ and $CaCO_3$ at the concrete-PCM interface, implying an increase in the extend of bond formation between silica compound and free $Ca(OH)_2$ after the hydration of cement to form more C-S-H at the interface.
- The ratio of Ca/Si quantified using SEM-EDS test can be used as an indirect method to measure the contents of C-S-H and free alkali at the interface. The use of silica fume reduces the value of Ca/Si ratio that reflects the higher possibility of formation of more C-S-H at the concrete-PCM interface with silica fume inclusion with PCM.

6.1.2 Material level testing

The test results at micro level confirms an increase of the extend of chemical bonding between the concrete substrate and overlay material with silica fume addition, subsequently to enhance the interfacial performance. For practitioners better understanding and with an aim to achieve the great potential in practical design implications of the modified PCM overlay strengthening method, the effects of various influencing factors on the concrete-PCM interfacial bond performance and the bonding durability under severe environmental condition was evaluated at material level testing. From the test results, following conclusions can be reached.

- Surface roughness preparation techniques of the substrate concrete had a profound effect on the interfacial bonding strength. Surface roughed by sand blasting results higher interfacial bond strength. In comparison with interfacial shear strength, the splitting tension strength are not so sensitive to variation of interface roughness of the substrate concrete.
- The failure at adhesion layer with smooth fracture surface results in lower bond strength, while the failure at adhesion layer or mixed-mixed mode failure results in lower bond strength.
- With a sufficient roughness level of substrate concrete, interfacial strength increases with the increase of the substrate concrete compressive strength.
- Applying surface penetrant at the interface decreases the interfacial shear strength and results pure interfacial fracture mode (I) even if the surface roughness is high.
- The interfacial strength is predominantly influenced with the moistness of the substrate concrete surface, the saturated surface dry interface state of substrate concrete facilitate bond strength development.

- Exposure under severe environmental conditions of the strengthened members had significant negative influences on its long-term performance. The freeze-thaw cycles had significant negative influences on bonding behaviors of substrate concrete-PCM interface. Exposure of cyclic temperature condition had more detrimental effect than the exposure of constant temperature condition. The influence of moisture under continuous immersion results lower reduction of interfacial strength compared to the exposure under wetting and drying cycle.
- The inclusion of 5% silica fume in PCM
  - significantly increases the interfacial bonding strength compared to normal PCM specimens.
  - shifts the interfacial fracture (I) with lower fracture energy to a composite fracture mode (I-P) or (I-C) or mixed (C-P) fracture mode with higher fracture energy.
  - increases significantly the bond strength from the very first day of pouring of overlay mortar due the predominant reaction of silica compound with $Ca(OH)_2$ during the early hydration stage.
  - significantly increases the interfacial bonding strength, provides better adhesion with substrate concrete and improves the durability of the interfacial performance of concrete-PCM interface under harsh freeze-thaw environments.
  - reduces the degradation of the interfacial bonding strength (about 40% compared to normal PCM cases), provides better adhesion with substrate concrete (occurrence of composite or mixed mode fracture instead of pure interface fracture that happened in normal PCM cases) and improves the durability of the interfacial performance of concrete-PCM interface under constant and cyclic temperature conditions.
  - significantly improves the interfacial bonding strength compared to without silica fume cases under the influence of moisture by wetting/drying and continuous immersion.

6.1.3 Material level testing

For real application of the current work by modified PCM, member level testing was performed on strengthened RC beams. It was concluded from the testing at micro and material level that the inclusion of silica fume exert positive influences on strength of concrete-PCM interface. The performance of the interface was also investigated at member level by conducting loading test of RC beams strengthened with various amount of reinforcement at bottom of beam which was embedded in both normal and modified PCM overlay. From the experimental and analytical results, following conclusions can be reached.

- PCM overlaying method significantly increases the load carrying capacity compared to the unstrengthen structure. The increase of the strengthening reinforcement area increase the failure load but reduces the ductility level and triggers the occurrence of debonding failure.
- Different types of strengthening reinforcement has important effect on the mechanical performances of the strengthened structural. The use of CFRP grid performs better in terms of peak load, debonding load, ductility level and load-displacement relationship compared to convention steel rebar and CFRP strand sheet.
- The use of larger amount of strengthening reinforcement having very high tensile stiffness triggers the occurrence of debonding failure. Reinforcement amount (area X tensile strength) ratio of the strengthening reinforcement and main steel bar should not exceed 0.5 in order to get better structural performance.
- The inclusion of 5% silica fume in PCM
  - increases the load carrying capacity of the strengthened beam in comparison with normal PCM cementitious matrix.
  - led to more ductile failure and dispersed more uniformly the shear stress transfer at the interface between the strengthening layer and the substrate concrete.

- reduces the decrease of ductility level the increase in strengthening reinforcement area in comparison with normal PCM case.
- delays the occurrence of the debonding failure and improve the overall performance of the strengthened beam because of the relatively stronger bond achieved between the cementitious mortar and the concrete substrate with the silica fume inclusion. Therefore, the flexural capacity of the modified PCM strengthened RC beams can be predicted with acceptable accuracy based on conventional procedure (sectional analysis) considering perfect bond between the cementitious mortar and the concrete substrate.
- improves the ultimate bending moment and enhance the performance of the bonding surface, thus reflecting a good repair effect.

In conclusion, considering easy applicability of silica fume with PCM in practical application, environmentally friendly nature and ability to achieve adequate bond strength with concretes substrate, this study can provide an indication for engineering application of silica fume in polymer cement-based repair materials.

6.2 Recommendations

6.2.1 Suggestions for Engineering Applications

Based on the experimental work conducted in this study, the following suggestions were made for the practical application on repairing structure by modified 5% silica PCM.

- It is commonly hold view that the interface should be roughened enough to ensure proper bonding of cement matrix based repair material and substrate concrete. The inclusion of silica fume makes the repair material chemically reactive and performs better even with smooth or very low roughness level. In real scenario, there might be some cases where the substrate concrete surface could not roughen enough. In such cases, current data can be used as a guideline to the practitioner.
- No information is available by manufacturers of PCM about the mechanical properties of PCM with the inclusion of silica fume. In this research work, it is confirmed that the inclusion of silica fume with PCM significantly improves the interfacial bond strength and performs better under severe environmental conditions. Current data may be used by the manufacturers of PCM to produce other types of PCM with improved functionality.

6.2.2 Suggestions for future studies

This dissertation describes the influence of silica fume to enhance the interfacial behavior of concrete-PCM, considering the effects of various influencing factors on the concrete-PCM interfacial bond performance and the bonding durability under severe environmental condition. Extensive experimentations were conducted at micro, material, and member level to precisely understand its influence and for practical application to real structures. Still there are a lot of works to be done prior to use this method in practical design implications which are recommended as follows.

- ✓ In this work, micro level testing was done after 28 days of specimen preparation. However, some stress is induced by the continuous traffic movement during/after the construction work from the early stages as the PCM overlaying method enables its construct without preventing traffic. Therefore, it is essential to evaluate the performances of silica fume quantitively from the very first day of pouring of overlay material.
- ✓ Only the content of C-S-H at the interface was indirectly measured from the results of Ca/Si ratio obtained from SEM-EDS test. It is suggested to do more precise investigation to establish a relationship between bond strength and Ca/Si ratio. It is also suggested to perform loading test and Ca/Si measurement on the same day as the exposure in air may affects the measurement of Ca/Si ratio.
- ✓ The influence of interface roughness was considered in this research work. In practice, there prevails many cracks in the substrate concrete. These cracks generally cleaned before

overlaying, but an extent of damage still exist. Therefore, the effect of the existing damage should be taken into account in the future study.

- ✓ The bonding durability of the interface under severe environmental conditions were evaluated with respect to strength measurement and fracture mode only in this work. The observation of material change at micro level and stress analysis considering thermal stress are two basic targets in the future study.
- ✓ The effects of severe environmental conditions were evaluated by exposing the specimens for a short period of time compared to the service life of RC structures. Long-time exposure period (about 2-3 years) should be used in the future study to investigate the bonding durability issue that resemble service life of the strengthened structures.
- ✓ The load carrying capacity of the strengthened RC beams was predicted in this work considering perfect bond between substrate concrete and overlay layer. Attention should be paid to establish bond-slip relationship to incorporate in the analytical and numerical simulation purpose.
- ✓ In this work, only RC beams were tested under static loading though many structures repaired by overlaying method are exposed to fatigue loading. Therefore, it is recommended to investigate the performance of the PCM strengthened members under fatigue loading, both experimentally and numerically.